# Nonlinear Control of Mechanical Systems: A Riemannian Geometry Approach

Thesis by
Francesco Bullo

Technical Report CDS 98-010
for the
Control and Dynamical Systems Option


California Institute of Technology
Pasadena, California

1999

(Thesis defended August 7, 1998)

*to Lily*

# Acknowledgements

First and foremost, I would like to thank my advisor Richard Murray. Richard introduced me to the wonders of geometric control theory and managed to keep me focused all these years. His advice and words of wisdom always came at the right time. His encouragement and support towards my work have been invaluable.

I particularly wish to thank Naomi Ehrich Leonard for having extended to me an invitation and an opportunity to work side by side at Princeton University. It has truly been a pleasure to collaborate with her over the years. Her creativity and enthusiasm are contagious.

During my years at Caltech I had the opportunity to work with many amazing professors. I thank Jerry Marsden, whose vision and work are a constant source of inspiration and Joel Burdick for his continuous support and for allowing me to collaborate with many of his students. Also, I would like to thank John Doyle for stimulating and thought-provoking discussions and Pietro Perona for his help during important moments.

I would like to express my sincere gratitude to my co-workers Andrew Lewis and Miloš Žefran. With them I have had the pleasure of sharing inspiring conversations dealing with subjects such as control theory and mechanics. In fact I want to emphasize how instrumental our collaborations have been. In addition, I would also like to extend my gratitude to Bill Goodwine, Jim Radford, and Scott Kelly for having taken the time to engage in such interesting discussions with me.

I would like to take a moment to mention my great group of friends at Caltech that have supported me from day one. Particular thanks go to Bob Behnken, Michiel van Nieuwstadt, Sudipto Sur, and Chung-Hei Yeung for welcoming me during my first year in the Thomas lab. Thanks are also in order for Bob M'Closkey, Mark Milam, Muruhan Rathinam, Pablo Parrilo, Willem Sluis, Wang-Sang Koon, Yong Wang, Roberto Zenit and many others. Also, I would like to thank Charmaine, Shauna, and Wendy for all their help. A special thank you goes to Sanjay Lall for joining me in countless coffee breaks, dinners, and open-minded discussions on topics ranging from pizza to politics to academics.

At Caltech I also had the pleasure of meeting my "agent" friends: Alberto, Chris, George, Enrico, Jean-Yves, Luis, Mario, Wayez, and many more. Their friendship has been invaluable during my years in LA. During the time I spent at Princeton, many people such as Craig Woolsey and Mario Iodice took the time to make my stay more enjoyable and I sincerely thank them for that. In addition, I want to give thanks to everyone whose name or importance may have slipped the controls of my keyboard.

Finally, I would like to thank my family back in Padova. To my parents Aurelio and Carla for their loving care, their unconditional support, and their firm belief in me. To my brother and sister, Federico and Valentina, for always being there for me. Although we were geographically separated, and although phone calls never sufficed, they were always in my heart. Also, I would like to thank Lily's parents Juan and Martha, and her brother Carlos for their encouragement and support over the years and for providing me with a home away from home.

My last thought goes to Lily and her great smile. She has given me the strength to keep going and has filled these years with enthusiasm and joy. Ti ringrazio con tutto il cuore.

# Abstract

Nonlinear control of mechanical systems is a challenging discipline that lies at the intersection between control theory and geometric mechanics. This thesis sheds new light on this interplay while investigating motion control problems for Lagrangian systems. Both stability and motion planning aspects are treated within a unified framework that accounts for a large class of devices such as robotic manipulators, autonomous vehicles and locomotion systems.

One distinguishing feature of mechanical systems is the number of control forces. For systems with as many input forces as degrees of freedom, many control problems are tractable. One contribution of this thesis is a set of trajectory tracking controllers designed via the notions of configuration and velocity error. The proposed approach includes as special cases a variety of results on joint and workspace control of manipulators as well as on attitude and position control of vehicles.

Whenever fewer input forces are available than degrees of freedom, various control questions arise. The main contribution of this thesis is the design of motion algorithms for vehicles, i.e., rigid bodies moving in Euclidean space. First, an algebraic controllability analysis characterizes the set of reachable configurations and velocities for a system starting at rest. Then, provided a certain controllability condition is satisfied, various motion algorithms are proposed to perform tasks such as short range reconfiguration and hovering.

Finally, stabilization techniques for underactuated systems are investigated. The emphasis is on relative equilibria, i.e., steady motions for systems that have a conserved momentum. Local exponential stabilization is achieved via an appropriate splitting of the control authority.

# Contents

# List of Figures

# List of Tables

# Chapter 1

# Introduction

Mechanical control systems provide an important and challenging research area that fall between the study of classical mechanics and modern nonlinear control. Mechanical and more generally Lagrangian systems pervade modern applications in science and industry and this thesis aims towards the development of a rigorous control theory applicable to this large class of systems.

From a theoretical standpoint, the geometric structure of mechanical systems gives way to stronger control algorithms than those obtained for generic nonlinear systems. In other words, it is precisely because we specialize to this rich class that we can exploit a typical structure and solve relevant control problems.

## 1.1 Nonlinear Control and Mechanics

The history of mechanics is extraordinarily rich and varied. Unlike a more classic approach in the works of Whittaker [105] and Goldstein [41], recent books by Marsden and co-workers [1], [71] and [72] develop a geometric, covariant theory that emphasizes the role of symmetry and reduction. Both Hamiltonian and Lagrangian viewpoints benefit greatly from this renewed attention to the more geometric aspects.

Similarly, control theory is also a well developed field. Beginning in the late 1970s, the results of numerous authors such as Brockett, Hermann, Isidori, Krener and Sussmann, e.g., [18], [44], [46], [93], have brought the methods of differential geometry to bear on nonlinear control problems. The classic feedback linearization problem is just an example of control theory understood as a geometric equivalence problem. Now, various books describe nonlinear control in a geometric light: Isidori [45], Nijmeijer and van der Schaft [78], and Sontag [90] are examples. Recent years have also witnessed large amounts of activity on nonlinear stability and stabilization; see for example the contribution in Khalil [51], the development of backstepping [55] and the theory on input-to-state stability [91].

The study of mechanical control systems has always been an elegant and exciting discipline that has taken advantage of, and sometimes inspired, this large body of literature. One early reference is the work of Brockett on control theory and analytical mechanics [17], and the related contributions [15], [16] on systems defined on groups and spheres. Optimal control, integrability, Hamiltonian and gradient flows, rigid body dynamics, and nonholonomic constraints are only a few of the subjects treated by various authors. A very incomplete list includes Baillieul [7], Bloch [9], Crouch [32], [34], Koditschek [53], Krishnaprasad [54], Marsden [10], and van der Schaft [97], [98]. Finally, recent exciting results obtained at Caltech by Murray's group and at Princeton by Leonard's group are surveyed in [75] and [61].

As a side note it is worth mentioning that a number of application areas is affected by both nonlinear control and mechanics: examples are robotic manipulation, see Murray and

co-workers [76] and Craig [31], design and control of aircrafts, see Etkin [37], and of ocean vehicles see Fossen [40], control of electro-mechanical systems, see Arimoto [4].

### Modeling via Riemannian Geometry Tools

This thesis investigates various control problems for a large class of mechanical systems. The latter are roughly classified as robotic manipulators and multibody systems, aerospace and underwater vehicles, and devices that locomote via nonholonomic constraints. All these systems are described by a second order nonlinear differential equation on a manifold, and a unified modeling approach is provided in this dissertation via some geometric tools.

In our investigation the geometry of *affine connections* plays a key role in modeling and characterizing control problems for this class of systems. As opposed to the more common languages of variational principles or symplectic geometry, the treatment in this thesis relies on some notions from Riemannian geometry, see [52] and the review in Chapter 2. These are efficient tools, as numerous contributions on modeling [9], stabilization [53], controllability [64], and [67], interpolation [79], [106] and dynamic feedback linearization [83] attest.

It is originally in the work of Smale [89] that the notion of *simple mechanical system* was formalized. These are systems whose configuration space is a tangent bundle (i.e., the phase space is divided into configuration and velocity variables) and whose Lagrangian is composed of kinetic and potential energy. Here we extend this definition by introducing forces. For example we describe a robotic manipulator in terms of a configuration space, a kinetic and a potential energy and a set of input forces. These four objects characterize a simple mechanical control system.

Underwater vehicles, satellites, surface vessels, airships and hovercrafts are all examples of simple mechanical control systems of a special kind. Their configuration space is endowed with a natural group operation, e.g., composition of rotations and translations in the Euclidean space. Also, their kinetic energy is invariant under this operation and the forces applied to the vehicle are fixed with respect to a body frame. Accordingly, we say that these are mechanical control systems on a *Lie group*; see Chapter 3 for a precise definition. One fundamental assumption on these systems is that lift/drag type effects are negligible, so that the first principle models we derive describe accurately the system's dynamics.

Finally, constraints of both holonomic and nonholonomic type, i.e., constraints on configuration or velocity variables, can also be treated within the affine connection framework. This is obtained by means of the procedure called elimination of multipliers, see [66] and [9] for an intrinsic exposition.

### Motion Control Problems and Applications

After introducing the basic models, we now describe various control problems of interest. In this dissertation we put the emphasis on motion control problems, where motion is intended as movement in Euclidean space. In other words, a prototypical problem is how to steer the configuration of a mechanical system from one point to another, either in a planar or in a three-dimensional setting. It goes without saying that the geometry of group of rigid displacements plays an important role. It is precisely this geometric structure that we exploit for advantage in control.

Both theoretical and practical motivations inspire our work. The more theoretical motivations involve the desire to formalize a set of loosely connected results from the robotic and the vehicle control literature, see Section 1.2.1, and to bring to bear some powerful mechanics on some stabilization problems, see Section 1.2.2. In addition, inspired by the field of robotic locomotion, we investigate how to design motion algorithms for so-called underactuated systems; see Section 1.2.3.

The driving applications are motion control problems that arise in the study and design of aerospace and underwater vehicles. Recent important trends in this field include a push toward the design of increasingly autonomous vehicles, an emphasis on reconfigurable systems and on control schemes amenable to implementation on-line. Additionally, the availability of inexpensive computing devices and sensors is leading to a renewed attention on how to design, deploy and utilize actuators.

All these factors make it possible to introduce innovative concepts in the control design phase. The goal of this dissertation is a deeper understanding of the interaction between control forces and Lagrangian dynamics. We believe this will lead to improved control algorithms for existing mechanisms and novel design schemes for future devices, see for example the work on underwater vehicles [61] and carangiform locomotion [50], on nonholonomic and multi-legged robots [42, 80], and on flatness for aerial vehicles [83, 99, 100].

## 1.2 Statement of Contributions

This section presents a brief outline of the contributions in this dissertation and a more detailed description in the following three subsections. One salient feature of mechanical control systems is the number of input forces. Control design based on Lyapunov functions has proven successful with fully actuated systems, that is, systems with as many inputs as degrees of freedom. More sophisticated tools are required in the underactuated case.

The first contribution of this dissertation consists of a trajectory tracking controller for fully actuated systems. The structure of the controller is traditional in that it is the sum of so-called proportional, derivative and feedforward terms. The way these terms are designed, however, is innovative. The key concepts are how to define state errors on a nonlinear space and how to perform the Lyapunov analysis in a coordinate-independent fashion. In other words, the synthesis of the control law is intrinsic and it therefore applies to robotic manipulators and multibody systems, as well as aerospace and underwater vehicles.

Despite the large number of fully actuated systems, the study of underactuated systems has gained much attention in the recent literature. From a practical point of view, we are motivated by vehicles that are underactuated either because of an actuator failure or because of a design choice. In the former case, our results will improve robustness to actuator failure and thus will provide autonomous vehicles with greater reliability. In the latter case, our results may allow for vehicle designs that include fewer actuators than typical leading to lighter, less costly designs. From a theoretical perspective, these systems when underactuated offer a control challenge as they have non-zero drift, the linearization at zero velocity is not controllable, and they are not stabilizable by continuous state feedback. Further, they are generically not feedback linearizable, not "configuration flat," as defined in [83], and no test is available to establish whether they are differentially flat.

The second contribution of this dissertation is a systematic procedure for the exponential stabilization of relative equilibria of underactuated systems. A key design idea is to distinguish between horizontal forces, which preserve the momentum, and vertical forces that affect it. A proportional, derivative control in the horizontal directions and a first order regulator in the vertical direction lead to exponential stability of the closed loop provided some assumptions hold. In particular, two necessary conditions are that the relative equilibrium be Lyapunov stable and that the system satisfy a certain linear controllability test.

The main contribution of this thesis is a controllability analysis and some motion control algorithms for underactuated vehicles in the small velocity regime. Since these systems have a non–controllable linearization at zero velocity, only a nonlinear analysis can determine what configurations and velocities can be reached. The contribution lies in some algebraic

tests that characterize these controllability properties. These results indicate the location and number of actuators needed for controllability.

Based on the controllability analysis, two motion primitives are designed to perform the basic tasks of changing and maintaining the system's velocity. This is achieved by a perturbation analysis under the assumption of small amplitude input and velocity. The primitives rely on in-phase sinusoidal inputs that exploit the system's dynamics, as opposed to traditional out-of-phase controls for kinematic systems. Using multiple calls to the motion primitives, motion algorithms are designed to steer the system from point to point and to exponentially stabilize the system to a fixed location.

In what follows we present a more detailed account and a review of the relevant literature for the various contributions in the thesis.

### 1.2.1 Tracking for Fully Actuated Systems

Chapter 4 deals with the trajectory tracking problem for fully actuated systems: the control objective is to track a trajectory with exponential convergence rates in order to guarantee performance and robustness. The tracking problem for robot manipulators has received much attention in the literature. Examples are the contributions in [95], [102] and [88], where asymptotic, exponential and adaptive tracking are achieved via a nonlinear analysis. These results are now standard in textbooks on control [78] and robotics [76]. Since then, similar techniques have been applied to the attitude control problem for satellites [103], and likewise to the attitude and position control for underwater vehicles [40, Section 4.5.4]. A further example is the spin axis stabilization problem for satellites [96]. A common feature in all these works is the preliminary choice of a parametrization, i.e., a choice of coordinates for the configuration manifold. The synthesis of both control law and corresponding Lyapunov function is performed in this specific parametrization. This set of coordinate plays then an important role, when the control system is characterized in terms of, for example, singularities and exponential convergence, and when adaptive capabilities are included.

In this thesis we propose a unifying framework that applies to a large class of mechanical systems. In the spirit of Koditschek [53], this is achieved by avoiding the parametrization step. Our design algorithm focuses on basic, intrinsic issues such as how to define a state error and how to exploit the Lagrangian dynamics. The notions of "error function" and "transport map" yield to a coordinate-free definition of errors between configurations and between velocities. Together with a dissipation function these ingredients determine the feedback law. The feedforward control is devised using the theory of Riemannian connections. Provided a compatibility condition between error function and transport map holds, our control strategy achieves globally stable tracking. As discussed in [53], (possible) topological properties of the configuration manifold preclude global asymptotic stabilization. However, we prove local exponential stability under some boundedness conditions and we provide an estimate of the region of attraction. Useful extensions to adaptive control and to more general mechanical systems can be included via standard techniques. We remark that the design process, the statement and the proof of the main theorem are all performed without choosing coordinates on the configuration manifold.

The resulting design algorithm is then set to work in a variety of applications, recovering previous controllers and suggesting new ones. Examples are the standard "augmented PD control" for robot manipulators, see [76], and the novel tracking controller for systems on the two sphere. Most instructive is the treatment of the tracking problem on the group of rigid rotations SO(3) and on the group of rigid motions SE(3). In the latter case, for example, we design a large set of error functions with matrix gains and we characterize transport maps as changes of reference frame. These ideas lead to a comparison of various previous approaches and to new results. Finally, some computationally simple feedforward

controls are derived via an extension of the main theorem.

### 1.2.2 Stabilization of Relative Equilibria for Underactuated Systems

Chapter 5 presents some stabilization techniques for the steady motions called relative equilibria. This family of trajectories is of interest in vehicle control applications; see for example the gliding underwater motions in [61] and the so-called spin axis stabilization problem for satellites in [96].

Point stabilization of underactuated Hamiltonian systems was originally investigated in [98]; see [78] for a standard treatment. Recently, geometric tools have been employed to address the class of mechanical systems with symmetries. Stability of underwater vehicles is studied in [60] where symmetry breaking potentials were employed to shape the energy of the closed loop system. In Bloch, Leonard and Marsden [11], a novel and powerful approach is introduced to deal with an even larger class of systems. In Jalnapurkar and Marsden [47] the authors obtain stabilizing controllers for underactuated mechanical systems with non-Abelian symmetry. In their treatment the family of input forces is assumed momentum preserving and stability in the reduced space is characterized in terms of certain Poisson brackets.

In this thesis we build on the work of Leonard in [60] and focus on the exponential stabilization problem (as opposed to Lyapunov or asymptotic stabilization). The control design is based on ideas from two areas: the theory of Hamiltonian reduction (and the Energy–Momentum method in particular), see [86], and the theory of passive nonlinear systems, see [98]. We divide the control synthesis into three steps: first we split the control authority along the momentum-preserving subspace and its orthogonal complement. Then we design a controller for the reduced system employing only the momentum-preserving forces, and finally we regulate the value of the momentum with the remaining control authority. A set of intrinsic conditions ensures the exponential stability for the *full* (internal variables and momentum) system. A key feature of this approach is that we focus on one-dimensional (Abelian) symmetries because applications to control of vehicles usually satisfy this assumption. This restriction leads to strong results and a simple exposition.

### 1.2.3 Controllability and Motion Planning for Underactuated Systems

Chapter 6 and Chapter 7 present controllability tests and motion algorithms for underactuated vehicles. Relevant past contributions include work on both the nonlinear controllability problem and the constructive controllability problem (including both motion planning and stabilization). Within the context of this thesis, the important references for controllability are the works of Sussmann on small-time local controllability [93] and of Lewis and Murray on configuration controllability for simple mechanical systems [67, 68]. Other contributions include local controllability results for other classes of mechanical systems, see [49, 80], and work on global controllability issues, see [12, 33, 70]. Regarding the constructive controllability problem, we employ the same approach as Leonard and Krishnaprasad in [62] and [58], where motion algorithms for a class of kinematic systems on Lie groups were designed with small-amplitude periodic inputs. In a later work [84] similar techniques were applied to a different class of mechanical system. Other contributions on oscillatory controls and Lagrangian systems include [7], [43] and [94]. A somewhat different approach, based on homogeneous time-varying strategies, was employed in [74, 82] to design exponentially stabilizing control laws for underactuated satellites and surface vessels.

To derive controllability tests for our class of systems, we apply the controllability analysis described in [93] and [67] to simple mechanical control systems on Lie groups. Key features of the analysis are a focus on the evolution of the system's configuration when the initial velocity is zero and the result that computations are performed on the Lie algebra of the Lie group. The local controllability properties are characterized by the algebraic operations of symmetric product and Lie bracket. The symmetric product, which is defined more formally in Section 2.3, depends upon the metric that defines the kinetic energy and, as we shall see, explicitly describes motions that involve both input vector fields and the drift dynamics. Our tests describe which velocities and configurations are reachable, independent of the initial configuration. The notions of good and bad symmetric products play a central role.

Guided by our interpretation of the controllability tests, we apply perturbation theory to investigate the response of the mechanical system to small-amplitude forcing. The initial velocity is also assumed to have small amplitude. The approximations we obtain give further insight into the controllability tests and are instrumental in the subsequent control design. Numerous examples illustrate the meaning of good and bad symmetric products and the effects of in-phase and out-of-phase sinusoidal inputs.

On the basis of a controllability assumption, we design two motion primitives that perform the basic tasks of changing and maintaining velocity. These motion primitives use in-phase inputs and compensate for contributions along bad symmetric product directions (see also [22]). The two motion primitives synthesize the controllability analysis and are the building blocks for designing high-level motion procedures. Using discrete-time feedback and multiple calls to the motion primitives, we design motion algorithms to solve the point-to-point reconfiguration problem (i.e., how to steer the system to a desired configuration) and the static interpolation problem (i.e., how to steer the system through a set of desired configurations). We solve point-to-point reconfiguration using a constant velocity algorithm. A second approach to point-to-point reconfiguration consists of interpolating a sequence of segments connecting initial to final configuration. We show the advantage of the latter solution in the case the segments are steady motions of the unforced mechanical system. Next, iterating an approximate stabilization step we design an algorithm that locally exponentially stabilizes the system to a desired configuration. Recall that exponential stabilization cannot be achieved by smooth time-varying feedback, and indeed our motion primitives are continuous, but not smooth, functions of the state. Accordingly, our approach relies on discrete-time continuous feedback, see [92], and on the iteration of a motion planning step, see [56]. Finally, the three algorithms are implemented numerically to verify the approximations and illustrate the control design.

## 1.3 Outline of the Thesis

A brief outline of the content of the various chapters is as follows:

*Chapter 2:* Here we review the necessary mathematical tools from differential geometry, Lie group theory and Riemannian geometry.

*Chapter 3:* In this chapter we present models based on Riemannian geometry for general second order differential equations on a manifold. The treatment includes the notion of simple mechanical control system, some extensions and numerous examples.

*Chapter 4:* This chapter presents the solution to the trajectory tracking problem for fully actuated mechanical systems.

*Chapter 5:* Here we presents some stabilization techniques for underactuated systems moving along a relative equilibrium.

*Chapter 6:* This chapter contains a review of the theory of nonlinear controllability and of configuration controllability. In addition, we present a novel treatment for systems on Lie groups and some initial results for systems that undergo impacts.

*Chapter 7:* In this chapter we present some approximate solutions to forced mechanical systems and some motion algorithms for underactuated systems.

*Chapter 8:* The chapter presents some conclusions, a summary and some directions for future research.

# Chapter 2

# Mathematical Preliminaries

In this chapter we review some mathematical tools. For an introduction to Riemannian geometry, we refer to [13], [35] and [52]. For an introduction to Lie group theory, we refer to [85] and [101].

The chapter is organized as follows. In Section 2.1 we review some notation in differential geometry. Section 2.2 presents some notions in Lie group theory and Section 2.3 some notions in Riemannian geometry. Finally, Section 2.4 presents some illustrative examples.

## 2.1 Differential Geometry

We assume the reader to be familiar with some differential geometry, to the extent presented for example in the appendices of [76] or [78]. A complete reference is [2]. We here quickly review some notation and state the results we will need later.

### Manifolds and Tensor Fields

A smooth *manifold* $Q$ is a locally Euclidean space, i.e., a space that is locally homeomorphic to $\mathbb{R}^n$ via a diffeomorphism. A *local coordinate chart* is a pair $(U, \phi)$, where $U$ is an open subset of $Q$ and $\phi$ is a smooth map from $U$ to $\mathbb{R}^n$. In what follows, a differentiable object is smooth whenever it is analytic.

We let $C^\infty(Q)$ denote the set of a smooth real valued functions on $Q$. The *tangent space* $T_qQ$ to the manifold $Q$ at the point $q$ is the set of all derivations on $C^\infty(Q)$. Elements of the tangent space are *tangent vectors*. The *cotangent space* $T_q^*Q$ is the dual space to $T_qQ$, i.e., the set of linear functionals on $T_qQ$. We let $\langle \cdot, \cdot \rangle$ denote the standard pairing between tangent and cotangent spaces. The *tangent (and cotangent) bundle* $TQ$ (respectively $T^*Q$) is defined as the union over all $q \in Q$ of tangent (respectively cotangent) space.

A *vector field* $X$ on $Q$ is a smooth map that associates to each point $q \in Q$ a tangent vector $X_q \in T_qQ$. Similarly, a *one-form* $\alpha$ on $Q$ associates to each $q \in Q$ a cotangent vector $\alpha_q$. Finally, a *tensor field* $t$ of contravariant order $r$ and covariant order $s$ associates to each $q \in Q$ a multi-linear map $t : T^*Q \times \cdots \times T^*Q \times TQ \times \cdots \times TQ \to \mathbb{R}$ (with $r$ copies of $T^*Q$ and $s$ copies of $TQ$).

Given a function $f$ in $C^\infty(Q)$, we let $\mathcal{L}_X f$ denote the Lie derivative of $f$ with respect to $X$ and we let $\mathrm{d}f$ denote the one-form such that for all vector fields $X$:

$$\langle \mathrm{d}f, X \rangle = \mathcal{L}_X f.$$

Given a smooth function $\Phi : Q \to Q$, define its *tangent map* $T\Phi : TQ \to TQ$ as

$$(T_q\Phi \cdot X_q)f \triangleq X_q(f \circ \Phi), \qquad \forall q,$$

where $f$ is a real valued function in $C^\infty(Q)$ and $X_q$ is a tangent vector in $T_qQ$.

Given a pair of smooth vector fields $X, Y$, we let $[X, Y]$ denote their Lie bracket and let $\mathcal{L}_X Y$ denote the Lie derivative of $Y$ with respect to $X$.

### Distributions and Integrable Manifolds

Given a pair of vector fields $X, Y$, their *Lie bracket* is the vector field defined by

$$\mathcal{L}_{[X,Y]}f = \mathcal{L}_X\mathcal{L}_Y f - \mathcal{L}_Y\mathcal{L}_X f, \qquad \forall f \in C^\infty(Q). \tag{2.1}$$

The Lie bracket operation satisfies two fundamental properties: skew symmetry and the Jacobi identity:

$$[[X, Y], Z] + [[Z, X], Y] + [[Y, Z], X] = 0.$$

A *distribution* $\mathcal{D}$ on $Q$ is a subbundle of $TQ$, i.e., the union over all $q \in Q$ of linear subspaces of $T_qQ$. The rank of $\mathcal{D}$ at $q$ is the dimension of the subspace $\mathcal{D}(q)$. Given a family of vector fields $\mathcal{X} = \{X_1, \ldots, X_k\}$, we can define a distribution by

$$\mathcal{D}_\mathcal{X} = \text{span}_{C^\infty(Q)}\{X_1, \ldots, X_k\}.$$

In what follows, we assume that distributions have constant rank and that it is possible to find a family of smooth vector fields that span them.

A distribution $\mathcal{D}_\mathcal{X}$ is *involutive* if for any pair of vector fields $X, Y \in \mathcal{X}$, their Lie bracket $[X, Y]$ also belongs to $\mathcal{X}$. An *integral manifold* $N$ of $\mathcal{D}$ is a submanifold of $Q$ such that $T_qN \subset \mathcal{D}(q)$ for all $q \in N$. A distribution $\mathcal{D}$ is *integrable* if, for all $q \in Q$, there exist an integrable manifold with the same dimension as the rank of $\mathcal{D}$. This submanifold of $Q$ is called the *maximal integral manifold*. Involutivity and integrability of a distribution are proven equivalent in Frobenius Theorem.

### Codistributions

Similarly to the notion of distribution, a *codistribution* $\mathcal{I}$ on $Q$ is a subbundle of $T^*Q$, i.e., the union over all $q \in Q$ of linear subspaces of $T_q^*Q$. The rank of $\mathcal{I}$ at $q$ is the dimension of the subspace $\mathcal{I}(q)$.

Given a distribution $\mathcal{D}$ on a manifold $Q$, we define its *annihilator* $\text{Ker}\,\mathcal{D}$ as the set of one-forms $\alpha$ such that $\langle \alpha, X \rangle = 0$, for all $X \in \mathcal{D}$. Similarly, given a codistribution $\mathcal{I}$, we define its annihilator $\text{Ker}\,\mathcal{I}$ as the set of vector fields $X$ such that $\langle \alpha, X \rangle = 0$, for all $\alpha \in \mathcal{I}$.

The $k$ dimensional codistribution $\mathcal{I}$ is *integrable* if there exist $k$ functions $\phi_1, \ldots, \phi_k$, such that $\mathcal{I} = \text{span}\{\text{d}\phi_1, \ldots, \text{d}\phi_k\}$. Integrability of the codistribution $\mathcal{I}$ is equivalent to the integrability of its annihilator $\text{Ker}\,\mathcal{I}$. Computable tests for the integrability of a codistribution are found in [38].

## 2.2 Lie Groups

A *Lie group* $G$ is a smooth manifold endowed with a smooth binary operation called group multiplication (satisfying associativity and existence of identity and inverse elements). A *Lie*

*algebra* is a vector space endowed with a skew symmetric, bilinear operation called the Lie bracket (satisfying the Jacobi identity).

The letters $g, h$ denote elements in the group $G$ and $e = \mathrm{Id}$ is the group identity. The map $L_g : G \to G; h \mapsto gh$ is called *left translation*. A vector field $X$ is said to be *left invariant* if it satisfies the equality

$$X(gh) = T_h L_g \, X(h),$$

where $T_h L_g$ is the tangent map to $L_g$ at $h$. We let Greek letters denote vectors in the tangent space at the identity $T_e G$, for example $X(e) = \xi$, and we denote left invariant vector fields as

$$X(g) = T_e L_g \, \xi \triangleq g \cdot \xi.$$

Since the value of $X(g)$ is uniquely determined by its values at $g = e$, we identify $T_e G$ with the set of left invariant vector fields $\mathfrak{g}$. It can be shown that the Lie bracket of two left invariant vector fields is still left invariant, so that we can define a Lie bracket on $\mathfrak{g}$ by

$$g \cdot [\xi, \eta] \triangleq [g \cdot \xi \ , \ g \cdot \eta]. \tag{2.2}$$

Therefore, the set of left invariant vector fields $\mathfrak{g}$ is a (finite dimensional) Lie algebra.

We let $\mathrm{ad}_\xi \, \eta = [\xi, \eta]$. Let $\mathfrak{g}^*$ denote the dual space of $\mathfrak{g}$, that is the set of covectors $\alpha$ such that $\langle \alpha, \xi \rangle$ is a linear function of $\xi \in \mathfrak{g}$. Let $\mathrm{ad}^*_\xi : \mathfrak{g}^* \to \mathfrak{g}^*$ be the dual operator of $\mathrm{ad}_\xi$ defined by $\langle \mathrm{ad}^*_\xi \, \alpha, \eta \rangle = \langle \alpha, [\xi, \eta] \rangle$ for all $\alpha \in \mathfrak{g}^*$.

In a *matrix Lie group* the group operation is matrix multiplication. The corresponding Lie algebra $\mathfrak{g}$ is also a matrix Lie algebra with Lie bracket given by matrix commutation, i.e., $[\xi, \eta] = \xi\eta - \eta\xi$.

### The Rotation and Rigid Displacement Groups

An example of a matrix Lie group is the rotation group

$$\mathrm{SO}(3) = \{R \in \mathbb{R}^{3\times 3} \,|\, RR^T = I_3, \ \det(R) = +1\}.$$

(SO stands for special orthogonal group; more details are available in [101]). Its associated matrix Lie algebra is the space of skew symmetric matrices

$$\mathfrak{so}(3) = \{S \in \mathbb{R}^{3\times 3} \,|\, S^T = -S\}.$$

Let $\times$ denote the cross product on $\mathbb{R}^3$ and define the operator $\widehat{\cdot} : \mathbb{R}^3 \to \mathfrak{so}(3)$ by $\widehat{x}y \triangleq x \times y$ for all $x, y \in \mathbb{R}^3$. The $\widehat{\cdot}$ operator is a Lie algebra isomorphism between $\mathfrak{so}(3)$ (with matrix commutator) and $\mathbb{R}^3$ (with cross product). Under this identification, the adjoint operator on $\mathfrak{so}(3)$ is $\mathrm{ad}_x = \widehat{x}$, for all $x \in \mathbb{R}^3$.

The special Euclidean group $\mathrm{SE}(n)$ is the group of rigid displacements, that is rotations and translations, on $\mathbb{R}^n$. In the three-dimensional case, this set of matrices has the structure of a Cartesian product between $\mathrm{SO}(3)$ and $\mathbb{R}^3$. As a Lie group $\mathrm{SE}(3)$ has the structure of a semi-direct product between $\mathrm{SO}(3)$ and $\mathbb{R}^3$. The corresponding Lie algebra $\mathfrak{se}(3)$ also has the structure $\mathfrak{so}(3) \times \mathbb{R}^3$ and it is isomorphic to $\mathbb{R}^6$. We represent a group element $g = (R, p) \in \mathrm{SO}(3) \times \mathbb{R}^3$ and an algebra element $\xi = (\widehat{\Omega}, V) \in \mathfrak{so}(3) \times \mathbb{R}^3$ using homogeneous coordinates:

$$g = \begin{bmatrix} R & p \\ 0_{1\times 3} & 1 \end{bmatrix} \quad \text{and} \quad \xi = \begin{bmatrix} \widehat{\Omega} & V \\ 0_{1\times 3} & 0 \end{bmatrix}.$$

The adjoint operator on $\mathfrak{se}(3) = \mathbb{R}^6$ is

$$\mathrm{ad}_{(\Omega,V)} = \begin{bmatrix} \widehat{\Omega} & 0 \\ \widehat{V} & \widehat{\Omega} \end{bmatrix}.$$

**Exponential Coordinates**

On a matrix Lie group we define the *exponential map* $\exp : \mathfrak{g} \to G$ as

$$\exp \xi = \sum_{k=0}^{\infty} \frac{\xi^n}{n!}.$$

If the set $G$ is the Cartesian product of an arbitrary number of copies of SE(3) and its proper subgroups, then the exponential map is surjective and it is a local diffeomorphism between the group and its algebra. We refer to [72] for more details. For example, given $\widehat{x} \in \mathfrak{so}(3)$, Rodrigues' formula gives

$$\exp(\widehat{x}) = I_3 + \sin \|x\| \frac{\widehat{x}}{\|x\|} + (1 - \cos \|x\|) \frac{\widehat{x}^2}{\|x\|^2},$$

where $\| \cdot \|$ is the standard Euclidean norm. The logarithmic map is the local inverse of the exponential map and provides us with a local chart on the manifold $G$. In other words, in an open neighborhood of the origin $\mathrm{Id} \in G$, we define $x = \log(g) \in \mathfrak{g}$ to be the *exponential coordinates* of the group element $g$. For example, if $R \in \mathrm{SO}(3)$ is such that $\mathrm{tr}(R) \neq -1$, then

$$\log(R) = \frac{\phi}{2 \sin(\phi)} (R - R^T) \in \mathfrak{so}(3),$$

where $\phi$ satisfies $2\cos(\phi) = \mathrm{tr}(R) - 1$ and $|\phi| < \pi$. In other words, $\log(R)$ is the product of the axis and angle of rotation of $R$. Corresponding definitions for the group SE(3) are presented in [76].

**Metrics on Lie Groups**

On the Lie algebra $\mathfrak{g}$ an inner product is defined by a self–adjoint positive definite tensor $\mathbb{I} : \mathfrak{g} \to \mathfrak{g}^*$, so that, for example, the inner product between $\xi$ and $\eta$ is $\langle \mathbb{I}\xi, \eta \rangle$ and the norm of $\xi$ is $\|\xi\| = \langle \mathbb{I}\xi, \xi \rangle^{1/2}$. Locally, this induces a metric on the group $G$ using the logarithm map as $d(g,h) = \|\log(gh^{-1})\|$. We refer to [62] and to [81] for a detailed treatment on metrics on Lie groups, and we investigate in the next section Riemannian metrics on Lie groups.

## 2.3 Riemannian Geometry

A *Riemannian metric* on a manifold $Q$ is a smooth map that associates to each tangent space $T_qQ$ an inner product $\langle\!\langle \cdot\,, \cdot \rangle\!\rangle_q$. A manifold endowed with a Riemannian metric is said to be a *Riemannian manifold.*

**Definition 2.1.** An affine connection on $Q$ is a smooth map that assigns to each pair of smooth vector fields $X, Y$ a smooth vector field $\nabla_X Y$ such that for all functions $f, g$ on $Q$ and for all vector fields $X, Y, Z$:

(i) $\nabla_{fX+gY} Z = f \nabla_X Z + g \nabla_Y Z$,

(ii) $\nabla_X(Y+Z) = \nabla_X Y + \nabla_X Z$, and

(iii) $\nabla_X fY = f\nabla_X Y + (\pounds_X f)\, Y$.

We also say that $\nabla_X Y$ is the *covariant derivative* of $Y$ with respect to $X$. Given any three vector fields $X, Y, Z$ on $Q$, we say that the affine connection $\nabla$ on $Q$ is *torsion-free* if

$$[X,Y] = \nabla_X Y - \nabla_Y X, \tag{2.3}$$

and is *compatible* with the metric $\langle\!\langle \cdot\,,\,\cdot \rangle\!\rangle$ if

$$\pounds_X \langle\!\langle Y\,,\,Z \rangle\!\rangle = \langle\!\langle \nabla_X Y\,,\,Z \rangle\!\rangle + \langle\!\langle Y\,,\,\nabla_X Z \rangle\!\rangle. \tag{2.4}$$

The Levi-Civita theorem states that on the Riemannian manifold $Q$ there exists a unique affine connection which is torsion-free and compatible with the metric. Indeed, combining equations (2.3), (2.4) and their permutations, one obtains the equality

$$\begin{aligned} 2\langle\!\langle X\,,\,\nabla_Z Y \rangle\!\rangle = \pounds_Z \langle\!\langle X\,,\,Y \rangle\!\rangle + \langle\!\langle Z\,,\,[X,Y] \rangle\!\rangle + \pounds_Y \langle\!\langle X\,,\,Z \rangle\!\rangle \\ + \langle\!\langle Y\,,\,[X,Z] \rangle\!\rangle - \pounds_X \langle\!\langle Y\,,\,Z \rangle\!\rangle - \langle\!\langle X\,,\,[Y,Z] \rangle\!\rangle, \end{aligned} \tag{2.5}$$

which uniquely determines the connection $\nabla$ as a function of the metric $\langle\!\langle \cdot\,,\,\cdot \rangle\!\rangle$. We call this $\nabla$ the *Riemannian (or Levi-Civita) connection* on $Q$.

In the remainder of the section, we present various constructions related to the notion of an affine connection. First we define various covariant derivatives with respect to a vector field $X$:

(i) the covariant derivative of a function $f$ is the function defined by $\nabla_X f = \pounds_X f$,

(ii) the covariant derivative of one-form $\omega$ is the one-form $\nabla_X \omega$ such that

$$\langle \nabla_X \omega, Y \rangle = \nabla_X \langle \omega, Y \rangle - \langle \omega, \nabla_X Y \rangle, \qquad \forall Y,$$

(iii) the covariant derivative of a tensor field $Z : T^*Q \times TQ$, i.e., of a tensor field of order (1,1), is the (1,1) tensor field $\nabla_X t$ such that

$$(\nabla_X Z)(\omega, Y) = \nabla_X (Z(\omega, Y)) - Z(\nabla_X \omega, Y) - Z(\omega, \nabla_X Y).$$

In addition, it is possible to define covariant derivatives along curves. Consider a smooth curve $c = \{c(t) \in Q, t \in [0,1]\}$, and a vector field $\{v(t) \in T_{c(t)}Q, t \in [0,1]\}$ defined along the curve $c$. Let $X$ and $Y$ be two vector fields such that $X(c(t)) = \dot{c}(t)$ and $Y(c(t)) = v(t)$. The *covariant derivative of the vector field $v$ along $c$* is defined by

$$\nabla_{\dot{c}(t)} v(t) = \nabla_X Y(q)\big|_{q=c(t)}.$$

Finally, we introduce the useful operation of symmetric product, see [67] and [32] for more details. Given a pair of smooth vector fields $X, Y$ on $Q$, the *symmetric product* $\langle X : Y \rangle$ is the smooth vector field defined by

$$\langle X : Y \rangle = \nabla_X Y + \nabla_Y X. \tag{2.6}$$

## 2.4 Examples of Covariant Derivatives

Loosely speaking, covariant derivatives are directional derivatives of quantities defined on manifolds. Equation (2.3) relates them to the notion of Lie differentiation, whereas equa-

tion (2.4) plays the role of the Leibniz rule. In the following we present some useful approaches on how to compute covariant derivatives.

### 2.4.1 On a Submanifold of $\mathbb{R}^n$

A first instructive case is when the manifold $Q$ is a submanifold of $\mathbb{R}^n$. In this case the Euclidean norm $\|\cdot\|$ on $\mathbb{R}^n$ induces a Riemannian metric and connection on the submanifold $Q$. Let $\pi_q$ denote the orthogonal projection from $\mathbb{R}^n$ onto the tangent space $T_qQ$. Given any two vector fields $X, Y$ on $Q$, it holds that

$$(\nabla_X Y)(q_0) = \pi_{q_0}\left(\frac{d}{dt}\Big|_{t=0} Y(q(t))\right), \tag{2.7}$$

where $\{q(t), t \in \mathbb{R}\}$ is any curve on $Q$ with $q(0) = q_0$ and $\dot{q}(0) = X(q_0)$. We refer to [13, Chapter VII] for more details on this description of covariant differentiation.

We further illustrate these ideas applying them to the two sphere $\mathbb{S}^2 \triangleq \{p \in \mathbb{R}^3 | \, p^T p = 1\}$. Since $\mathbb{S}^2$ is embedded in $\mathbb{R}^3$, we identify points, tangent and cotangent vectors on the sphere with their corresponding components in $\mathbb{R}^3$. If $\{q(t), t \in \mathbb{R}\}$ is a curve and $Y(q)$ is a vector field on $\mathbb{S}^2 \subset \mathbb{R}^3$, then

$$(\nabla_{\dot{q}} Y)(q) = \pi_q\left(\dot{Y}(q(0))\right) = \dot{Y}(q(t)) - \left(q(t)^T \dot{Y}(q(t))\right) q(t),$$

where both $q(t)$ and $Y(q(t))$ are thought of as vectors on $\mathbb{R}^3$.

### 2.4.2 In a System of Local Coordinates

In full generality we can express covariant derivatives in a system of local coordinates. Given the chart $(q^1, \ldots, q^n)$, we define the *Christoffel symbols* $\Gamma_{ij}^k$ by

$$\nabla_{\frac{\partial}{\partial q^i}}\left(\frac{\partial}{\partial q^j}\right) = \Gamma_{ij}^k \frac{\partial}{\partial q^k},$$

where the summation convention is enforced here and in what follows. The Christoffel symbols of a Riemannian connection are computed from equation (2.5) as follows. Let $M$ be a matrix representation of the metric; in other words let $M_{ij} = \langle\!\langle \frac{\partial}{\partial q^i}, \frac{\partial}{\partial q^j} \rangle\!\rangle$. We have

$$\Gamma_{ij}^k = \frac{1}{2} M^{mk}\left(\frac{\partial M_{mj}}{\partial q^i} + \frac{\partial M_{mi}}{\partial q^j} - \frac{\partial M_{ij}}{\partial q^m}\right), \tag{2.8}$$

where $M^{ij}$ is the inverse of the tensor $M_{ij}$. The covariant derivative of a vector field is then written as

$$\nabla_X Y = \left(\frac{\partial Y^i}{\partial q^j} X^j + \Gamma_{jk}^i X^j Y^k\right) \frac{\partial}{\partial q^i}, \tag{2.9}$$

and of a one-form as

$$\nabla_X \omega = \left(\frac{\partial \omega_i}{\partial q^j} X^j - \Gamma_{ij}^k \omega_k X^j\right) dq^i. \tag{2.10}$$

### 2.4.3 On a Lie Group

Finally, we describe Riemannian connections within the context of Lie groups. Invariant connections on Lie groups are nicely described in [85] and employed by V. I. Arnold in the study of hydrodynamic of ideal fluids, see [5] and [6, Appendix 1 and 2].

As in the previous section, $g$ is an element in $G$ and Greek letters denote vectors in the Lie algebra $\mathfrak{g}$. An inner product on the Lie algebra $\mathfrak{g}$, that is a tensor $\mathbb{I} : \mathfrak{g} \to \mathfrak{g}^*$, induces a left invariant Riemannian metric on $G$ by left translation:

$$\langle\!\langle X(g)\,,\, Y(g) \rangle\!\rangle \triangleq \mathbb{I}(g^{-1} \cdot X(g)) \cdot (g^{-1} \cdot Y(g)).$$

The Riemannian connection $\nabla$ associated to this metric is of interest. An application of equation (2.5) shows that this connection satisfies

$$\nabla_{(g\cdot\xi)}\,(g \cdot \eta) = g \cdot \Big({}_{\mathfrak{g}}\nabla_{\xi}\eta\Big)\,, \tag{2.11}$$

where the map ${}_{\mathfrak{g}}\nabla : \mathfrak{g} \times \mathfrak{g} \to \mathfrak{g}$ is defined by

$${}_{\mathfrak{g}}\nabla_{\xi}\eta = \frac{1}{2}[\xi, \eta] - \frac{1}{2}\mathbb{I}^{-1}\big(\operatorname{ad}^*_{\xi}\mathbb{I}\eta + \operatorname{ad}^*_{\eta}\mathbb{I}\xi\big). \tag{2.12}$$

Connections that satisfy equation (2.11) are said to be *left invariant*. Such connections have the property that the Lie bracket, see equation (2.2), and the covariant derivative, see equation (2.11), of two left invariant vector fields are still left invariant. This also applies to the symmetric product. Specifically, it holds

$$\langle g \cdot \xi : g \cdot \eta \rangle = g \cdot \langle \xi : \eta \rangle\,,$$

where the symmetric product between two vectors on $\mathfrak{g}$ is defined as:

$$\langle \xi : \eta \rangle \triangleq -\mathbb{I}^{-1}\big(\operatorname{ad}^*_{\xi}\mathbb{I}\eta + \operatorname{ad}^*_{\eta}\mathbb{I}\xi\big). \tag{2.13}$$

For example, on $\mathfrak{so}(3) \approx \mathbb{R}^3$ with the inertia tensor $\mathbb{J}$ and with the equality $\operatorname{ad}^*_{\xi} = -\hat{\xi}$, we compute $\langle \xi : \eta \rangle = \mathbb{J}^{-1}\big(\xi \times \mathbb{J}\eta + \eta \times \mathbb{J}\xi\big)$.

# Chapter 3

# Models of Mechanical Control Systems

In this chapter we introduce models for various classes of mechanical systems. We focus on writing the equations of motion for a mechanical system in a coordinate free fashion. The key idea is to regard the kinetic energy of the system as a Riemannian metric and to write the Euler-Lagrange equations in terms of the associated Riemannian connection. A similar approach is taken in the dissertation of A. D. Lewis [64]. For an introduction to geometric mechanics we refer to [72] and [6], and for a modern introduction to robotics we refer to [76].

The chapter is organized as follows. In Section 3.1 we define a mechanical control system. Section 3.2 treats the additional structure of mechanical systems on Lie groups. Finally in Section 3.3 and 3.4 we present mechanical systems subject to constraints and impacts. Most of the content in this chapter is taken from the literature. For example, the treatment on constrained mechanical systems follow the approach advocated in [9, 66]. The treatment on hybrid mechanical systems in Section 3.4 is joint work with Miloš Žefran; see [29].

## 3.1 Simple Mechanical Control Systems

A *simple mechanical control system* is defined by the following objects:

(i) an $n$-dimensional configuration manifold $Q$, with local coordinates $q = \{q^1, \ldots, q^n\}$,

(ii) a Riemannian metric $M_q : TQ \times TQ \to \mathbb{R}$ on $Q$ (the kinetic energy), alternatively denoted by $\langle\!\langle \cdot, \cdot \rangle\!\rangle$,

(iii) a function $V$ on $Q$ describing the potential energy, and

(iv) an $m$-dimensional codistribution $\mathcal{F} = \text{span}\{F^1, \ldots, F^m\}$ defining the input forces.

The word "simple" refers to the Lagrangian being equal to kinetic minus potential energy and comes originally from the definition in Smale [89]. Let $q(t) \in Q$ be the configuration of the system and $\dot{q}(t) \in T_qQ$ its velocity. In a system of local coordinates, the Lagrangian is written as

$$L(q, \dot{q}) = \frac{1}{2}(M_q)_{ij}\, \dot{q}^i \dot{q}^j - V(q).$$

(Note that the summation convention is assumed throughout the dissertation.) We let $\Gamma^i_{jk}(q)$ denote the Christoffel symbols of the Levi-Civita connection associated with $M_q$, see equation (2.8), and we let $M^{ij}$ denote the inverse matrix of $M_{ij}$. Then the forced

Euler-Lagrange equations are

$$\ddot{q}^i + \Gamma^i_{jk}\dot{q}^j\dot{q}^k = M^{ij}\left(-\frac{\partial V}{\partial q^j} + F_j\right), \qquad i = 1, \ldots, n, \tag{3.1}$$

where $F_j$ is the $j$th component of the resultant force $F(q,t) = \sum_1^m F^k(q)u_k(t)$ and where the controls $\{u_1(t), \ldots, u_m(t), t \in \mathbb{R}^+\}$ belong to the space of piecewise smooth functions $\mathcal{U}^m$. Note that the Euler-Lagrange equations are coordinate independent (intrinsic), in the sense that they are satisfied in every system of local coordinates.

Using the formalism introduced in the previous chapter, these equations can be written in a coordinate independent form. We let $\nabla$ denote the Riemannian connection of the metric $M_q$ on $Q$, and with a slight abuse of notation, we let $M_q$ denote the map $M_q : TQ \to T^*Q$ defined by $M_q(X,Y) = \langle M_q X, Y\rangle$. The forced Euler-Lagrange equations in intrinsic form are then

$$\nabla_{\dot{q}}\dot{q} \;=\; M_q^{-1}\Big(-\mathrm{d}V(q) + \sum_{k=1}^{m} F^k(q)u_k\Big), \tag{3.2}$$

where $\mathrm{d}V(q)$ is the differential of the potential function $V$.

One distinguishing feature of Lagrangian control systems is the number of input forces. Accordingly we have the two definitions:

(i) A mechanical control system is said to be *fully actuated* if for all $q \in Q$, the family of covectors $\{F^1(q), \ldots, F^m(q)\}$ spans the whole cotangent space $T_q^*Q$. In other words, a system is fully actuated if there exists an independent input force corresponding to each degree of freedom.

(ii) A mechanical control system is said to be *underactuated* if the number of available input forces $m$ is less than the degrees of freedom $n$.

*Remark 3.1 (Time scaling).* Consider a mechanical system without potential energy $V$, and for $\lambda > 0$ define $\tau = \lambda t$. The following property holds: if $(q(t), \dot{q}(t))$ is a solution for $t \in [0,1]$ to the forced system (3.2) with external forcing $u_i(t)$, then $(q(\tau/\lambda), \dot{q}(\tau/\lambda)/\lambda)$ is a solution for $\tau \in [0,\lambda]$ with external forcing $u_i(\tau/\lambda)/\lambda^2$. In other words, if we find an input $u(t)$ that achieves a desired motion in time 1, then $u(t/\lambda)/\lambda^2$ achieves the same motion in time $\lambda$.

### 3.1.1 Robotic Manipulators

In this section we relate the abstract definition above to the classical coordinate-based description of robotic manipulators. As Figure 3.1 illustrates, the configuration of a robotic manipulator can be described by $n$ generalized joint angles $\theta = (\theta^1, \ldots, \theta^n) \in \mathbb{S}^n$, where $\mathbb{S}$ is the torus. The kinetic energy is described by the inertia matrix $M(\theta)$ and the joint forces are $\mathcal{F} = \{\mathrm{d}\theta^1, \ldots, \mathrm{d}\theta^n\}$. The equations of motion eqrefeq:mechsys:coords are then written in vector form as

$$M(\theta)\ddot{\theta} + C(\theta,\dot{\theta})\dot{\theta} = F, \tag{3.3}$$

where both left and right hand side have been pre-multiplied by the inertia matrix $M(\theta)$. $C(\theta,\dot{\theta})$ is the *Coriolis matrix* and can be related to the inertia matrix $M$ and its Christoffel symbols by:

$$C_{ij}(\theta,\dot{\theta}) = \sum_{k=1}^{n} M_{i\ell}\Gamma^{\ell}_{jk}\dot{\theta}^k = \frac{1}{2}\sum_{k=1}^{n}\left(\frac{\partial M_{ij}}{\partial\theta^k} + \frac{\partial M_{ik}}{\partial\theta^j} - \frac{\partial M_{kj}}{\partial\theta^i}\right)\dot{\theta}^k. \tag{3.4}$$

The fundamental difference between equation (3.2) and equation (3.3) is that the latter is a coordinate-dependent representation of the Euler-Lagrange differential equation, while the first one is coordinate-free.

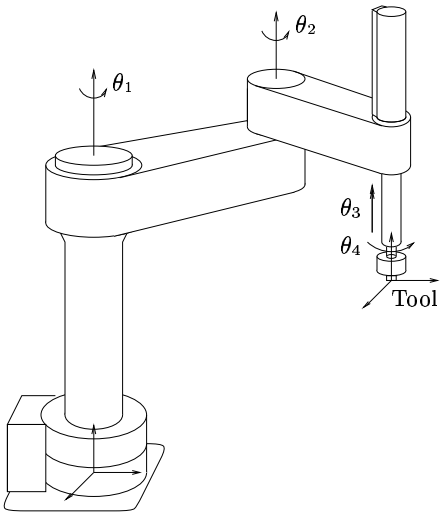


Figure 3.1: A Robotic Manipulator

### 3.1.2 A Pointing Device on the Two Sphere

An alternative way of controlling a manipulator is to focus on the motion of the end effector, for example the Tool in Figure 3.1. In the robotics literature this is referred to as "workspace control." The key idea is to rewrite the equations of motion and to specify the control goal in terms of the end-effector variables, as opposed to the joint variables. As an example, we study here a system whose configuration space is the two sphere $\mathbb{S}^2$: a fully actuated spherical pendulum in absence of gravity. This example is motivated by applications to workspace control of a robot manipulator such as a pan tilt unit and the so called "spin axis stabilization" problem for a satellite.

Let $q \in \mathbb{S}^2$ be the configuration and consider a latitude/longitude parametrization:

$$q = \begin{bmatrix} \cos(\phi)\cos(\theta) \\ \cos(\phi)\sin(\theta) \\ \sin(\phi), \end{bmatrix}$$

where $(\phi, \theta) \in [0, 2\pi]^2$. This parametrization has a singularity at $\cos(\phi) = 0$. The kinetic energy of the system is $\frac{1}{2}\|\dot{q}\|^2 = \frac{1}{2}(\dot{\phi}^2 + \cos(\phi)\dot{\theta}^2)$. The unforced Euler-Lagrange equations for the spherical pendulum are written in coordinates as

$$\begin{aligned} \ddot{\phi} + \cos(\phi)\sin(\phi)\dot{\theta}^2 &= 0, \\ \ddot{\theta} - 2\tan(\phi)\dot{\phi}\dot{\theta} &= 0, \end{aligned} \tag{3.5}$$

or coordinate-free as

$$\nabla_{\dot{q}}\dot{q} = 0,$$

where the Riemannian connection $\nabla$ on $\mathbb{S}^2$ is induced by the natural metric on $\mathbb{R}^3$. One additional way of writing the equations of motion involves parametrizing $\mathbb{S}^2$ by means of $q \in \mathbb{R}^3$. There is of course a redundancy, but the advantage is the simple expression the equation of motion have:

$$\ddot{q} + (\dot{q}^T \dot{q})q = 0. \tag{3.6}$$

By workspace control, we mean a strategy that specifies the desired task in terms of the end-effector $q \in \mathbb{S}^2 \subset \mathbb{R}^3$ as opposed to some joint space coordinates as for example $(\phi, \theta)$. Accordingly, the focus is the formulation in equation (3.6) and not on equation (3.5).

## 3.2 Vehicles as Mechanical Systems on Lie Groups

A large class of vehicle models fit our definition of simple mechanical control systems. Since their configuration manifold is also a group, the equations of motion of these systems enjoy additional structure and properties. In this section we describe these properties and illustrate them via numerous examples.

A *simple mechanical control system on a Lie group* is described by the following objects:

(i) an $n$-dimensional matrix Lie group $G$, defining the configuration space,

(ii) an inertia tensor $\mathbb{I} : \mathfrak{g} \to \mathfrak{g}^*$ on the Lie algebra $\mathfrak{g}$, defining the kinetic energy, and

(iii) a set of input covectors $\mathcal{F} = \{f_1, \ldots, f_m\} \subset \mathfrak{g}^*$, defining the body-fixed forces. To simplify notation, we denote the covectors $f_i$ with subscripts instead of superscripts.

Potential energy effects are neglected in order to preserve full symmetry of the system.

As described in Section 2.4.3, the inertia tensor $\mathbb{I}$ defines via left translation a Riemannian metric (representing the kinetic energy on $G$). In other words, let $g : [0, 1] \to G$ be a smooth curve in $G$, and define the *velocity in body frame* as the vector in $\mathfrak{g}$ defined by

$$\xi(t) = T_{g(t)} L_{g^{-1}(t)} \, \dot{g}(t).$$

On a matrix Lie group this corresponds to the matrix equation $\xi = g^{-1}\dot{g}$. Then the kinetic energy associated with the curve is $KE = \frac{1}{2} \langle \mathbb{I}\xi, \xi \rangle$. We refer to the treatment in [76] for the standard notion of "body frame."

Let $g \in G$ be the configuration of the mechanical system and let $\xi \in \mathfrak{g}$ be its velocity in body frame. The kinematic and dynamic equations of motion for the system with Lagrangian equal to the kinetic energy are given by

$$\dot{g} = g \cdot \xi, \tag{3.7}$$

$$\mathbb{I}\dot{\xi} = \mathrm{ad}^*_\xi \, \mathbb{I}\xi + \sum_{i=1}^{m} f_i u_i(t), \tag{3.8}$$

where the controls $\{u_1(t), \ldots, u_m(t), t \in \mathbb{R}^+\}$ belong to the space of piecewise smooth functions $\mathcal{U}^m$, and $\sum_1^m f_i u_i(t)$ is the resultant force acting on the mechanical system. In geometric mechanics, the dynamic equation (3.8) is called the Euler-Poincaré equation; in robotics, the kinematic equation (3.7) is usually expressed in some choice of coordinate system, for example, Euler angles for SO(3).

For later reference it is useful to rewrite the dynamic equation (3.8) in terms of the

inverse inertia $\mathbb{I}^{-1}$. If we define $b_i \triangleq \mathbb{I}^{-1} f_i$, we have

$$\dot{\xi} = \mathbb{I}^{-1} \mathrm{ad}^*_\xi \mathbb{I}\xi + \sum_{i=1}^{m} b_i u_i(t).$$

*Remark 3.2 (Relative equilibria).* For any vector $\eta$ with the property that $\mathrm{ad}^*_\eta \mathbb{I}\eta = 0$, the curve $t \in \mathbb{R} \mapsto (\exp(t\eta), \eta)$ is a solution to the system (3.7)–(3.8) with no inputs. These curves are studied in mechanics [72] under the name of *relative equilibria* and describe motion that corresponds to constant body-fixed velocity for the uncontrolled system.

We conclude this section with a few examples of mechanical control systems in Lie groups. We present models for planar bodies, satellites and underwater vehicles. They will be referred to later, as we study controllability and design control laws. To simplify notation, we let $\{\mathsf{e}_1, \ldots, \mathsf{e}_n\}$ denote the standard basis on $\mathbb{R}^n$; for example, for $n = 3$ we set $\mathsf{e}_1 = (1,0,0)$, $\mathsf{e}_2 = (0,1,0)$ and $\mathsf{e}_3 = (0,0,1)$.

### 3.2.1 A Planar Rigid Body

Let $g = (\theta, x, y) \in \mathrm{SE}(2)$ denote the configuration of the planar body and $\xi = (\omega, v_1, v_2)$ its body-fixed velocity. The kinetic energy is $KE = \frac{1}{2}J\omega^2 + \frac{1}{2}m(v_1^2 + v_2^2)$ where $J$ is the moment of inertia and $m$ the mass of the body. On $\mathfrak{se}(2)$ the adjoint operator is computed as

$$\mathrm{ad}_{(\omega, v_1, v_2)} = \begin{bmatrix} 0 & 0 & 0 \\ v_2 & 0 & -\omega \\ -v_1 & \omega & 0 \end{bmatrix}.$$

The two control inputs consist of forces applied at a distance $h$ from the center of mass, see Figure 3.2. After inverting $\mathbb{I} = \mathrm{diag}\{J, m, m\}$, we have $b_1 = \frac{1}{m}\mathsf{e}_2$ and $b_2 = \frac{-h}{J}\mathsf{e}_1 + \frac{1}{m}\mathsf{e}_3$. In coordinates the equations of motion (3.7)–(3.8) read

$$\begin{aligned} \dot{\theta} &= \omega & J\dot{\omega} &= -hu_2(t) \\ \dot{x} &= \cos(\theta)v_1 - \sin(\theta)v_2 & m\dot{v}_1 &= m\omega v_2 + u_1(t) \\ \dot{y} &= \sin(\theta)v_1 + \cos(\theta)v_2 & m\dot{v}_2 &= -m\omega v_1 + u_2(t). \end{aligned}$$

These equations provide a model for planar vehicles, for example, a hovercraft that glides on the surface of a body of water with negligible friction.

### 3.2.2 Satellites with Thrusters or Rotors on the Rotation Group

The configuration of the satellite (rigid body) is the rotation matrix $R$ representing the position of a frame fixed with the rigid body with respect to an inertially fixed frame. The kinematic equation describing the evolution of $R(t)$ is

$$\dot{R} = R\widehat{\Omega},$$

where $\Omega \in \mathbb{R}^3$ is the body angular velocity expressed in the body frame, and where $\widehat{\Omega}$ belongs to the space of skew symmetric matrices $\mathfrak{so}(3) \approx \mathbb{R}^3$, see Section 2.2. The kinetic energy of the rigid body is $\frac{1}{2}\Omega^T \mathbb{J}\Omega$, where the inertia matrix $\mathbb{J} = \mathrm{diag}\{J_1, J_2, J_3\}$ is symmetric and positive definite. The adjoint operator is $\mathrm{ad}_\Omega = \widehat{\Omega}$. The Euler equations describing the time

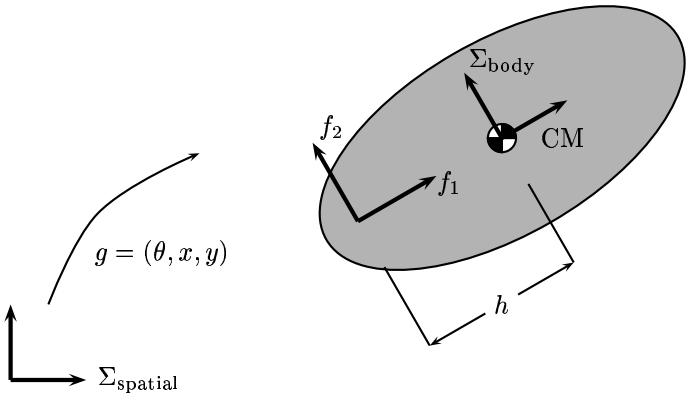


Figure 3.2: Rigid body in SE(2) with two forces $f_1$ and $f_2$ applied at a point a distance $h$ from the center of mass CM. $\Sigma_{\text{spatial}}$ denotes an inertial reference system, $\Sigma_{\text{body}}$ denotes a reference frame fixed with the body. $g = (\theta, x, y)$ denotes the position of the body.

evolution of $\Omega$ are

$$\mathbb{J}\dot{\Omega} = \mathbb{J}\Omega \times \Omega + f, \tag{3.9}$$

where $f \in \left(\mathbb{R}^3\right)^*$ is the resultant torque acting on the body. For example, assuming we have two thrusters aligned with the first two principal axes, the equations of motion are

$$\begin{aligned} \dot{R} &= R\widehat{\Omega}, \\ \mathbb{J}\dot{\Omega} &= \mathbb{J}\Omega \times \Omega \quad + \mathsf{e}_1 u_1(t) + \mathsf{e}_2 u_2(t). \end{aligned} \tag{3.10}$$

Accordingly, $b_1 = \frac{1}{J_1}\mathsf{e}_1$ and $b_2 = \frac{1}{J_2}\mathsf{e}_2$.

Satellites can alternatively be equipped with internal rotors (momentum wheels). Consider the case in which there are two rotors aligned with two principal axes of the satellite. The configuration of the satellite plus rotor system is described by $R \in \mathrm{SO}(3)$ and $(\theta_1, \theta_2) \in \mathbb{R}^2$ (describing the angular position of the wheels). Let $\Omega_{\text{rot}} = (\dot{\theta}_1, \dot{\theta}_2, 0)$ denote the angular velocities of the rotors and $\Omega$ the angular velocities of the carrier. The kinetic energy is

$$KE = \frac{1}{2}\Omega^T(\mathbb{J}_{\text{lock}} - \mathbb{J}_{\text{rot}})\Omega + \frac{1}{2}(\Omega + \Omega_{\text{rot}})^T\mathbb{J}_{\text{rot}}(\Omega + \Omega_{\text{rot}}),$$

where $\mathbb{J}_{\text{lock}} = \operatorname{diag}\{J_1, J_2, J_3\}$ is the inertia of the satellite-rotors system with the rotors locked, while $\mathbb{J}_{\text{rot}} = \operatorname{diag}(J_{\text{rot}1}, J_{\text{rot}2}, 0)$ is the inertia of the rotors about their spin axes. From the kinetic energy we compute the inertia matrix as

$$\mathbb{J}_{\text{sat-rot}} = \begin{bmatrix} \mathbb{J}_{\text{lock}} & \mathbb{J}_{\text{rot}} \\ \mathbb{J}_{\text{rot}} & \mathbb{J}_{\text{rot}} \end{bmatrix}.$$

Also, the adjoint operator satisfies $\operatorname{ad}_{(\Omega,\Omega_{\text{rot}})}(v, w) = (\Omega \times v, 0)$. The dynamic equations are

$$\begin{bmatrix} \mathbb{J}_{\text{lock}} & \mathbb{J}_{\text{rot}} \\ \mathbb{J}_{\text{rot}} & \mathbb{J}_{\text{rot}} \end{bmatrix} \begin{bmatrix} \dot{\Omega} \\ \dot{\Omega}_{\text{rot}} \end{bmatrix} = \begin{bmatrix} (\mathbb{J}_{\text{lock}}\Omega + \mathbb{J}_{\text{rot}}\Omega_{\text{rot}}) \times \Omega \\ 0 \end{bmatrix} + \begin{bmatrix} 0 \\ \mathsf{e}_1 u_1(t) + \mathsf{e}_2 u_2(t) \end{bmatrix},$$

and, by inverting the inertia matrix, the input vectors are

$$b_1 = \frac{1}{J_{\text{rot}1} - J_1}\mathsf{e}_1 + \frac{J_1}{J_{\text{rot}1}(J_{\text{rot}1} - J_1)}\mathsf{e}_4,$$
$$b_2 = \frac{1}{J_{\text{rot}2} - J_2}\mathsf{e}_2 + \frac{J_2}{J_{\text{rot}2}(J_{\text{rot}2} - J_2)}\mathsf{e}_5.$$

### 3.2.3 A Six DOF Underwater Vehicle in Ideal Fluid

This example is motivated by recent interest in the area of underwater vehicle dynamics, see [59], [63] and [40]. The configuration of an underwater vehicle is described by the position $p$ and attitude $R$ of a body frame with respect to an inertial frame. Therefore the configuration manifold is the group of rigid displacement SE(3). As described in Section 2.2, we introduce the so-called homogeneous coordinates:

$$g = \begin{bmatrix} R & p \\ 0_{1\times 3} & 1 \end{bmatrix} \quad \text{and} \quad \xi = \begin{bmatrix} \widehat{\Omega} & V \\ 0_{1\times 3} & 0 \end{bmatrix}.$$

Accordingly, the standard kinematic equations are

$$\begin{aligned} \dot{R} &= R\widehat{\Omega}, \\ \dot{p} &= RV, \end{aligned} \tag{3.11}$$

where $\xi = (\widehat{\Omega}, V) \in \mathfrak{se}(3) = \mathfrak{so}(3) \times \mathbb{R}^3$ is the body velocity expressed in the body frame.

The motion of a rigid body in incompressible, irrotational and inviscid fluid is Hamiltonian with an inertia tensor which includes added masses and inertias, see [57], [59] or the original work of Kirchhoff. If the underwater vehicle is an ellipsoidal body with uniformly distributed mass, the kinetic energy of the body-fluid system is $\frac{1}{2}\Omega^T\mathbb{J}\Omega + \frac{1}{2}V^T\mathbb{M}V \equiv \frac{1}{2}\xi^T\mathbb{I}\xi$, the mass and inertia matrices of the body-fluid system are $\mathbb{M} = \text{diag}\{m_1, m_2, m_3\}$ and $\mathbb{J} = \text{diag}\{J_1, J_2, J_3\}$. The Kirchhoff equations describing the time evolution of the body velocity $\xi$ are

$$\begin{aligned} \mathbb{J}\dot{\Omega} &= \mathbb{J}\Omega \times \Omega + \mathbb{M}V \times V + f_\Omega, \\ \mathbb{M}\dot{V} &= \mathbb{M}V \times \Omega + f_V, \end{aligned} \tag{3.12}$$

where $f = [f_\Omega \ f_V] \in \mathfrak{se}(3)^*$ is the resultant generalized force acting on the body. For example, we can assume there are three body-fixed forces applied at a point a distance $h$ from the center of mass, as depicted in Figure 3.3. The corresponding input vectors are

$$b_1 = \frac{1}{m_1}\mathsf{e}_4, \qquad b_2 = -\frac{h}{J_3}\mathsf{e}_3 + \frac{1}{m_2}\mathsf{e}_5, \qquad \text{and} \qquad b_3 = \frac{h}{J_2}\mathsf{e}_2 + \frac{1}{m_3}\mathsf{e}_6.$$

## 3.3 Locomotion Devices as Constrained Mechanical Systems

In this section we model mechanical devices subject to constraints. Our interest is motivated by locomotion devices that interact with the surrounding environment via holonomic and nonholonomic constraints. Since the underlying Lagrange-d'Alembert principle applies to both type of constraints, this section presents a unified treatment.

The most common constraints on mechanical systems are of the following two types:

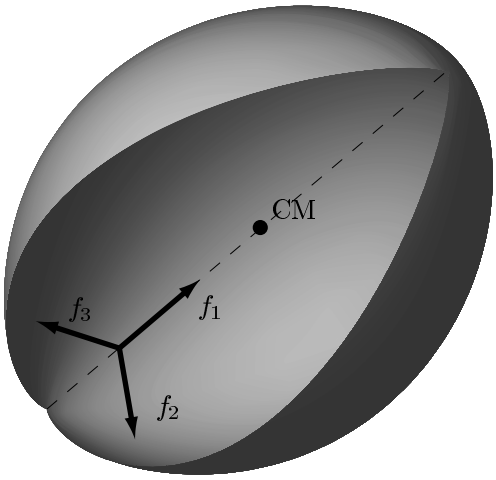


Figure 3.3: Rigid body in SE(3) with three forces applied at a point a distance $h$ from the center of mass.

(i) Clamping a sliding body to a surface is an example of a constraint on the configuration variables $q$. Such constraints are called *holonomic*. Formally, a holonomic constraint is described by the equation $\varphi(q) = 0$ where the map $\varphi : Q \to \mathbb{R}^{n-p}$ is smooth. We assume that 0 is a regular value of $\varphi$ so that $R = \varphi^{-1}(0)$ defines a submanifold $R \subset Q$. The constraint on $q(t)$ induces constraint on $\dot{q}(t)$ via

$$0 = \frac{d}{dt}\varphi^i(q(t)) = \mathrm{d}\varphi^i \cdot \dot{q}.$$

This implies that at each point $q \in R$, the set of feasible velocities $\mathcal{D}(q)$ is the annihilator of $\{\mathrm{d}\varphi^1(q), \ldots, \mathrm{d}\varphi^{n-p}(q)\}$.

In this thesis we are interested in holonomic constraints which are defined at each point. Heuristically, we model the possibility of clamping a sliding object at any point of its path over a smooth surface: at each point $q_0$, the constraint is $\varphi(q) = \varphi(q_0)$. In this case, we assume that the set of regular values of $\varphi$ contains an open non-empty neighborhood of $\varphi(q_0) \in \mathbb{R}^{n-p}$. Correspondingly, at each configuration $q$ in a neighborhood $W \subset Q$ of $q_0$ the constraint distribution $\mathcal{D}(q)$ is defined as the annihilator of $\{\mathrm{d}\varphi^1(q), \ldots, \mathrm{d}\varphi^{n-p}(q)\}$.

(ii) Non-integrable constraints on the evolution of the velocity variable $\dot{q}$ are called *nonholonomic*. Rolling without sliding is one such case. We describe a nonholonomic constraint by a $p$-dimensional *constraint distribution* $\mathcal{D}$. At each point $q \in Q$, $\mathcal{D}(q)$ describes the set of feasible velocities.

Both holonomic and nonholonomic constraints can therefore be written in the form $\dot{q} \in \mathcal{D}(q)$, for an appropriate distribution $\mathcal{D}(q)$. A mechanical control system together with a constrained distribution is said to be a *constrained mechanical control system*. In what follows we denote one such system as

$$\Sigma_{\mathrm{CMCS}} = \{Q, M_q, \mathcal{F}, \mathcal{D}\}. \tag{3.13}$$

Let $\mathcal{D}^\perp$ denote the orthogonal complement to $\mathcal{D}$ with respect to the metric $M_q$. Accordingly, let $P : TQ \to \mathcal{D}$ and $P^\perp : TQ \to \mathcal{D}$ denote the orthogonal projections onto $\mathcal{D}$ and its complement, $P^\perp = I - P$. The (Lagrange-d'Alembert) constrained variational principle leads to the equations of motion

$$\nabla_{\dot{q}}\dot{q} = \lambda(t) + (M_q^{-1}F^k)u_k, \tag{3.14}$$

$$P^\perp(\dot{q}) = 0, \tag{3.15}$$

where $\lambda(t) \in \mathcal{D}^\perp$ is the Lagrange multiplier enforcing the constraint.

### 3.3.1 Control Systems Described by Affine Connections

In this section we provide a unified treatment of both constrained and unconstrained mechanical control systems. The key idea is to allow for general affine connections and not only for Riemannian connections. The treatment in this section follows the work of Lewis and Murray [66, 68], and is similar in spirit to the work of Bloch and Crouch [9].

Given a simple mechanical control system $\{Q, M_q, V, \mathcal{F}\}$, let the input vector fields be $Y_k = M_q^{-1}\, F^k$. Then the Euler-Lagrange equations (3.2) can be written as

$$\nabla_{\dot{q}}\dot{q} = \sum_{k=1}^{m} Y_k u_k, \tag{3.16}$$

where for simplicity we assume zero potential energy. When a constraint is present, the Lagrange-d'Alembert equations can be simplified by eliminating the multiplier. We formalize this concept following the treatment in [66]:

**Lemma 3.3.** *Given a constrained mechanical system $\{Q, M_q, \mathcal{F}, \mathcal{D}\}$, let $P$ be the orthogonal projection onto the constraint distribution and let the input vector fields be $Y_k = P(M_q^{-1}F^k)$. The equations of motion* (3.14)–(3.15) *can be written as*

$$\widetilde{\nabla}_{\dot{q}}\dot{q} = \sum_{k=1}^{m} Y_k u_k, \tag{3.17}$$

*or equivalently in coordinates as*

$$\ddot{q}^i + \widetilde{\Gamma}^i_{jk}\dot{q}^j\dot{q}^k = \sum_{k=1}^{m}(Y_k u_k)^i,$$

*where the affine connection $\widetilde{\nabla}$ and its Christoffel symbols $\widetilde{\Gamma}^i_{jk}$ are defined according to*

$$\widetilde{\nabla}_X Y = \nabla_X Y + \left(\nabla_X P^\perp\right)(Y), \tag{3.18}$$

*for any pair $X, Y$ of vector fields on $Q$, and*

$$\widetilde{\Gamma}^i_{jk} = \Gamma^i_{jk} + \frac{\partial (P^\perp)^i_j}{\partial q^k} + \Gamma^{km}_i (P^\perp)^m_j - \Gamma^{kj}_m (P^\perp)^i_m.$$

*Proof.* First, start by noting that $\tilde{\nabla}$, as defined in equation (3.18), is in fact an affine connection. The proof is a direct verification of the three conditions in Definition 2.1 and is omitted.

By projecting equation (3.14) onto $\mathcal{D}^{\perp}$ and by covariantly differentiating equation (3.15) we obtain

$$P^{\perp}(\nabla_{\dot{q}}\dot{q}) = \lambda(t) + P^{\perp}(Y_k u_k),$$
$$P^{\perp}(\nabla_{\dot{q}}\dot{q}) = -\left(\nabla_{\dot{q}} P^{\perp}\right)(\dot{q}).$$

Hence it holds that

$$\lambda(t) = -\left(\nabla_{\dot{q}} P^{\perp}\right)(\dot{q}) - P^{\perp}(Y_k u_k),$$

and equation (3.14) becomes

$$\nabla_{\dot{q}}\dot{q} + \left(\nabla_{\dot{q}} P^{\perp}\right)(\dot{q}) = P(Y_k u_k).$$

According to equation (3.18), we therefore have $\widetilde{\nabla}_{\dot{q}}\dot{q} = P(Y_k u_k)$. This concludes the proof. □

We summarize the result in this section as follows. In both constrained and unconstrained regimes, let $\mathcal{Y} = \text{span}\{Y_1, \ldots, Y_m\}$ denote the input distribution. In both cases the equations of motion are

$$\nabla_{\dot{q}}\dot{q} = \sum_{k=1}^{m} Y_k u_k, \tag{3.19}$$

and are determined by the three objects: the configuration manifold $Q$, the affine connection $\nabla$, and the input distribution $\mathcal{Y}$. We call one such system a *control system on a manifold with an affine connection.*

*Remark 3.4.* If the constraint is holonomic, we can write Euler-Lagrange equations on a reduced space $R$, instead of invoking the Lagrange-d'Alembert principle on the full space [72]. Let $r \in R$, let $M_r'$ be the restriction of the metric $M_q$ on $T_r R \subset T_r Q$, and let $\nabla^R$ denote the corresponding Riemannian connection. The unforced equations for the constrained system can be then written as

$$\nabla^R_{\dot{r}}\dot{r} = 0.$$

It can be shown [66] that on the equations of motion obtained on reduced space via the connection $\nabla^R$ agree with the ones provided by the constraint connection $\widetilde{\nabla}$.

## 3.4 Locomotion Devices as Mechanical Control Systems with Impacts

In this section we model mechanical devices that locomote via impacts with the surrounding environment. We start by presenting a geometric treatment of the classical model of impacts, see for example in [19]. Loosely speaking, an impact results when an impulsive force that enforces a constraint acts on the system. Accordingly, an impact in general causes a switch in the equations of motions and a jump in the system's velocity.

Let $\{Q, M_q, \mathcal{F}\}$ be a mechanical control system, let $\mathcal{D}^-$ and $\mathcal{D}^+$ be two constraint distributions, and let $(\nabla^-, \mathcal{Y}^-)$ and $(\nabla^+, \mathcal{Y}^+)$ be the corresponding affine connections and input

distributions. We say that the mechanical systems undergoes an *impact* at time $t$ if the following events occur:

(i) the dynamic equations switch from $(\nabla^-, \mathcal{Y}^-)$ to $(\nabla^+, \mathcal{Y}^+)$,

(ii) the state $(q, \dot{q})$ undergoes a discontinuous change in velocity described by a tensor field $J_q : T_qQ \to T_qQ$. In other words, if we let $q(t^-)$ and $q(t^+)$ refer to the limiting processes $\lim_{s->t^-} q(s)$ and $\lim_{s->t^+} q(s)$, we have:

$$q(t^+) = q(t^-),$$
$$\dot{q}(t^+) = J_q\left(\dot{q}(t^-)\right).$$

This definition of impact describes both holonomic and nonholonomic impacts, since the nature of the constraint distribution $\mathcal{D}^+$ is unspecified. Additionally, this definition embeds the classic notions of purely plastic and elastic impacts as special cases. For example, if a particle hits a surface with nonzero velocity, then the linear operator $J_q$ annihilates the normal component of the velocity in the plastic impact case and reverses it in the elastic impact case (a coefficient of restitution $0 < e < 1$ can be included). Formally, we define:

**Plastic impact:** The two constraint distributions $\mathcal{D}^-$ and $\mathcal{D}^+$ are distinct (for example $\mathcal{D}^- = TQ$ and $\mathcal{D}^+ = TR$ is the tangent space of a submanifold $R \subset Q$). The operator $J_q = P_{\mathcal{D}^+}$ is the orthogonal projection onto $\mathcal{D}^+$.

**Elastic impact:** The equations of motion do not change, as connection and input distributions are the same before and after the impact. There exists a submanifold $R$ such that

$$J_q = P_{TR} + (-e)P^{\perp}_{\mathcal{TR}},$$

where $P_{TR}$ is the orthogonal projection onto the tangent space to $R$ and where $0 < e < 1$ is the coefficient of restitution.

Notice that these definitions are in agreement with the classic simplified models of elastic and plastic impacts, see [19].

### 3.4.1 Hybrid Mechanical Control Systems

In this section we expand on the notion of control systems on manifolds with an affine connection and we construct a special class of hybrid systems. In this construction we adapt some ideas from the notion of "controlled general hybrid dynamical system" as described in [14].

The fundamental discrete phenomena we want to model are controlled jumps between distinct sets of constraints. Our setting is therefore a mechanical control system $(Q, M_q, \mathcal{F})$ with a given set of $\mathcal{D}_i$, where $i$ belongs to an index set $I$. For each constraint $\mathcal{D}_i$, we consider the constrained mechanical control system $\Sigma_i = \{Q, M_q, \mathcal{F}, \mathcal{D}_i\}$, with associated affine connection $\nabla_i$ and input distribution $\mathcal{Y}_i$.

Formally we define the *hybrid mechanical control system* as

$$\Sigma_{\text{HMCS}} = \{I, Q, \Sigma_Q, \mathbf{V}, \Delta\}, \tag{3.20}$$

where:

(i) $I$ is the *index set* of constraints,

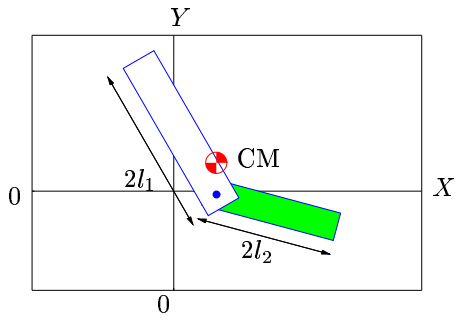


Figure 3.4: Sliding and clamping device with two legs. Leg #2 is allowed to fully clamp on the floor reducing the system's degrees of freedom from 4 to 1 (only the joint angle). Alternatively we pin only its center and allow two angles to change.

(ii) $Q$ is the $n$-dimensional *configuration manifold*,

(iii) $\Sigma_Q = \{\Sigma_i = \{Q, M_q, \mathcal{F}, \mathcal{D}_i\}\}_{i\in I}$ is the collection of constrained mechanical control systems on $Q$,

(iv) $\mathbf{V} = \{V_{ij}\}_{i,j\in I}$ is the set of discrete controls. We require $V_{ij} \neq \emptyset$.

(v) $\Delta = \{\delta_{ij} | i, j \in I\}$ is the set of *jump transition maps*, where $\delta_{ij} : V_{ij} \times \cup_{q\in Q}\mathcal{D}_i(q) \to \cup_{q\in Q}\mathcal{D}_j(q)$, and $\delta_{ij}(v)(q, \dot{q}) = (q, J_{ij}(q, v) \cdot \dot{q})$. The operator $J_{ij}(q, v)$ is linear for each $q \in Q$ and each $v \in V_{ij}$.

The evolution of a hybrid mechanical control system can be described as follows. The system starts in the state $((q, \dot{q}), i) \in TQ \times I$ and it evolves according to the dynamics given by $\nabla_i$ and the chosen set of continuous controls. At any point, we can choose to jump to any other discrete state through impact. This is modeled by the discrete control $V_{ij}$. Additionally we allow for different possible impacts to choose from: for example, we can choose to undergo an elastic impact and thus remain in the same discrete state. This is modeled by the jump transition map $\delta_{ij}$.

*Remark 3.5 (Autonomous jumps).* It would be possible to augment the model with autonomous jumps by adding a collection $\mathbf{A} = \{A_i\}_{i\in I}$ of *autonomous jump set* and a collection $\delta_A = \{\delta_{A_i}\}_{i\in I}$ of *autonomous jump transition maps* as described in [14]. However, in this dissertation we concentrate on the controlled jumps and do not pursue this matter any further.

### 3.4.2 A Sliding and Clamping Device

We study a simple example: two homogeneous bars of unit density and lengths $(2l_1, 2l_2)$, connected by a joint. See Figure 3.4 for a representation where CM is the center of mass of the two body system. We denote with $(\theta_j, x_j, y_j)$ the center of mass of the $j$th joint and with $(x_{\text{CM}}, y_{\text{CM}})$ the position of CM. We assume that we can actuate the joint and that we can at any point in time and space enforce one of the following two constraints. First, we can instantaneously clamp position and orientation the second bar to the ground, resulting in fixing the position $\varphi_1(q) = (\theta_2, x_2, y_2)$ of the second bar. Alternatively, we can clamp only the center of mass of the second bar $\varphi_2(q) = (x_2, y_2)$.

### Constrained Mechanical Control Systems

The mechanical control system is defined according to the treatment in the previous sections by the following objects: The configuration manifold of the two body system is $Q = \mathbb{T}^2 \times \mathbb{R}^2$ and we let $q = (\theta_1, \theta_2, x_{\text{CM}}, y_{\text{CM}})$ be the configuration. The inertia matrix is

$$M_q = \frac{1}{6(l_1^2 + l_2^2)} \begin{bmatrix} 5l_1^4 + 5l_1^2 l_2^2 + 12 l_1^4 l_2^2 & 12 l_1^3 l_2^3 \cos(\theta_1 - \theta_2) & 0 & 0 \\ 12 l_1^3 l_2^3 \cos(\theta_1 - \theta_2) & 5l_1^2 l_2^2 + 5l_2^4 + 12 l_1^2 l_2^4 & 0 & 0 \\ 0 & 0 & 12\left(l_1^2 + l_2^2\right)^2 & 0 \\ 0 & 0 & 0 & 12\left(l_1^2 + l_2^2\right)^2 \end{bmatrix}.$$

The input force is $F = \mathrm{d}\theta_1 - \mathrm{d}\theta_2$.

Next, we characterize the two constrained regimes. Recall that two constrained mechanical control systems are defined by the two submanifolds $R_1(q_0) = \{q \in Q \mid \varphi_1(q) = \varphi_1(q_0) = (\theta_{20}, x_{20}, y_{20})\}$ and $R_2(q_0) = \{q \in Q \mid \varphi_2(q) = \varphi_2(q_0) = (x_{20}, y_{20})\}$. As discussed in Section 3.3, these holonomic constraints induce two constraint distributions $\mathcal{D}_1(q)$ and $\mathcal{D}_2(q)$. We compute them as:

$$\begin{aligned} \mathcal{D}_1(q) &= \operatorname{span}\left\{ (l_1^2 + l_2^2)\frac{\partial}{\partial \theta_1} + l_1^3 \sin(\theta_1)\frac{\partial}{\partial x_{\text{CM}}} - l_1^3 \cos(\theta_1)\frac{\partial}{\partial y_{\text{CM}}} \right\}, \\ \mathcal{D}_2(q) &= \operatorname{span}\left\{ (l_1^2 + l_2^2)\frac{\partial}{\partial \theta_1} + l_1^3 \sin(\theta_1)\frac{\partial}{\partial x_{\text{CM}}} - l_1^3 \cos(\theta_1)\frac{\partial}{\partial y_{\text{CM}}}, \right. \\ &\qquad \left. (l_1^2 + l_2^2)\frac{\partial}{\partial \theta_2} + l_2^3 \sin(\theta_2)\frac{\partial}{\partial x_{\text{CM}}} - l_2^3 \cos(\theta_2)\frac{\partial}{\partial y_{\text{CM}}} \right\}. \end{aligned}$$

Summarizing, if we label with 0 the unconstrained system and if we set $\mathcal{D}_0 = TQ$, we formally have a set of three distinct constrained mechanical control systems $\{Q, M_q, \mathcal{F}, \mathcal{D}_i\}$, for $i \in \{0, 1, 2\}$.

### Constrained Dynamics and Projected Inputs

Next, we compute the dynamics on the three distinct regimes. We start by exhibiting the Christoffel symbols for the un-clamped regime. The only non-vanishing symbols are

$$\begin{aligned} \Gamma^1_{11}(q) &= 72\,\eta(\theta_1, \theta_2)\, l_1^4 l_2^4 \sin(2\theta_2 - 2\theta_1), \\ \Gamma^2_{11}(q) &= 12\,\eta(\theta_1, \theta_2)\, l_1^3 l_2 \left(5l_2^2 + 5l_1^2 + 12 l_1^2 l_2^2\right) \sin(\theta_1 - \theta_2), \\ \Gamma^1_{22}(q) &= 12\,\eta(\theta_1, \theta_2)\, l_1 l_2^3 \left(5l_2^2 + 5l_1^2 + 12 l_1^2 l_2^2\right) \sin(\theta_2 - \theta_1), \\ \Gamma^2_{22}(q) &= 72\,\eta(\theta_1, \theta_2)\, l_1^4 l_2^4 \sin(2\theta_1 - 2\theta_2), \end{aligned}$$

where $\eta(\theta_1, \theta_2)^{-1} = \left(12 l_1^2 l_2^2 \cos(\theta_1 - \theta_2)\right)^2 - \left(5l_2^2 + 5l_1^2 + 12 l_1^2 l_2^2\right)^2$.

The Christoffel symbols of the two constrained connections can be computed via a symbolic manipulation software. We do not present these values here for brevity's sake, but we emphasize that the computations are performed on the reduced space, as described in Remark 3.4.

Next we present the input vector field on each of the three regimes. We call $Y_i$ the input vector field corresponding to the $i$th regime. We start by inverting the kinetic energy and

defining the input in the unconstrained regime as

$$Y_0 = \eta(\theta_1,\theta_2)\left(6\left(l_1^2+l_2^2\right)\left(5l_2^2+l_1^2\left(5+12l_2^2\right)+12l_1^3l_2\cos(\theta_1-\theta_2)\right)\frac{\partial}{\partial\theta_1}\right.$$
$$\left.-6\left(l_1^2+l_2^2\right)\left(5l_2^2+l_1^2\left(5+12l_2^2\right)+12l_1l_2^3\cos(\theta_1-\theta_2)\right)\frac{\partial}{\partial\theta_2}\right).$$

By projecting $Y_0$ onto the appropriate constraint distributions, we compute

$$Y_1 = \zeta(\theta_1,\theta_2)\left((l_1^2+l_2^2)\frac{\partial}{\partial\theta_1}+l_1^3\sin(\theta_1)\frac{\partial}{\partial x_{\mathrm{CM}}}-l_1^3\cos(\theta_1)\frac{\partial}{\partial y_{\mathrm{CM}}}\right),$$

for an appropriate scalar function $\zeta(\theta_1,\theta_2)$. Additionally, assuming $l_1 = l_2 \equiv l$

$$Y_2 = \xi(\theta_1,\theta_2)\left(6\frac{\partial}{\partial\theta_1}-6\frac{\partial}{\partial\theta_2}+3l\left(\sin(\theta_1)-\sin(\theta_2)\right)\frac{\partial}{\partial x_{\mathrm{CM}}}-3l\left(\cos(\theta_1)-\cos(\theta_2)\right)\frac{\partial}{\partial y_{\mathrm{CM}}}\right),$$

where we set $\xi(\theta_1,\theta_2)^{-1} = l^2\left(5+12l^2-12l^2\cos(\theta_1-\theta_2)\right)$.

# Chapter 4

# Tracking for Fully Actuated Systems

In this chapter we assume that the mechanical control system is fully actuated, i.e., there exist an independent control input for each degree of freedom. Under this assumption we show how it is possible to design a trajectory tracking controller that achieves exponential stability.

The chapter is organized as follows. First we introduce the notions of error function and transport map and we illustrate them by means of the two sphere example. These ideas lead to the main theorem, with proof and comments, in Section 4.3. Finally, we present numerous examples and applications of the main result. The content of this chapter is joint work with Richard M. Murray and was originally presented at various conferences; see [28, 25, 27], and the final journal version is [26].

## 4.1 Review of Stabilization Theory for Mechanical Systems

In this section we review some classic notion useful in the stabilization of mechanical systems. Main concept is the use of the total energy, i.e., the Hamiltonian of the system, as Lyapunov function. Our main reference is the work of Koditschek [53].

The setting is as follows. Consider a simple mechanical system with no potential energy

$$\nabla_{\dot{q}}\dot{q} = M_q^{-1}F,$$

where $q(t) \in Q$ is the configuration, $M$ and $\nabla$ are the kinetic energy metric and the corresponding connection, and $F \in T_q^*Q$ is the input force. The control goal is to design a stabilizing controller for a point $q_0$.

The following two objects are instrumental in the control design. Let $\varphi : Q \in \mathbb{R}$ be a smooth real valued function on $Q$. We shall say that $\varphi$ is positive definite about $q_0$, if $\varphi(q) \geq 0$ for all $q$, and $\varphi(q) = 0$ if and only if $q = q_0$. Let $(K_d)(q) : T_qQ \to T_q^*Q$ be a smooth, self-adjoint (i.e., symmetric in a matrix representation), positive definite tensor field on $Q$.

These two objects play the role of a potential and dissipation function in the classic proportional (PD) control:

$$F_{\mathrm{PD}} = -\mathrm{d}\varphi(q) - K_d\dot{q}.$$

Closed loop stability is assessed as follows. Consider the candidate Lyapunov function $\varphi + \frac{1}{2}\|\dot{q}\|^2$. Since both a potential and a kinetic energy like term are present, the function is

positive definite in both the configuration and the velocity. Its time derivative is computed using the tools from Chapter 2 as:

$$\begin{aligned}\frac{d}{dt}(\varphi + \frac{1}{2}\|\dot{q}\|^2) &= \nabla_{\dot{q}}\varphi + \frac{1}{2}\nabla_{\dot{q}}\|\dot{q}\|^2 \\ &= \langle \mathrm{d}\varphi, \dot{q}\rangle + \langle\!\langle \nabla_{\dot{q}}\dot{q}\,,\, \dot{q}\rangle\!\rangle \\ &= \langle \mathrm{d}\varphi, \dot{q}\rangle + \langle -\mathrm{d}\varphi(q) - K_d\dot{q}, \dot{q}\rangle = -\langle K_d\dot{q}, \dot{q}\rangle\,.\end{aligned}$$

Since the time derivative of the Lyapunov function is negative semi-definite, the closed loop is Lyapunov stable. Asymptotic stability is usually proven via Lasalle principle, see for example [53].

In the following sections we extend this classic result in various directions. In particular, we focus on tracking as opposed to stabilization and exponential convergence as opposed to asymptotic.

## 4.2 Configuration and Velocity Errors

In this section we study the geometric objects involved in the design of a tracking controller. To measure the distance between reference and actual configuration, we introduce the notion of error function. To measure the distance between reference and actual velocity, we introduce the notion of transport map. A design on two sphere manifold provides an example of our definitions. Finally we study the time derivative of the transport map. Together with a dissipation function, these ingredients are crucial in designing a tracking controller.

### 4.2.1 Error Function and Configuration Error

Let $\varphi$ be a smooth real valued function on $Q \times Q$. We shall call $\varphi$ an *error function* if it is *positive definite*, that is $\varphi(q,r) \geq 0$ for all $q$ and $r$, and $\varphi(q,r) = 0$ if and only if $q = r$. We shall say that the error function $\varphi$ is *symmetric*, if $\varphi(q,r) = \varphi(r,q)$ for all $q$ and $r$.

Let $\mathrm{d}_1\varphi$ and $\mathrm{d}_2\varphi$ denote the differential of $\varphi(q,r)$ with respect to its first and second argument. We shall say that the error function $\varphi$ is *(uniformly) quadratic with constant $L$* if for all $\epsilon > 0$ there exist two constants $b_1 \geq b_2 > 0$ such that $\varphi(q,r) < L - \epsilon$ implies

$$b_1\|\mathrm{d}_1\varphi(q,r)\|^2_{M_q} \;\geq\; \varphi(q,r) \;\geq\; b_2\|\mathrm{d}_1\varphi(q,r)\|^2_{M_q}. \tag{A1}$$

Here and in what follows, the tag (A$n$) denotes design assumptions that will play a crucial role in later sections.

*Remark 4.1.* The quadratic assumption on the error function is necessary in order to prove exponential convergence rates. This is a weak requirement, since smooth positive definite functions are always of at least quadratic order in a neighborhood of their critical point.

When $q$ and $r$ are actual and reference configuration, we will sometimes call the quantity $\varphi(q,r)$ configuration error. As mentioned above, the error function $\varphi$ will be instrumental in designing the proportional action.

### 4.2.2 Transport Map and Velocity Error

Given two points $q, r \in Q$, we shall call a linear map $\mathcal{T}_{(q,r)} : T_rQ \to T_qQ$ a *transport map* if it is *compatible with the error function*, that is if

$$\mathrm{d}_2\varphi(q,r) = -\mathcal{T}^*_{(q,r)}\mathrm{d}_1\varphi(q,r), \tag{A2}$$

where $\mathcal{T}^*_{(q,r)} : T^*_q Q \to T^*_r Q$ is the dual map of $\mathcal{T}_{(q,r)}$. The transport map $\mathcal{T}$ is also required to be *smooth*, i.e., for all points $r$ in $Q$ and tangent vectors $Y_r$ in $T_r Q$, the vector field $\mathcal{T}_{(q,r)} Y_r$ is smooth.

Given a transport map, velocities belonging to different tangent bundles can be compared. In the following, we shall call *velocity error* the quantity

$$\dot{e} \triangleq \dot{q} - \mathcal{T}_{(q,r)}\dot{r} \quad \in T_q Q. \tag{4.1}$$

Note the slight abuse of terminology, given that the velocity error is not the time derivative of a position error. Also note that since the definition of $\mathcal{T}$ and $\dot{e}$ are equivalent, we will sometimes talk about compatibility between configuration and velocity errors. The next lemma provides some insight into the meaning of the velocity error and of condition (A2).

**Lemma 4.2 (Time derivative of an error function).** *Let $\{q(t), t \in \mathbb{R}_+\}$ and $\{r(t), t \in \mathbb{R}_+\}$ be two smooth curves in $Q$. Let $\varphi$ be an error function and $\mathcal{T}$ a compatible transport map. Then*

$$\frac{d}{dt}\varphi\big(q(t), r(t)\big) = \mathrm{d}_1\varphi\big(q(t), r(t)\big) \cdot \dot{e}(t), \qquad \forall t \in \mathbb{R}_+.$$

*Proof.* Applying the compatibility condition (A2), we have:

$$\begin{aligned}\frac{d}{dt}\varphi(q(t), r(t)) &= \mathrm{d}_1\varphi(q, r) \cdot \dot{q} \;+\; \mathrm{d}_2\varphi(q, r) \cdot \dot{r} \\ &= \mathrm{d}_1\varphi(q, r) \cdot \dot{q} \;+\; \big(-\mathcal{T}^*_{(q,r)}\mathrm{d}_1\varphi(q, r)\big) \cdot \dot{r} \\ &= \mathrm{d}_1\varphi(q, r) \cdot \big(\dot{q} - \mathcal{T}_{(q,r)}\dot{r}\big).\end{aligned}$$

□

The result can be restated as follows. As both $q$ and $r$ are functions of time, the time derivative of $\varphi : Q \times Q \to \mathbb{R}$ reduces to a derivative only with respect to the first argument

$$\mathcal{L}_{(\dot{q},\, \dot{r})}\varphi \;=\; \mathcal{L}_{(\dot{e},\, 0)}\varphi, \tag{4.2}$$

where $(X,\ Y)$ denotes a vector field on the product manifold $Q \times Q$.

Last, we introduce the notion of dissipation function, which will be useful in defining a derivative action. We define a *(linear Rayleigh) dissipation function* as a smooth, self-adjoint, positive definite tensor field $(K_d)(q) : T_q Q \to T^*_q Q$. We shall say that $K_d$ is bounded if there exist $d_2 \geq d_1 > 0$ such that

$$d_2 \geq \sup_{q \in Q} \|K_d(q)\|_{M_q} \geq \inf_{q \in Q} \|K_d(q)\|_{M_q} \geq d_1, \tag{B1}$$

where $\|\cdot\|_M$ is the operator norm for $(1,1)$ type tensors on $T_q Q$ induced by the metric $M_q$ on $T_q Q$. Here and in what follows, the tag (B$n$) denotes boundedness assumptions that will play a crucial role in later sections.

### 4.2.3 Example Design for the Two Sphere

To illustrate the previous ideas we apply them to the two sphere $\mathbb{S}^2 \triangleq \{p \in \mathbb{R}^3 \,|\, p^T p = 1\}$. Since $\mathbb{S}^2$ is embedded in $\mathbb{R}^3$, we identify points, tangent and cotangent vectors on the sphere, with their corresponding components in $\mathbb{R}^3$. Note that the Euclidean norm $\|\cdot\|$ on $\mathbb{R}^3$ induces a metric on the submanifold $\mathbb{S}^2$. Given an error function $\varphi : \mathbb{S}^2 \times \mathbb{S}^2 \to \mathbb{R}_+$, the norm of its differential $\|\mathrm{d}_1\varphi\|$ is therefore well defined. Recall that we let $a \times b$ denote the outer product

between the two vectors $a, b \in \mathbb{R}^3$, and we let $\widehat{a}$ or $a\widehat{\ }$ denote the $3 \times 3$ skew symmetric matrix such that $\widehat{a}\, b = a \times b$.

**Lemma 4.3 (Design on the sphere).** *Let $q$ and $r$ belong to $\mathbb{S}^2$. It holds that*

*(i)* $\varphi(q,r) \triangleq 1 - q^T r$ *is a symmetric error function with differential* $\mathrm{d}_1\varphi(q,r) = \widehat{q}^2 r = -r + (q^T r)q$,

*(ii)* $\varphi(q,r)$ *is a quadratic error function with constant* $L = 2$, *and*

*(iii)* $\mathcal{T}_{(q,r)} \triangleq (q^T r) I_3 + (r \times q)\widehat{\ }$ *is a compatible transport map.*

*Proof.* As mentioned above, recall that we identify points, tangent and cotangent vectors on the sphere, with their corresponding components in $\mathbb{R}^3$. Since the orthogonal projection of $r \in \mathbb{S}^2$ onto $\mathrm{span}\{q\}^\perp$ is $r - (q^T r)q = -\widehat{q}^2 r$, we have

$$\mathcal{L}_{(\dot{q},0)}\varphi = -\dot{q}^T r = -\dot{q}^T (r - (q^T r)q) = (\widehat{q}^2 r)^T \dot{q}.$$

This proves (i). We prove (ii) as follows. By assumption we are given an $\epsilon > 0$ such that $0 \le \varphi(q,r) \le 2 - \epsilon$, or equivalently $1 \ge q^T r \ge -1 + \epsilon$. The differential of the error function satisfies

$$\|\mathrm{d}_1\varphi\|^2 = \|r - (q^T r)q\|^2 = 1 - (q^T r)^2 = (1 + q^T r)\varphi(q,r).$$

Since at $\varphi(q,r) = 0$ the bounds in assumption (A1) are verified, we only need to check that there exist $b_1 \ge b_2 > 0$ such that

$$b_1(1 + q^T r) \ge 1 \ge b_2(1 + q^T r).$$

This holds true for $b_1 = 1/2$ and $b_2 = 1/\epsilon$, proving (ii). Next we show that $\varphi$ and $\mathcal{T}$ are compatible (A2). This is verified with some algebraic simplifications based on the equality $v \times (w \times z) = (v^T z)w - (v^T w)z$. We have

$$\begin{aligned}
\mathcal{T}^* \mathrm{d}_1\varphi(q,r) &= -(q^T r)r + (q^T r)^2 q - \big(r - (q^T r)q\big) \times (r \times q) \\
&= -(q^T r)r + (q^T r)^2 q - \big((r - (q^T r)q)^T q\big)\, r - \big((r - (q^T r)q)^T r\big)\, q \\
&= -(q^T r)r + (q^T r)^2 q + \big(1 - (q^T r)^2\big) q \\
&= q - (q^T r)r \;\equiv\; -\mathrm{d}_2\varphi(q,r).
\end{aligned}$$

□

Next, we present some figures to compare our design with a traditional one. To warn of the effects of a design performed in local coordinates, Fig. 4.1 shows various paths connecting the same two points on a sphere. In each figure we employ a different projection, that is a different set of coordinates $x(q)$, and we draw the flow of the gradient[1] of the (error) function $\|x(q) - x(r)\|^2$, that is a straight line in the particular set of coordinates. Note how the resulting paths depend on the choice of projection.

In Fig. 4.2, we focus on two different choices of transport map and velocity error. Given a fixed reference velocity $\dot{r}$ (which is represented in both pictures by a thick arrow on top of the sphere), we draw for various points $q$ the vector field $\mathcal{T}_{(q,r)}\dot{r}$. The left picture portrays the global, smooth design described above. On the right picture, we show the velocity error

[1] The gradient of a scalar function $f$ is the vector field $\nabla f$ such that $\langle\!\langle \nabla f\,,\, X \rangle\!\rangle \triangleq \mathcal{L}_X f$.

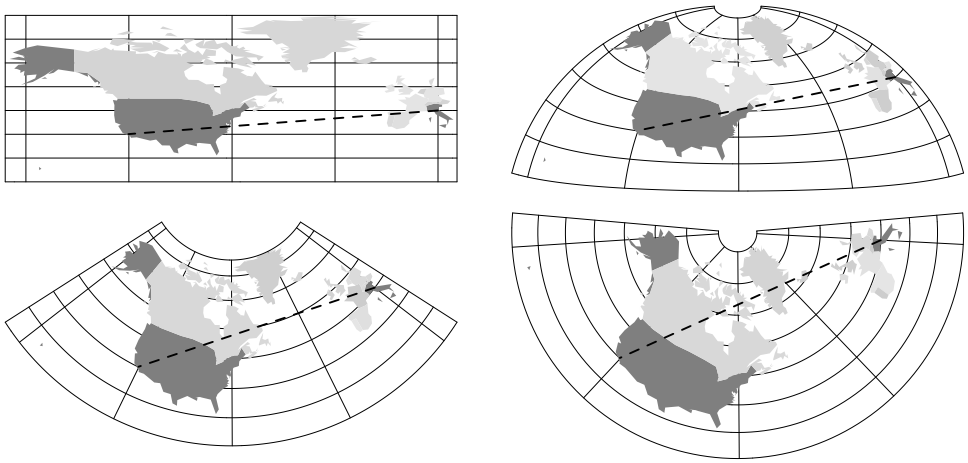

Figure 4.1: Comparison of error functions based on four coordinate systems: the flow of their gradient is depicted . As expected, straight lines in different coordinate systes give rise to different curves.

computed in a latitude, longitude parametrization. This is the procedure: if $(\theta_1, \theta_2)$ are the local coordinates, then we can write

$$\dot{r} = \dot{r}_1 \frac{\partial}{\partial \theta_1}(r) + \dot{r}_2 \frac{\partial}{\partial \theta_2}(r).$$

We computed the "velocity error" vector field as

$$\mathcal{T}_{\text{lat/long}} \dot{r} = \dot{r}_1 \frac{\partial}{\partial \theta_1}(q) + \dot{r}_2 \frac{\partial}{\partial \theta_2}(q).$$

At the north pole of the latitude, longitude chart the singularity is evident.

### 4.2.4 Derivatives of the Transport Map

So far we have introduced configuration and velocity errors that will be key ingredients in designing a proportional and derivative feedback in the next section. We now study how the quantity $(\mathcal{T}_{(q,r)}\dot{r})$ varies as a function of both $q(t)$ and $(r, \dot{r})(t)$. This will be useful in designing the feedforward action. Let the total derivative of $(\mathcal{T}_{(q,r)}\dot{r})$ be

$$\frac{D\left(\mathcal{T}\dot{r}\right)}{dt} = \nabla_{\dot{q}}\left(\mathcal{T}\dot{r}\right) + \frac{d}{dt}\Big|_{q \text{ fixed}}\left(\mathcal{T}\dot{r}\right), \tag{4.3}$$

where the two terms are described as follows:

(i) At $(r, \dot{r})$ fixed, $\mathcal{T}_{(q,r)}\dot{r}$ is a vector field on $Q$ and therefore its covariant derivative $\nabla_{\dot{q}}\left(\mathcal{T}\dot{r}\right)$ is well-defined on $Q$. We call the *covariant derivative of the transport map* the map $\nabla\mathcal{T} : T_qQ \times T_rQ \to T_qQ$ defined as

$$(\nabla_X \mathcal{T})Y_r \triangleq \nabla_X(\mathcal{T}Y_r),$$

for all tangent vectors $X \in T_qQ$ and $Y_r \in T_rQ$.

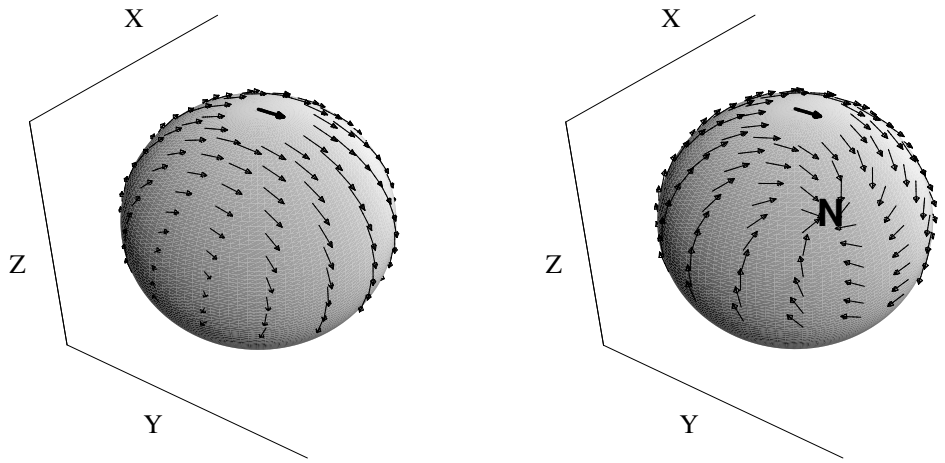


Figure 4.2: Transport maps on $\mathbb{S}^2$. We depict the vector $\mathcal{T}_{(q,r)}\dot{r}$ for two different transport maps: on the left our smooth global design, on the right a design based on a latitude, longitude chart, with the north pole denoted by the letter N.

(ii) At $q$ fixed, $\mathcal{T}_{(q,r)}\dot{r}$ is a vector on the vector space $T_qQ$ and therefore its time derivative is well-defined. We denote it with the symbol:

$$\left.\frac{d}{dt}\right|_{q \text{ fixed}} (\mathcal{T}\dot{r}) \quad \in T_qQ.$$

Next, we compute coordinate expressions for the previous quantities. Let $\{\frac{\partial}{\partial q^1}, \dots \frac{\partial}{\partial q^n}\}$ be a basis for $T_qQ$ and $\{\frac{\partial}{\partial r^1}, \dots \frac{\partial}{\partial r^n}\}$ a basis for $T_rQ$. Then we have the decompositions

$$\dot{r} = \dot{r}^\alpha \tfrac{\partial}{\partial r^\alpha}, \quad \text{and} \quad \mathcal{T}\dot{r} = \mathcal{T}^k_\alpha \dot{r}^\alpha \tfrac{\partial}{\partial q^k}.$$

If $\Gamma^k_{ij}$ are the Christoffel symbols of $\nabla$ and if $X$ is a tangent vector in $T_qQ$, then we have

$$(\nabla_X \mathcal{T})^k_\alpha \;=\; \frac{\partial \mathcal{T}^k_\alpha}{\partial q^j} X^j \;+\; \Gamma^k_{ij} \mathcal{T}^i_\alpha X^j. \tag{4.4}$$

Regarding the time derivative at $q$ fixed, we have

$$\left( \left.\frac{d}{dt}\right|_{q \text{ fixed}} (\mathcal{T}\dot{r}) \right)^k = \frac{\partial \mathcal{T}^k_\alpha}{\partial r^\beta} \dot{r}^\alpha \dot{r}^\beta + \mathcal{T}^k_\alpha \ddot{r}^\alpha. \tag{4.5}$$

*Remark 4.4.* Assume for an instant that the reference trajectory $r(t)$ obeys the same equations of motion as the actual mechanical system, that is

$$\nabla_{\dot{r}} \dot{r} \;=\; M_r^{-1} F_r(t),$$

for some appropriate reference force $F_r(t) \in T_rQ$. Since in coordinates we have $(\nabla_{\dot{r}} \dot{r})^\alpha =$

$\ddot{r}^\alpha + \Gamma^\alpha_{\beta\gamma}(r)\dot{r}^\beta\dot{r}^\gamma$, then we can rewrite the equation (4.5) as

$$\begin{aligned}\frac{d}{dt}\Big|_{q \text{ fixed}}(\mathcal{T}\dot{r}) &= \mathcal{T}\nabla_{\dot{r}}\dot{r} + \left(\frac{\partial \mathcal{T}^k_\alpha}{\partial r^\beta} - \mathcal{T}^k_\gamma \Gamma^\gamma_{\alpha\beta}(r)\right)\dot{r}^\alpha\dot{r}^\beta \frac{\partial}{\partial q^k}. \\ &\triangleq \mathcal{T}\left(M_r^{-1}F_r(t)\right) + \left(\nabla_{(0,\dot{r})}\mathcal{T}\right)\dot{r},\end{aligned}$$

where the last equality defines implicitly the map $\nabla_{(0,\dot{r})}\mathcal{T} : T_rQ \to T_qQ$. Note that the definition is coordinate independent, hence well-posed. Roughly speaking, this map is the covariant derivative of $\mathcal{T}$ with respect to $\dot{r}$. This statement can be made precise by defining $\mathcal{T}$ as a tensor on the product Riemannian manifold $Q \times Q$. We do not pursue this direction here.

We conclude the section with some boundedness assumptions. We shall say that the transport map $\mathcal{T}$ has bounded covariant derivative and that the error function $\varphi$ has bounded second covariant derivative if

$$\sup_{(q,r)\in Q\times Q} \|\nabla \mathcal{T}_{(q,r)}\|_M < \infty, \tag{B2}$$

and

$$\sup_{(q,r)\in Q\times Q} \|\nabla \mathrm{d}_1\varphi\,(q,r)\|_M < \infty, \tag{B3}$$

where $\|\cdot\|_M$ is the operator norm on the inner product space $(T_qQ,\, M_q)$. We shall say that the twice differentiable curve $\{r(t), t \in \mathbb{R}_+\} \subset Q$ is a reference trajectory with bounded time derivative if

$$\sup_{t\in\mathbb{R}} \|\dot{r}\|_{M_r} < \infty. \tag{B4}$$

Given the equalities (2.10) and (4.4), a sufficient condition for the bounds (B2)-(B3) to hold, is that the quantities $M_{ij}$, $M^{ij}$, $\Gamma^k_{ij}$, $\partial \mathcal{T}^i_\alpha/\partial q^k$ and $\partial^2\varphi/(\partial q^i \partial q^j)$ are bounded over $(q,r) \in Q \times Q$ for all $i, j, k, \alpha$. On a compact manifold these conditions are implied by the smoothness of $M$, $K_d$, $\mathcal{T}$ and $\varphi$.

## 4.3 Tracking on Manifolds

In this section we state and solve the exponential tracking problem for general mechanical control systems on manifolds.

### 4.3.1 Problem Statement and Control Design

In what follows we let $\{r(t), t \in \mathbb{R}_+\}$ denote a reference trajectory, $(\varphi, \mathcal{T})$ denote a pair of error function and transport map and we focus on a simple mechanical control system with no potential energy:

$$\nabla_{\dot{q}}\dot{q} = M_q^{-1}F, \qquad q \in Q. \tag{4.6}$$

We loosely state the control objective as follows:

**Problem 4.5.** Design a control law $F = F(q, \dot{q};\, r, \dot{r})$ such that the configuration $q(t)$ tracks $r(t)$ with an exponentially decreasing error.

Special care is needed to make this statement precise, as no trivial definition of exponential stability exists for systems on manifolds. We start by introducing a total energy function, defined as the sum of a generalized potential (the configuration error) and a kinetic energy function (the norm of the velocity error):

$$W_{\text{total}}(q, \dot{q};\ r, \dot{r}) \ \triangleq\ \varphi(q, r) + \frac{1}{2}\|\dot{q} - \mathcal{T}_{(q,r)}\dot{r}\|^2_{M_q}. \tag{4.7}$$

Alternatively we will write $W_{\text{total}}(t)$ for $W_{\text{total}}(q(t), \dot{q}(t);\ r(t), \dot{r}(t))$. Next we introduce the following definitions:

(i) the curve $q(t) = r(t)$ is *stable with Lyapunov function* $W_{\text{total}}$ if it holds $W(t) \leq W_{\text{total}}(0)$ from all initial conditions $(q(0), \dot{q}(0))$.

(ii) the curve $q(t) = r(t)$ is *exponentially stable with Lyapunov function* $W_{\text{total}}$ if there exist two positive constants $\lambda, k$ such that $W_{\text{total}}(t) \ \leq\ k\, W_{\text{total}}(0)e^{-\lambda t}$, from all initial conditions $(q(0), \dot{q}(0))$.

We are now ready to state the main result.

**Theorem 4.6 (Bullo and Murray [26]).** *Consider the control system in equation* (4.6)*, and let* $\{r(t), t \in \mathbb{R}_+\}$ *be a twice differentiable reference trajectory. Let* $\varphi$ *be an error function,* $\mathcal{T}$ *be a transport map satisfying the compatibility condition* (A2) *and* $K_d$ *be a dissipation function.*

*If the control input is defined as* $F = F_{\text{PD}} + F_{\text{FF}}$ *with*

$$\begin{aligned} F_{\text{PD}}(q, \dot{q};\ r, \dot{r}) \ &=\ -\mathrm{d}_1\varphi(q, r) - K_d\,\dot{e}, \\ F_{\text{FF}}(q, \dot{q};\ r, \dot{r}) \ &=\ M_q\left((\nabla_{\dot{q}}\mathcal{T}_{(q,r)})\dot{r} \ +\ \frac{d}{dt}\Big|_{q\ \text{fixed}}(\mathcal{T}_{(q,r)}\dot{r})\right), \end{aligned}$$

*then the curve* $q(t) = r(t)$ *is stable with Lyapunov function* $W_{\text{total}}$*.*

*In addition, if the error function* $\varphi$ *satisfies the quadratic assumption* (A1) *with a constant* $L$*, and if the boundedness assumptions* (B1–B4) *hold, then the curve* $q(t) = r(t)$ *is exponentially stable with Lyapunov function* $W_{\text{total}}$ *from all initial conditions* $(q(0), \dot{q}(0))$ *such that*

$$\varphi\big(q(0), r(0)\big) + \frac{1}{2}\|\dot{e}(0)\|^2_{M_q} < L.$$

*Proof.* The proof is divided into three parts: first we prove Lyapunov stability using the total energy as a Lyapunov function. Second, we add an additional "cross" term to the Lyapunov function. Finally, we conclude local exponential stability with a bounding argument.

The proof is based on the properties of covariant derivatives described in Section 2.3 and on the definitions in Section 4.2.4. This approach makes the proof straightforward and independent from any choice of local coordinates: the Lyapunov function, its time derivative and the final bounding argument are coordinate-free.

### Part I: Lyapunov Stability from Total Energy

We employ the total energy function $W_{\text{total}} = \varphi + \frac{1}{2}\|\dot{e}\|^2_{M_q}$ as candidate Lyapunov function. By Lemma 4.2 the time derivative of the first term is $\dot{\varphi} = \mathrm{d}_1\varphi \cdot \dot{e}$. We compute the time

derivative of the second term in two steps. At $r$ fixed, the equality (2.4) allows us to write

$$\begin{aligned}\frac{d}{dt}\Big|_{r \text{ fixed}} \frac{1}{2}\|\dot{e}\|_{M_q}^2 &= \frac{1}{2}\mathcal{L}_{\dot{q}}\langle\langle \dot{e}\,,\,\dot{e}\rangle\rangle = \langle\langle \dot{e}\,,\,\nabla_{\dot{q}}\dot{e}\rangle\rangle \\ &= \langle\langle \dot{e}\,,\,\nabla_{\dot{q}}\,(\dot{q}-\mathcal{T}\dot{r})\rangle\rangle \\ &= \langle\langle \dot{e}\,,\,M_q^{-1}(F_{\mathrm{PD}}+F_{\mathrm{FF}}) - (\nabla_{\dot{q}}\mathcal{T})\dot{r}\rangle\rangle.\end{aligned}$$

At $q$ fixed, we have instead

$$\frac{d}{dt}\Big|_{q \text{ fixed}} \frac{1}{2}\|\dot{e}\|_{M_q}^2 = \langle\langle \dot{e}\,,\,\frac{d}{dt}\Big|_{q \text{ fixed}}(\dot{q}-\mathcal{T}\dot{r})\rangle\rangle = -\langle\langle \dot{e}\,,\,\frac{d}{dt}\Big|_{q \text{ fixed}}(\mathcal{T}\dot{r})\rangle\rangle.$$

Plugging in we have

$$\begin{aligned}\frac{d}{dt}W_{\mathrm{total}} &= \mathrm{d}_1\varphi\cdot\dot{e} + \langle\langle \dot{e}\,,\,M_q^{-1}(F_{\mathrm{PD}}+F_{\mathrm{FF}}) - (\nabla_{\dot{q}}\mathcal{T})\dot{r} - \frac{d}{dt}\Big|_{q \text{ fixed}}(\mathcal{T}\dot{r})\rangle\rangle \\ &= \mathrm{d}_1\varphi\cdot\dot{e} + \langle\langle M_q^{-1}F_{\mathrm{PD}}\,,\,\dot{e}\rangle\rangle \\ &= \mathrm{d}_1\varphi\cdot\dot{e} + (-\mathrm{d}_1\varphi - K_d\,\dot{e})\cdot\dot{e} \;=\; -K_d\dot{e}\cdot\dot{e}\end{aligned}$$

so that $\frac{d}{dt}W_{\mathrm{total}}$ is negative semidefinite and Lyapunov stability as defined in Theorem 4.6 is proven.

**Part II: Introduction of Cross Term**

To construct a strict Lyapunov function (i.e., a function with a time derivative strictly definite), we add a "small" cross term to $W_{\mathrm{total}}$. Let $\epsilon$ be a positive constant, let

$$W_{\mathrm{cross}}(t) \;=\; \dot{\varphi} \;=\; \mathrm{d}_1\varphi\cdot\dot{e},$$

and consider the candidate Lyapunov function

$$W \;\triangleq\; W_{\mathrm{total}} + \epsilon\, W_{\mathrm{cross}}.$$

We need to show that there exists a sufficiently small $\epsilon$, such that $W$ is positive definite in $\varphi$ and $\|\dot{e}\|_{M_q}$. We start by noting that from Part I and the assumptions on the initial conditions, we have

$$W_{\mathrm{total}}(t) \le W_{\mathrm{total}}(0) < L \quad\Longrightarrow\quad \varphi(t) < L,$$

which implies that the bounds (A1) on the differential of the error function hold for all time. Then we have

$$\begin{aligned}W &\ge \varphi + \frac{1}{2}\|\dot{e}\|_{M_q}^2 - \epsilon\|\mathrm{d}_1\varphi\|_{M_q}\cdot\|\dot{e}\|_{M_q} \\ &\ge \varphi + \frac{1}{2}\|\dot{e}\|_{M_q}^2 - \epsilon(1/\sqrt{b_2})\sqrt{\varphi}\,\|\dot{e}\|_{M_q},\end{aligned}$$

and therefore

$$W \ge \frac{1}{2}\begin{bmatrix}\sqrt{\varphi}\\ \|\dot{e}\|_{M_q}\end{bmatrix}^T\begin{bmatrix}2 & -\epsilon/\sqrt{b_2}\\ -\epsilon/\sqrt{b_2} & 2\end{bmatrix}\begin{bmatrix}\sqrt{\varphi}\\ \|\dot{e}\|_{M_q}\end{bmatrix} \;\triangleq\; \begin{bmatrix}\sqrt{\varphi}\\ \|\dot{e}\|_{M_q}\end{bmatrix}^T\mathcal{P}\begin{bmatrix}\sqrt{\varphi}\\ \|\dot{e}\|_{M_q}\end{bmatrix}.$$

By choosing $\epsilon < 2\sqrt{b_2}$, the matrix $\mathcal{P}$ and the function $W$ are positive definite with respect to $\sqrt{\varphi}$ and $\|\dot{e}\|_{M_q}$.

Next, we compute the time derivative of $W_{\text{cross}}$. At $r$ fixed, we have

$$\begin{aligned}\frac{d}{dt}\Big|_{r \text{ fixed}}\dot{\varphi} &= \nabla_{\dot{q}}\left(\mathrm{d}_1\varphi \cdot \dot{e}\right) = (\nabla_{\dot{q}}\mathrm{d}_1\varphi)\cdot\dot{e} + \mathrm{d}_1\varphi\cdot(\nabla_{\dot{q}}\dot{e}) \\ &= (\nabla_{\dot{q}}\mathrm{d}_1\varphi)\cdot\dot{e} + \mathrm{d}_1\varphi\cdot\left(M_q^{-1}F - (\nabla_{\dot{q}}\mathcal{T})\dot{r}\right). \end{aligned} \tag{4.8}$$

At $q$ fixed, we have

$$\frac{d}{dt}\Big|_{q \text{ fixed}}(\mathrm{d}_1\varphi) = \mathrm{d}_1\left(\frac{d}{dt}\Big|_{q \text{ fixed}}\varphi\right) = \mathrm{d}_1\left(\mathrm{d}_1\varphi\cdot(-\mathcal{T}\dot{r})\right),$$

and therefore

$$\begin{aligned}\frac{d}{dt}\Big|_{q \text{ fixed}}\dot{\varphi} &= \left(\frac{d}{dt}\Big|_{q \text{ fixed}}\mathrm{d}_1\varphi\right)\cdot\dot{e} + \mathrm{d}_1\varphi\cdot\left(\frac{d}{dt}\Big|_{q \text{ fixed}}\dot{e}\right) \\ &= \mathrm{d}_1\left(\mathrm{d}_1\varphi\cdot(-\mathcal{T}\dot{r})\right)\cdot\dot{e} + \mathrm{d}_1\varphi\cdot\left(-\frac{d}{dt}\Big|_{q \text{ fixed}}(\mathcal{T}\dot{r})\right) \\ &= -\mathcal{L}_{\dot{e}}(\mathrm{d}_1\varphi\cdot(\mathcal{T}\dot{r})) - \mathrm{d}_1\varphi\cdot\left(\frac{d}{dt}\Big|_{q \text{ fixed}}(\mathcal{T}\dot{r})\right) \\ &= -\left(\nabla_{\dot{e}}\mathrm{d}_1\varphi\right)\cdot(\mathcal{T}\dot{r}) - \mathrm{d}_1\varphi\cdot\left(\nabla_{\dot{e}}(\mathcal{T}\dot{r})\right) - \mathrm{d}_1\varphi\cdot\left(\frac{d}{dt}\Big|_{q \text{ fixed}}(\mathcal{T}\dot{r})\right). \end{aligned}$$

Summing the previous equation with equation (4.8) we obtain

$$\begin{aligned}\frac{d}{dt}\dot{\varphi} = (\nabla_{\dot{e}}\mathrm{d}_1\varphi)\cdot\dot{e} &+ \mathrm{d}_1\varphi\cdot\left(M_q^{-1}F - (\nabla_{\dot{q}}\mathcal{T})\dot{r} - \frac{d}{dt}\Big|_{q \text{ fixed}}(\mathcal{T}\dot{r})\right) \\ &- \mathrm{d}_1\varphi\cdot\left(\nabla_{\dot{e}}(\mathcal{T}\dot{r})\right),\end{aligned}$$

and substituting the control force $F$

$$\begin{aligned}&= (\nabla_{\dot{e}}\mathrm{d}_1\varphi)\cdot\dot{e} + \mathrm{d}_1\varphi\cdot\left(M_q^{-1}F_{\text{PD}}\right) - \mathrm{d}_1\varphi\cdot\left(\nabla_{\dot{e}}(\mathcal{T}\dot{r})\right) \\ &= -\|\mathrm{d}_1\varphi\|_{M_q}^2 + (\nabla_{\dot{e}}\mathrm{d}_1\varphi)\cdot\dot{e} + \mathrm{d}_1\varphi\cdot\left(M_q^{-1}K_d\dot{e}\right) - \mathrm{d}_1\varphi\cdot\left((\nabla_{\dot{e}}\mathcal{T})\dot{r}\right).\end{aligned}$$

Next, by means of the quadratic assumption (A1) on $\varphi$, we can express $\dot{W}_{\text{cross}} = \ddot{\varphi}$ as a function of $\varphi$ and $\|\dot{e}\|_{M_q}$. It holds that

$$\dot{W}_{\text{cross}} \;=\; \ddot{\varphi} \;\leq\; -\begin{bmatrix}\sqrt{\varphi}\\ \|\dot{e}\|_{M_q}\end{bmatrix}^T \mathcal{Q}_{\text{cross}}\begin{bmatrix}\sqrt{\varphi}\\ \|\dot{e}\|_{M_q}\end{bmatrix},$$

where the symmetric matrix $\mathcal{Q}_{\text{cross}}$ has the following entries:

$$\begin{aligned}(\mathcal{Q}_{\text{cross}})_{1,1} &= 1/b_1, \\ (\mathcal{Q}_{\text{cross}})_{2,1} &= -\left(\sup_{q\in Q}\|K_d\|_{M_q} \;+\; \sup_t\|\dot{r}\|_{M_r}\cdot\sup_{(q,r)\in Q\times Q}\|\nabla\mathcal{T}\|_M\right)/\sqrt{b_1} \\ (\mathcal{Q}_{\text{cross}})_{2,2} &= -\sup_{(q,r)\in Q\times Q}\|\nabla\mathrm{d}_1\varphi\|_M.\end{aligned}$$

Note that the operators in $\mathcal{Q}_{\text{cross}}$ are bounded: $(\mathcal{Q}_{\text{cross}})_{1,2}$ is upper bounded due to assump-

tions (B1), (B4) and (B2), $(\mathcal{Q}_{\text{cross}})_{2,2}$ is upper bounded due to the assumption (B3).

**Part III: Bounding Arguments**

As a last step, we bound the time derivative of the Lyapunov function $W = W_{\text{total}} + \epsilon W_{\text{cross}}$. We have

$$\frac{d}{dt}W \;\leq\; -\begin{bmatrix}\sqrt{\varphi}\\ \|\dot{e}\|_{M_q}\end{bmatrix}^T \mathcal{Q}\begin{bmatrix}\sqrt{\varphi}\\ \|\dot{e}\|_{M_q}\end{bmatrix},$$

where the symmetric matrix $\mathcal{Q}$ is positive definite for small enough $\epsilon$, since

$$\begin{aligned}\mathcal{Q}_{1,1} &= \epsilon(\mathcal{Q}_{\text{cross}})_{1,1},\\ \mathcal{Q}_{1,2} &= \epsilon(\mathcal{Q}_{\text{cross}})_{1,2},\\ \mathcal{Q}_{2,2} &= \inf_{q\in Q}\|K_d\|_{M_q} + \epsilon(\mathcal{Q}_{\text{cross}})_{2,2},\end{aligned}$$

and $\mathcal{Q}_{2,2}$ is bounded away from zero thanks to (B1). Hence, there exist a $\lambda > 0$ such that $\dot{W} < -\lambda W$. Finally, it holds that

$$W_{\text{total}} = \begin{bmatrix}\sqrt{\varphi}\\ \|\dot{e}\|_{M_q}\end{bmatrix}^T \begin{bmatrix}1 & 0\\ 0 & \frac{1}{2}\end{bmatrix}\begin{bmatrix}\sqrt{\varphi}\\ \|\dot{e}\|_{M_q}\end{bmatrix},$$

and for an appropriate positive $k_1$

$$\begin{aligned}&\leq\; k_1\begin{bmatrix}\sqrt{\varphi}\\ \|\dot{e}\|_{M_q}\end{bmatrix}^T \mathcal{P}\begin{bmatrix}\sqrt{\varphi}\\ \|\dot{e}\|_{M_q}\end{bmatrix}\\ &\leq\; k_1 W(t) \;\leq\; k_1 W(0)e^{-\lambda t} \;\leq\; 2k_1 W_{\text{total}}(0)e^{-\lambda t},\end{aligned}$$

where we used the fact that $W_{\text{total}}(0) + \epsilon W_{\text{cross}}(0) \leq 2W_{\text{total}}(0)$. □

### 4.3.2 Remarks

The design process and the theorem's results are global in the reference position $r(t)$ but only local in the configuration $q$ (the error function $\varphi(q, r)$ must remain smaller than the parameter $L$). This limitation cannot be avoided because of possible topological properties of the manifold $Q$. For additional details we refer to [53], where the author discusses the global aspects of the point stabilization problem and describes the usefulness of the so-called Morse property.

Theorem 4.6 achieves Lyapunov and exponential stability with respect to the particular total energy $W_{\text{total}}$ we synthesized. Therefore, the design of error function and transport map plays a central role in imposing performance requirements. For example the choice of error function $\varphi(q, r)$ affects the type of convergence we obtain: the configuration $q$ converges to the reference $r$ in the topology induced by $\varphi$. Additionally, the choice of $(\varphi, \mathcal{T})$ determines the (computational) complexity of the control action. For example, one particular transport map might be desirable since it generates a "simple" velocity error and a "simple" feedforward control. However, the compatibility condition (A2) constitutes a constraint on the set of admissible pairs $(\varphi, \mathcal{T})$. The next section, and in particular the SO(3) and SE(3) cases, illustrates some of the tradeoffs involved in the control design.

As expected, the final control law is sum of a feedback and a feedforward term. This is in agreement with the ideas exposed in [75] on "two degree of freedom system design"

for mechanical systems. While the feedforward term depends on the geometry of both the manifold and the mechanical system, the feedback term is designed knowing only the configuration manifold $Q$. We expect the ideas of configuration and velocity error to be relevant for more general second order nonlinear systems on manifolds.

Note finally that, while the theorem is stated for mechanical systems with Lagrangian equal to kinetic energy, it can be generalized to systems with potential functions, viscous forces and gyroscopic forces, by pre-compensating for these extra terms.

### 4.3.3 Extensions to Model-Based Adaptive Control

Since the control law in Theorem 4.6 requires full knowledge of the inertia tensor $M(q)$, our approach is of limited relevance whenever an exact measurement of this quantity is not available. Well-known solutions to this problem rely on model-based adaptive schemes. Three examples are the composite adaptive controller in [88], the passivity-based controller in [4] and the indirect adaptive controller in [104].

In what follows, we sketch the basic common idea behind these treatments. The key simplifying assumption is that the unknown parameters enter linearly the Euler-Lagrange equations. In particular, assume that the inertia tensor $M(q)$ satisfies $M(q) = \sum_i \lambda_i M_i(q)$, where $\lambda_i \in \mathbb{R}$ are unknown parameters and $M_i(q)$ are known tensors. Let $\widehat{\lambda}_i(t)$ be the estimate of $\lambda_i$ and define the tensor $\widehat{M}(q,t) = \sum_i \widehat{\lambda}_i(t) M_i(q)$.

**Lemma 4.7 (Stable adaptive tracking).** *Under the same setting as in Theorem 4.6, define the control input as*

$$F = -\mathrm{d}_1\varphi - K_d\,\dot{e} + \widehat{M}(q,t)\frac{D\left(\mathcal{T}\dot{r}\right)}{dt},$$

*where $D\left(\mathcal{T}\dot{r}\right)/dt$ is defined in equation (4.3), and set the update law*

$$\frac{d}{dt}\widehat{\lambda}_i = -M_i\dot{e}\cdot\frac{D\left(\mathcal{T}\dot{r}\right)}{dt}.$$

*Then the curve $q(t) = r(t)$ is stable with Lyapunov function*

$$W_{\text{adap}} = W_{\text{total}} + \frac{1}{2}\sum_i(\lambda_i - \widehat{\lambda}_i)^2 \;=\; \left(\varphi + \frac{1}{2}\|\dot{e}\|^2_{M_q}\right) + \frac{1}{2}\sum_i(\lambda_i - \widehat{\lambda}_i)^2,$$

*in the sense that $W_{\text{adap}}(t) \leq W_{\text{adap}}(0)$ from all initial conditions $(q(0), \dot{q}(0))$ and all initial estimates $(\lambda_i(0))$.*

*Proof.* Following the steps described in Part I of the previous proof, we have:

$$\begin{aligned}
\frac{d}{dt}W_{\text{total}} &= -K_d\dot{e}\cdot\dot{e} + (\widehat{M} - M)\dot{e}\cdot\frac{D\left(\mathcal{T}\dot{r}\right)}{dt} \\
&= -K_d\dot{e}\cdot\dot{e} + \sum_i(\widehat{\lambda}_i - \lambda_i)\left(M_i\,\dot{e}\cdot\frac{D\left(\mathcal{T}\dot{r}\right)}{dt}\right) \\
&= -K_d\dot{e}\cdot\dot{e} - \sum_i(\widehat{\lambda}_i - \lambda_i)\frac{d}{dt}\widehat{\lambda}_i,
\end{aligned}$$

where in the last step we have plugged in the update law for $\widehat{\lambda}_i$. Finally, since $\frac{d}{dt}\widehat{\lambda}_i =$

$\frac{d}{dt}(\widehat{\lambda}_i - \lambda_i)$, we have

$$\frac{d}{dt} W_{\text{adap}} = -K_d \dot{e} \cdot \dot{e}.$$

□

## 4.4 Applications and Extensions

In what follows we describe examples of the design techniques and of the stability results presented so far. We start by describing some general issues in the design of error functions and transport maps.

### 4.4.1 On the Design of Error Functions and Transport Maps

As briefly mentioned in Section 4.3.2, criteria for the design of error functions are studied by Koditschek [53], where certain topological properties are suggested to obtain large regions of attraction. A second, often useful criteria for the design of an error function is the availability of matrix, rather than scalar, gains as a way of enforce different weighting onto different "error directions."

Methods for the design of transport map are more difficult to describe. First of all, the compatibility condition must be examined:

$$\mathrm{d}_2\varphi(q,r) = -\mathcal{T}^*_{(q,r)}\mathrm{d}_1\varphi(q,r).$$

This equation can be read in two ways: First, given a transport map $\mathcal{T}$, a compatible error function is computed via a partial differential equation. Alternatively, given an error function $\varphi$, a transport map is computed via a under-determined set of linear equations. Clearly, the latter method is usually preferred. In fact, all the examples we shall present in the next sections share this feature: the error function is designed first, and a compatible transport map later.

The search for an algebraically simple transport map is usually aided by the properties of the error function and of the manifold in question. Incidentally, this method is also silently employed in the literature, see for example the treatment we provide in Section 4.4.4. However, the current literature does not give any attention on this design issue and on the freedom in choosing $\mathcal{T}$.

Finally, given an error function and given a set of compatible transport maps, one imagines chosing the optimal one with respect to some appropriate cost criteria. In what follows, we do not investigate this issue and we focus on computing computationally simple transport maps.

### 4.4.2 A Pointing Device on the Two Sphere

We start by applying the main theorem to the sphere example described in Section 3.1.2 and Section 4.2.3. Form the Section 3.1.2, recall that there exist a natural Riemannian metric and corresponding connection on the sphere. Exploiting this structure the equations of motion have the simple expression

$$\nabla_{\dot{q}}\dot{q} = F, \tag{4.9}$$

where, for simplicity, we identify tangent and cotangent space of the sphere and write the input force $F$ as living on $T_q\mathbb{S}^2$. In Section 4.2.3 we designed a quadratic error function and

a compatible transport map as

$$\varphi(q,r) \triangleq 1 - q^T r \qquad \text{and} \qquad \mathcal{T}_{(q,r)} \triangleq (q^T r) I_3 + (r \times q)\widehat{\ },$$

where $r$ is the reference configuration on $\mathbb{S}^2$.

**Lemma 4.8 (Tracking on the sphere).** *Consider the system in equation* (4.9) *and let* $\{r(t), t \in \mathbb{R}_+\}$ *be a reference trajectory with* $\sup_t \|\dot{r}\|$ *bounded . Let* $k_p$ *and* $k_d$ *be two positive constants. Then the control law* $F = F_{\mathrm{PD}} + F_{\mathrm{FF}}$*, with*

$$\begin{aligned} F_{\mathrm{PD}} &= -k_p \widehat{q}^2 r \; - \; k_d\big(\dot{q} - q \times (r \times \dot{r})\big) \\ F_{\mathrm{FF}} &= \big(\dot{r}^T r \times q\big)(q \times \dot{q}) \; + \; q \times (r \times \nabla_{\dot{r}} \dot{r}), \end{aligned}$$

*exponentially stabilizes* $k_p \varphi(q,r) + \frac{1}{2}\|\dot{q} - \mathcal{T}_{(q,r)}\dot{r}\|^2$ *to zero from any initial condition* $q(0) \neq -r(0)$ *and for all* $\dot{q}(0), \dot{r}(0), k_p$ *such that*

$$k_p > \frac{\|\dot{q}(0) - \mathcal{T}_{(q,r)}\dot{r}(0)\|^2}{2\big(1 + q(0)^T r(0)\big)}.$$

*Proof.* In Section 4.2.3 we proved that $\varphi$ is quadratic (A1) and $\mathcal{T}$ is compatible (A2). Additionally, since $\mathbb{S}^2$ is compact, the conditions (B1–3) are satisfied, because of the smoothness of the metric, of $k_d$, of $\mathcal{T}$ and of $\varphi$. The assumption (B4) is explicitly made in the text.

Hence we only need to prove that the $F_{\mathrm{PD}}$ and the $F_{\mathrm{FF}}$ above are designed as prescribed by Theorem 4.6. Applying twice the equality $v \times (w \times z) = (v^T z)w - (v^T w)z$, we have

$$\begin{aligned} \mathcal{T}\dot{r} &= (q^T r)\dot{r} + (r \times q) \times \dot{r} = (q^T r)\dot{r} - (\dot{r}^T q) r \\ &= q \times (r \times \dot{r}), \end{aligned}$$

and

$$\frac{d}{dt}\Big|_{q \text{ fixed}} \big(\mathcal{T}_{(q,r)}\dot{r}\big) = q \times (r \times \ddot{r}) = q \times (r \times \nabla_{\dot{r}}\dot{r}).$$

Finally, following the description in Section 2.4, we compute the covariant derivative of the vector field $\big(\mathcal{T}\dot{r}\big)(q)$ by differentiating it with respect to time and then projecting the result onto the tangent plane at $q$. In formulas this reads as:

$$(\nabla_{\dot{q}}\mathcal{T})\dot{r} = \pi_q \left( \frac{d}{dt}\Big|_{r \text{ fixed}} \mathcal{T}\dot{r} \right) = -\widehat{q}^2 \left( \frac{d}{dt}\Big|_{r \text{ fixed}} \mathcal{T}\dot{r} \right).$$

Summarizing some algebraic equalities, we have

$$\begin{aligned} \big(\nabla_{\dot{q}}\mathcal{T}\big)\dot{r} &= -\widehat{q}^2\big(\frac{d}{dt}\Big|_{r \text{ fixed}} q \times (r \times \dot{r})\big) = -\widehat{q}\big(q \times (\dot{q} \times (r \times \dot{r}))\big) \\ &= -\widehat{q}\big(q^T(r \times \dot{r})\dot{q} - q^T\dot{q}(r \times \dot{r})\big) = (q^T r \times \dot{r})(\dot{q} \times q). \end{aligned}$$

This completes the proof. □

### 4.4.3 A Robotic Manipulator

In this section, we shall recover the standard results on tracking control of manipulators contained in [76]. As in Section 3.1.1, let $\theta \in \mathbb{R}^n$ be the joint variables and $M(\theta)$ be the inertia matrix of the manipulator. The design described in Section 4.2 is performed as follows.

Let $K$ be a symmetric positive definite matrix and let $\varphi(\theta, r) = \frac{1}{2}(\theta - r)^T K_p(\theta - r)$ be a quadratic error function. Thanks to the identification $T_\theta \mathbb{R}^n = T_r \mathbb{R}^n$, we let the transport map be equal to the identity matrix: $\mathcal{T}_{(\theta,r)} = I_n$. Assumptions (A1) and (A2) are easily verified. To design the feedforward action, we compute the covariant derivative of $I_n$. Let $\{\frac{\partial}{\partial \theta^1}, \dots, \frac{\partial}{\partial \theta^n}\}$ be the standard basis in $\mathbb{R}^n$, let $\{i, j, k, \dots\}$ be indices over $\theta$ and $\{\alpha, \beta, \dots\}$ be indices over $r$. Then, from equation (4.4)

$$(\nabla I_n)^i_{\alpha j} = \frac{\partial (I_n)^i_\alpha}{\partial \theta^j} + \Gamma^i_{jk} (I_n)^k_\alpha = \Gamma^i_{j\alpha},$$

Therefore, in contrast to a naive guess, the covariant derivative of the identity map is different from zero. Given a symmetric positive definite $K_d$, the control law is

$$\begin{aligned} F_{\mathrm{PD}} &= -K_p(\theta - r) - K_d(\dot\theta - \dot r) \\ F_{\mathrm{FF}} &= M(\theta)\Big((\nabla_{\dot\theta} I_n)\dot r + \frac{d}{dt}\Big|_{\theta \text{ fixed}} \dot r\Big) \\ &= M(\theta)\big(\Gamma^i_{j\alpha} \dot\theta^j \dot r^\alpha \tfrac{\partial}{\partial \theta^i} + \ddot r\big) \;\equiv\; M(\theta)\ddot r + C(\theta, \dot\theta)\dot r, \end{aligned} \tag{4.10}$$

where $C(\cdot, \cdot)$ is the Coriolis matrix typically encountered in robotics. The control law $F = F_{\mathrm{PD}} + F_{\mathrm{FF}}$ agrees with the one presented in [76, Chapter 4, Section 5.3] under the name of *augmented PD control*. The assumptions (B1–B4) can be written in terms of $\Gamma^k_{ij}$ and $\dot r$ being bounded over $t \in \mathbb{R}$ and $\theta \in \mathbb{R}^n$.

### Linearization by state transformations and by feedback

Sometimes a simple state transformation suffices for the linearization of the Euler-Lagrange equations. This happens when there exists a choice of local coordinates such that the Christoffel symbols vanish. If the designed described above is performed in this specific set of coordinates, the expression (4.10) for the feedforward control simplifies considerably since the cross term $(\dot\theta, \dot r)$ vanishes. More details on this case are discussed in [8].

More generally the Euler-Lagrange equations can be linearized by means of a feedback transformation. By setting

$$F = M^{-1}(\theta)\Big(U - C(\theta, \dot\theta)\Big)\dot\theta, \tag{4.11}$$

we have that the equations of motion

$$M(\theta)\ddot\theta + C(\theta, \dot\theta)\dot\theta = F$$

become

$$\ddot\theta = U.$$

A tracking controller can then be designed using linear techniques. This design procedure is the so-called *computed torque method*; see [76, Chapter 4, Section 5.2]. Note that a controller designed this way depends on the initial choice of the coordinates system $(\theta^1, \dots, \theta^n)$.

We reconcile this method with our framework as follows. Let $\overline{\nabla}$ be the connection characterized by vanishing Christoffel symbols in the chart $\{\theta^1, \dots, \theta^n\}$. Then the equality $\ddot\theta = U$ can be written as $\overline{\nabla}_{\dot\theta}\dot\theta = U$, hence as a mechanical system. In other words, we regard the feedback transformation (4.11) as a "change of connection" from $\nabla$ to $\overline{\nabla}$. This idea is described in some theoretical details in [52, Proposition 7.10]. Summarizing, the computed torque method falls within the scope of Theorem 4.6 if feedback pre-transformations are allowed.

### 4.4.4 A Satellite with Three Thrusters

In the next two sections we design tracking controllers for mechanical systems defined on the group of rotations SO(3) and on the group of rigid motions SE(3). We focus on rigid bodies with body-fixed forces and invariant kinetic energy, as satellites and underwater vehicles. Nevertheless our treatment is relevant also for workspace control of robotic manipulators. This section presents the attitude control problem for a fully actuated satellite; see Section 3.2.2 for the model.

#### Error Functions

Let $\{R_d(t), t \in \mathbb{R}_+\}$ denote the reference trajectory corresponding to a desired or reference frame and let $\widehat{\Omega}_d = R_d^T \dot{R}_d$ denote the reference velocity in the reference frame. Using the group operation, we define right and left attitude errors as

$$R_{e,r} \triangleq R_d^T R \qquad \text{and} \qquad R_{e,\ell} \triangleq R R_d^T. \tag{4.12}$$

The matrix $R_{e,r}$ is the relative rotation from the body frame to the reference frame. Two error functions are then defined as $\varphi_r(R, R_d) \triangleq \phi(R_{e,r})$ and $\varphi_\ell(R, R_d) \triangleq \phi(R_{e,\ell})$, where $\phi : \mathrm{SO}(3) \to \mathbb{R}_+$ is defined as [53]

$$\phi(R_e) \triangleq \frac{1}{2} \operatorname{tr}\left(K_p(I_3 - R_e)\right).$$

If the eigenvalues $\{k_1, k_2, k_3\}$ of the symmetric matrix $K_p$ satisfy $k_i + k_j > 0$ for $i \neq j$, then both error functions $\varphi_\ell$ and $\varphi_R$ are symmetric, positive definite and quadratic with constant $L = \min_{i \neq j}(k_i + k_j)$. Locally near the identity the function $\phi$ assigns a weight $k_2 + k_3$ to a rotation error about the first axis (and similarly for the other axes). Appendix A contains the proof of these facts and the expression of $\phi$ in the unit quaternion representation.

#### Velocity Errors

To define compatible velocity errors, we compute the time derivative of the two error functions. Let the matrix $\mathrm{skew}(A)$ denote $\frac{1}{2}(A - A^T)$ and let $\cdot^\vee$ denote the inverse operator to $\widehat{\cdot} : \mathbb{R}^3 \to \mathfrak{so}(3)$. We have

$$\frac{d}{dt}\varphi_r = \left(\mathrm{skew}(K_p R_{e,r})^\vee\right)^T \Omega_{e,r}, \tag{4.13}$$

$$\frac{d}{dt}\varphi_\ell = \left(\mathrm{skew}(K_p R_{e,\ell})^\vee\right)^T R_d\, \Omega_{e,\ell}, \tag{4.14}$$

where we define right and left velocity errors in the body frame as

$$\Omega_{e,r} \triangleq \Omega - R_{e,r}^T \Omega_d \qquad \text{and} \qquad \Omega_{e,\ell} \triangleq \Omega - \Omega_d.$$

Note the slightly improper wording, since a velocity error $\dot{e} = \dot{R} - \mathcal{T}\dot{R}_d$ lives on the tangent bundle $T_R\mathrm{SO}(3)$. A precise statement is

$$\dot{e}_\ell = R\widehat{\Omega}_{e,\ell} \equiv \dot{R} - \left(R R_d^T\right)\dot{R}_d,$$
$$\dot{e}_r = R\widehat{\Omega}_{e,r} \equiv \dot{R} - \dot{R}_d\left(R_d^T R\right).$$

These equalities also motivate the names "left" and "right." A left (right) velocity error is obtained by left (right) translation of the velocity $\dot{R}_d$.

Next we describe compatible couples of configuration and velocity errors. Equation (4.13) suggests that a right attitude error $R_d^T R$ and a right velocity error $\Omega - R^T R_d \Omega_d$ are compatible. This couple is the most common choice in the literature; see for example [73, 53, 103, 36].

Left attitude and velocity error appear less frequently [69]. With this choice both the velocity error and, as we show below, the feedforward control have a simple expression. Remarkably, when the gain $K_p$ is a scalar multiple of the identity $k_p I_3$, the left and right error functions are equal and the couple $(\varphi_{e,r}, \Omega_{e,\ell})$ is compatible. Finally, coordinate based approaches are also possible. The velocity error in [87] is taken to be the difference between the rate of change of the Gibbs vectors for actual and reference attitude. Similarly, in the flight control literature, Euler angles and their rates are often used; see Etkin [37].

### Control Laws and Simulations

Finally we summarize the design process.

**Lemma 4.9.** *Consider the system in equation* (3.9). *Let* $\{R_d(t), t \in \mathbb{R}_+\}$ *denote the reference trajectory and let* $\widehat{\Omega}_d = R_d^T \dot{R}_d$ *denote its bounded body-fixed velocity. Corresponding to the two choices of attitude error, we define*

$$\begin{aligned} f_r &= -\operatorname{skew}(K_p R_{e,r})^\vee \quad -K_d \Omega_{e,r} + \Omega \times \mathbb{J}(R_{e,r}^T \Omega_d) + \mathbb{J}(R_{e,r}^T \dot{\Omega}_d), \\ f_\ell &= -R_d^T \operatorname{skew}(K_p R_{e,\ell})^\vee - K_d \Omega_{e,\ell} + \Omega_d \times \mathbb{J}\Omega + \mathbb{J}\dot{\Omega}_d, \end{aligned}$$

*where* $K_d$ *is a positive definite matrix and* $K_p$ *is a symmetric matrix with eigenvalues* $\{k_1, k_2, k_3\}$ *such that* $k_i + k_j > 0$ *for* $i \neq j$.

*Then, for both choices of attitude error, the total energy* $\phi(R_e) + \frac{1}{2}\|\Omega_e\|_{\mathbb{J}}^2$ *converges exponentially to zero from all initial conditions* $(R(0), \Omega(0))$ *such that*

$$\phi(R_e(0)) + \frac{1}{2}\|\Omega_e(0)\|_{\mathbb{J}}^2 \; < \; \min_{i \neq j}(k_i + k_j).$$

This lemma is a direct consequence of Theorem 4.6, except for the design of the feedforward control which is discussed in the next section. To the authors' knowledge, both control laws are novel: $f_\ell$ in the choice of velocity error, $f_r$ in the expression of the feedforward control.

To illustrate the difference between the two velocity errors, we run simulations without the PD action. The reference trajectory is a $2\pi$ radians rotation about the vertical $Z$ axis performed in 10 seconds with velocity profile of $2\pi(3t^2 - t)/100$ radians per second. The initial attitude error is a rotation of $\pi/4$ radians about the $X$ axis. Both the angular velocity and the reference angular velocity are zero at time $t = 0$ and therefore the velocity error is zero for all times. Indeed, the latter property characterizes the two simulations completely: on the left side of Figure 4.4 we have $\dot{R}(t) = R(t)\widehat{\Omega}_d(t)$, on the right side $\dot{R}(t) = (R_d(t)\Omega_d(t))\widehat{\ } R(t)$. We note the very different qualitative behavior of the two closed-loop simulations.

## 4.4.5 An Underwater Vehicle with Six Actuators

In this section we extend the treatment of the attitude tracking problem to the group of rigid rotations and translations $\mathrm{SE}(3) = \mathrm{SO}(3) \times \mathbb{R}^3$. We focus on the idealized model of an underwater vehicle, described in Section 3.2.3.

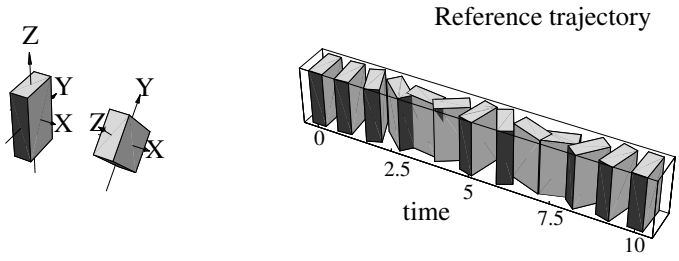


Figure 4.3: Bricks represent rotation matrices. On the left we depict initial reference attitude and initial error (i.e., a rotation of $\pi/4$ about the $X$ axis). On the right we depict the reference attitude trajectory.

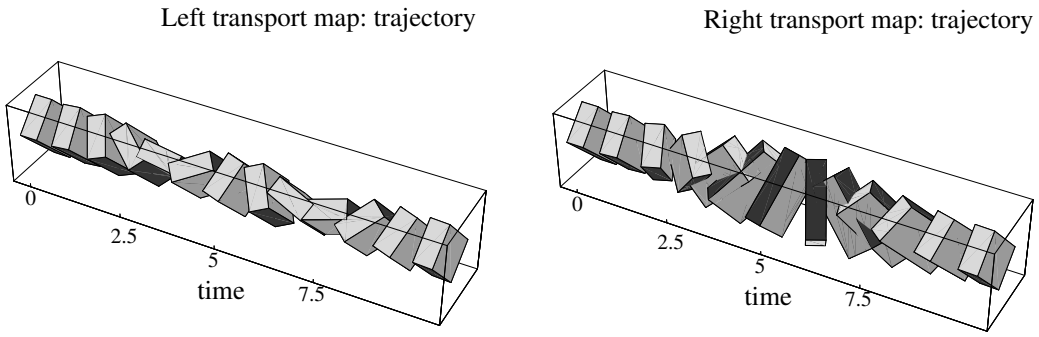


Figure 4.4: Trajectories in the closed loop help us compare feedforward policies. Left and right velocity errors are employed correspondingly on the left and right picture.

### Error Functions

Let $\{g_d = (R_d, p_d), t \in \mathbb{R}_+\}$ denote the reference trajectory corresponding to a desired frame and let $\xi_d = (\Omega_d, V_d)$ denote the reference velocity expressed in the desired frame, that is $\dot{g}_d = g_d \cdot \xi_d$. As in the SO(3) case, we design an error function $\varphi$ by composing a group error $g_e(g, g_d)$ and a positive definite function $\phi : \mathrm{SE}(3) \to \mathbb{R}$.

The group operation on SE(3) provides us with right and left group errors

$$g_{e,r} \triangleq g_d^{-1} g = \left(R_d^T R,\ R_d^T (p - p_d)\right),$$
$$g_{e,\ell} \triangleq g g_d^{-1} = \left(R R_d^T,\ p - R R_d^T p_d\right).$$

The group element $g_{e,r}$ is the relative motion from the body frame to the desired frame. Disregarding the group structure, two other group errors are

$$g_{e,1} \triangleq \left(R_d^T R,\ p - p_d\right) \quad \text{and} \quad g_{e,2} \triangleq \left(R R_d^T,\ R^T p - R_d^T p_d\right).$$

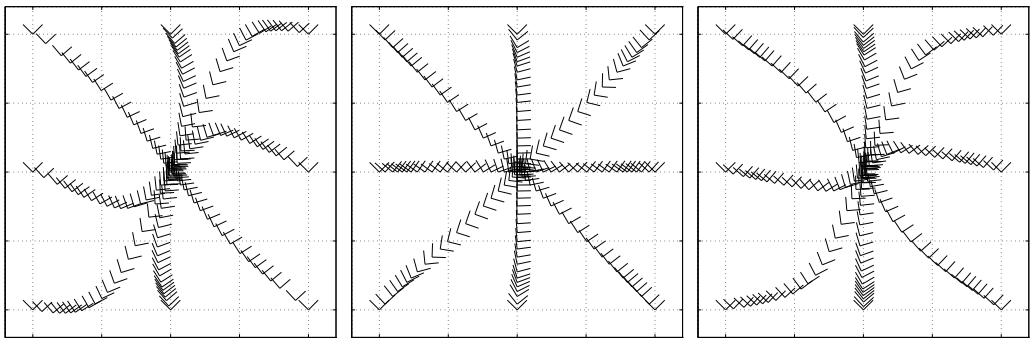

Figure 4.5: From left to right the functions $\phi_1$, $\phi_2$ and $\phi_3$ are compared in terms of the flow of their gradient. Each frame on the plane represents a configuration on SE(2).

Next we design some positive definite functions on SE(3). We set

$$\begin{aligned}
\phi_1(R,p) &= \frac{1}{2}\operatorname{tr}(K_1(I_3 - R)) + \frac{1}{2}p^T K_2 p \quad \triangleq \quad \phi_1(R) + \frac{1}{2}\|p\|^2_{K_2}, \\
\phi_2(R,p) &= \phi_1(R) + \frac{1}{2}\|R^T p\|^2_{K_2}, \\
\phi_3(R,p) &= \phi_1(R) + \frac{1}{2}\|(I_3 + R^T)p\|^2_{K_2},
\end{aligned}$$

where the eigenvalues $\{k_1, k_2, k_3\}$ of the symmetric matrix $K_1$ satisfy $k_i + k_j > 0$ for $i \neq j$, and where $K_2$ is positive definite. The presence of matrix gains in both the attitude and position variables is useful in applications.

In Fig. 4.5 we attempt to portray these functions restricted to SE(2), the group of rigid motions on the plane. We equip this space with an invariant metric (kinetic energy) of the form $J\omega^2 + m_x v_x^2 + m_y v_y^2$, where $(\omega, v_x, v_y)$ is the velocity in the body frame. Then we compute the gradient vector field for each of the three error functions and we draw their flow fields. The gains on rotational and translational components are chosen equal to $(J, m_x, m_y)$.

Finally we design error functions by combining a group error $g_e$ with a function $\phi$. For all choices of $g_e$ and $\phi$, the resulting error function $\varphi$ is quadratic with constant $\min_{i \neq j}(k_i + k_j)$, where $\{k_1, k_2, k_3\}$ are the eigenvalues of the matrix $K_1$. Since many combinations are possible, we report only the most instructive ones in the first column of Table 4.1. In the third column we characterize the error functions in terms of various properties. For example, we call $\varphi$ *invariant* if it is invariant under changes in the inertial coordinate frame. Also recall that $\varphi$ is symmetric if $\varphi(g, g_d) = \varphi(g_d, g)$. Additionally, we specify the frame in which the proportional gains $K_1$ and $K_2$ are expressed.

### Velocity Errors

We start by recalling some kinematics [76, Chapter 2]. We are interested in the adjoint map $\mathrm{Ad}_g : \mathfrak{se}(3) \to \mathfrak{se}(3)$ that transforms velocity vectors (elements in $\mathfrak{se}(3)$) from the body coordinate frame to the inertial coordinate frame. Identifying $\mathfrak{se}(3)$ with $\mathbb{R}^6$, this map is

$$\mathrm{Ad}_g = \mathrm{Ad}_{(R,p)} = \begin{bmatrix} R & 0 \\ \hat{p}R & R \end{bmatrix}.$$

Table 4.1: Error functions and transport elements on SE(3).

| Error function | Transport element | Comments |
|---|---|---|
| $\phi_1(R_d^T R) + \frac{1}{2}\|p - p_d\|^2_{K_2}$ | $(R^T R_d, 0)$ | $\phi_1(g_{e,1})$, not invariant, symmetric, gains expressed in inertial frame. |
| $\phi_1(R_d^T R) + \frac{1}{2}\|R_d^T(p - p_d)\|^2_{K_2}$ | $g^{-1}g_d$ | $\phi_1(g_{e,r})$, invariant, not symmetric, gains expressed in reference frame. |
| $\phi_1(R_d^T R) + \frac{1}{2}\|R^T(p - p_d)\|^2_{K_2}$ | $g^{-1}g_d$ | $\phi_2(g_{e,r})$, invariant, not symmetric, gains expressed in body frame. |
| $\phi_1(R_d^T R) + \frac{1}{2}\|(R^T + R_d^T)(p - p_d)\|^2_{K_2}$ | $g^{-1}g_d$ | $\phi_3(g_{e,r})$, invariant, symmetric. |
| $\phi_1(RR_d^T) + \frac{1}{2}\|(R + R_d)(p - p_d)\|^2_{K_2}$ | $(I_3, 0)$ | $\phi_3(g_{e,\ell})$, not invariant, symmetric. |
| $\phi_1(RR_d^T) + \frac{1}{2}\|R^T p - R_d^T p_d\|^2_{K_2}$ | $(I_3, R_d^T p_d - R^T p)$ | $\phi_1(g_{e,2})$, not invariant, symmetric. |

More generally, since $g_{e,r} = g_d^{-1} g$ is the relative motion from the body frame to the desired frame, the reference velocity in the desired frame $\xi_d$ is expressed in the body frame via the map $\mathrm{Ad}_{g^{-1}g_d} = \mathrm{Ad}_{g_{e,r}^{-1}}$. These ideas lead to a natural definition of velocity error as

$$\xi_{e,r} = \xi - \mathrm{Ad}_{g_{e,r}^{-1}} \xi_d,$$

where the body and the reference velocities are expressed in the same frame. We call $\xi_{e,r}$ the right velocity error. This is a useful definition since, with the aid of the homogeneous representation and some matrix algebra, we have

$$\begin{aligned} \dot{g}_{e,r} &= g_d^{-1}\left(\frac{d}{dt} g\right) + \left(\frac{d}{dt} g_d^{-1}\right) g = g_d^{-1} g \cdot \xi - \xi \cdot g_d^{-1} g \\ &\equiv g_{e,r}\left(\xi - \mathrm{Ad}_{g_{e,r}^{-1}} \xi_d\right). \end{aligned}$$

Therefore, every error function that relies on the right group error $g_{e,r}$ is compatible with the right velocity error.

More generally the adjoint map is useful in describing transport maps. In what follows, we parametrize the set of transport maps with the set of change of frames, that is with SE(3). For each transport map $\mathcal{T}$, we call *transport element* the unique motion $\tau \in \mathrm{SE}(3)$ such that

$$\dot{g} - \mathcal{T}\dot{g}_d = g \cdot (\xi - \mathrm{Ad}_\tau \xi_d).$$

In the Table 4.1, we report compatible transport elements for each error function. For each couple $(\varphi, \tau)$, the compatibility is verified with some straightforward algebra. Note that the choice of $\tau$ depends only on the group error $g_e$ employed to define $\varphi$.

### Control Laws

We here summarize the ideas exposed so far and design a proportional derivative feedback. Additionally we devise a set of feedforward control laws by means of a minor extension of Theorem 4.6. Let $\langle \cdot, \cdot \rangle$ denote the natural pairing between $\mathfrak{se}(3)$ and its dual $\mathfrak{se}(3)^*$, and let $(\varphi, \tau)$ be a compatible pair of error function and transport element. We define $f_{\mathrm{P}}, f_{\mathrm{D}} \in \mathfrak{se}(3)^*$ by means of

$$\begin{aligned} \langle f_{\mathrm{P}} \ , \ \eta \rangle &= -\mathcal{L}_{(g \cdot \eta, \, 0)} \varphi(g, g_d), \qquad && \forall \eta \in \mathfrak{se}(3), \\ f_{\mathrm{D}} &= -K_d \left( \xi - \mathrm{Ad}_\tau \, \xi_d \right), \end{aligned} \tag{4.15}$$

where $K_d : \mathfrak{se}(3) \mapsto \mathfrak{se}(3)^*$ is a self-adjoint (symmetric) and positive definite. For example, from the first row of Table 4.1 we compute

$$f_{\mathrm{P}} + f_{\mathrm{D}} = - \begin{bmatrix} \mathrm{skew}(K_1 R_e)^\vee \\ R^T K_2 p_e \end{bmatrix} - K_d \begin{bmatrix} \Omega - R_e^T \Omega_d \\ V - R_e^T V_d \end{bmatrix},$$

where $(R_e, p_e) = (R_d^T R, \ p - p_d)$, and likewise from the third row

$$f_{\mathrm{P}} + f_{\mathrm{D}} = - \begin{bmatrix} \mathrm{skew}(K_1 R_e)^\vee + (K_2 p_e) \times p_e \\ R^T K_2 p_e \end{bmatrix} - K_d \begin{bmatrix} \Omega - R_e^T \Omega_d \\ V - R_e^T \left( V_d + \Omega_d \times p_e \right) \end{bmatrix},$$

where $(R_e, p_e) = (R_d^T R, \ R_d^T (p - p_d))$. Next, we define a family of feedforward control laws as

$$f_{\mathrm{FF}} = - \mathrm{ad}^*_{(\mathrm{Ad}_\tau \, \xi_d)} \, \xi + \mathbb{I} \frac{d}{dt} (\mathrm{Ad}_\tau \, \xi_d) + S_\tau (\xi_e, \xi_d), \tag{4.16}$$

where the bilinear operator $S_\tau : \mathfrak{se}(3) \times \mathfrak{se}(3) \mapsto \mathfrak{se}(3)^*$ is skew symmetric with respect to its first argument, i.e., it holds

$$\langle S_\tau (\xi_e, \eta), \xi_e \rangle = 0, \qquad \forall \eta \in \mathfrak{se}(3). \tag{4.17}$$

For example, corresponding to $\tau = g^{-1} g_d$, (second, third and fourth row in Table 4.1, right group error $g_{e,r}$) and $\tau = (I_3, 0)$, (fifth row in Table 4.1, left group error $g_{e,\ell}$), an appropriate choice of $S_\tau$ leads to the simple feedforward controls:

$$\begin{aligned} f_{\mathrm{FF},r} &= \ - \mathrm{ad}^*_\xi \, \mathbb{I} \mathrm{Ad}_{g^{-1} g_d} \, \xi_d \ + \ \mathbb{I} \, \mathrm{Ad}_{g^{-1} g_d} \, \dot{\xi}_d, \\ f_{\mathrm{FF},\ell} &= \ - \mathrm{ad}^*_{\xi_d} \, \mathbb{I} \xi \ + \ \mathbb{I} \dot{\xi}_d. \end{aligned}$$

Note that, with the corresponding definition of Ad and ad operators, these choices are the same employed for the attitude tracking problem in Lemma 4.9.

**Lemma 4.10.** *Consider the system in equation* (3.11) *and* (3.12). *Let* $\{g_d(t), t \in \mathbb{R}_+\}$ *denote the reference trajectory and let* $\xi_d = g_d^{-1} \dot{g}_d \in \mathfrak{se}(3)$ *denote its bounded body-fixed velocity. From Table 4.1, let* $\varphi$ *be a quadratic error function with constant* $\min_{i \neq j}(k_i + k_j)$, *and let* $\tau$ *be a compatible transport element. Also, let* $S_\tau$ *be a bilinear operator satisfying* (4.17), *and according to equations* (4.15) *and* (4.16), *let*

$$f = f_{\mathrm{P}} + f_{\mathrm{D}} + f_{\mathrm{FF}} \quad \in \mathfrak{se}(3)^*.$$

*Then the total energy* $\varphi(g, g_d) + \frac{1}{2} \| \xi - \mathrm{Ad}_\tau \, \xi_d \|^2_{\mathbb{I}}$ *converges exponentially to zero from all*

*initial conditions* $(g(0), \xi(0))$ *such that*

$$\varphi\big(g(0), g_d(0)\big) + \frac{1}{2}\|\xi(0) - \mathrm{Ad}_{\tau(0)}\,\xi_d(0)\|_{\mathbb{I}}^2 \;<\; \min_{i\neq j}(k_i + k_j).$$

In what follows we present a sketch of the proof. First, the proportional and derivative feedback are devised according to the design procedure in Section 4.2, so that the only difference with the design in Theorem 4.6 regards the feedforward control. In fact, the latter theorem can be extended as follows.

**Lemma 4.11.** *Let the map* $S_{(q,r)} : T_qQ \times T_rQ \to T_q^*Q$ *satisfy*

$$S_{(q,r)}(X_q, Y_r) \cdot X_q = 0,$$

*for all* $X_q \in T_qQ$ *and* $Y_r \in T_rQ$. *Also consider the boundedness condition:*

$$\sup_{(q,r)\in Q\times Q} \|\nabla \mathcal{T}_{(q,r)} + M_q^{-1} S\|_M < \infty. \tag{B2'}$$

*The statement of Theorem 4.6 holds true if we set* $F = F_{\mathrm{PD}} + F_{\mathrm{FF}} + S(\dot{e}, \dot{r})$ *instead of* $F = F_{\mathrm{PD}} + F_{\mathrm{FF}}$, *and if we assume* (B2') *instead of condition* (B2).

The proof of this statement is a straightforward modification of the proof of Theorem 4.6. Thus we only need to show that feedforward action $f_{\mathrm{FF}}$ in equation (4.16) differs from the one defined in the main theorem, call it $f'_{\mathrm{FF}}$, by a skew symmetric operator. Indeed, using some of the tools introduced in Section (2.4), we compute

$$f'_{\mathrm{FF}} = \mathbb{I}\,{}_{\mathfrak{g}}\nabla_{\xi}\,(\mathrm{Ad}_t\,\xi_d) + \frac{d}{dt}\,(\mathrm{Ad}_t\,\xi_d)\,,$$

where the map ${}_{\mathfrak{g}}\nabla : \mathfrak{g} \times \mathfrak{g} \to \mathfrak{g}$ is defined in equation (2.12), and $f_{\mathrm{FF}} = f'_{\mathrm{FF}}$ when the operator $S_\tau$ is defined as

$$S_\tau(\xi_e, \xi_d) = \frac{1}{2}\left(\mathbb{I}[\xi_e, \mathrm{Ad}_t\,\xi_d] + \mathrm{ad}^*_{(\mathrm{Ad}_t\,\xi_d)}\,\mathbb{I}\xi_e - \mathrm{ad}^*_{\xi_e}(\mathrm{Ad}_t\,\xi_d)\right).$$

# Chapter 5

# Exponential Stabilization of Relative Equilibria of Underactuated Systems

In this chapter we present some stabilization techniques for underactuated mechanical systems. We focus on relative equilibria arising from one-dimensional symmetries. Recall that a mechanical system admits a symmetry whenever the Lagrangian is invariant under a group action on the configuration manifold. When this happens, it is possible to have steady motions, called relative equilibria, along the group action. The key design idea is to distinguish between horizontal forces, which preserve the momentum, and vertical forces that affect it.

The chapter is organized as follows. In Section 5.1 we review some key notions on the theory of nonlinear stabilization. Section 5.2 presents some concepts about symmetries and relative equilibria. An effort is made to present only the necessary notions. Section 5.3 presents the control design with assumptions, statement of the main result and proof. Finally, in Section 5.4 we apply the technique to a planar body with two forces and a satellite with two thrusters. A preliminary version of this chapter was presented in [20]; the treatment builds on the previous contributions in [60, 47].

## 5.1 Review of Stabilization Theory for Nonlinear Systems

In this section we review some basic tools in stabilization of nonlinear control systems. A combination of Lyapunov techniques and controllability analysis turns out to be quite useful.

**Nonlinear analysis**

Let $M$ be a smooth $n$-dimensional manifold and consider the smooth control system

$$\dot{x} = f(x) + \sum_i g_i(x)u_i. \tag{5.1}$$

Let $x_0$ be an equilibrium point for $f$, and assume $V : M \to \mathbb{R}_+$ is a smooth function and $\epsilon > 0$ such that

$$\begin{aligned} V(x) &> 0, \qquad \forall x \neq x_0 \in B_\epsilon(x_0), \\ V(x_0) &= 0, \end{aligned} \tag{5.2}$$

where $B_\epsilon(x_0)$ is a neighborhood of $x_0$. If

$$\begin{aligned} 0 &= \mathcal{L}_f V(x), \\ u_i(x) &= -\mathcal{L}_{g_i} V(x), \end{aligned} \tag{5.3}$$

the solution $x(t)$ of the differential equation above with initial condition in a neighborhood of $x_0$ will converge to the largest invariant set contained in $\mathcal{L}_{g_i} V(x) = 0$. This is proven via Lasalle's principle.

Additionally, if

$$\dim\{g_i, \mathrm{ad}_f\, g_i, \ldots, \mathrm{ad}_f^n\, g_i,\ \forall i\}(x_0) = n, \tag{5.4}$$

the solution $x(t)$ will converge asymptotically to the point $x_0$. This is proven as follows. Points $x$ in the invariant set of $f$ that satisfy $\mathcal{L}_{g_i} V(x) = 0$ must also satisfy $\mathcal{L}_f^k \mathcal{L}_{g_i} V(x) = 0$ for all $k$. But this is equivalent to satisfying $\mathcal{L}_{\mathrm{ad}_f^k\, g_i} V(x) = 0$ for all $k$. Equation (5.4) says that the distribution $\{\mathrm{ad}_f^k\, g_i, \forall i, k\}$ has full rank at $x_0$ and therefore in a neighborhood of the point. It follows that the invariant set is locally characterized by $0 = \mathcal{L}_X V(x) = \langle \mathrm{d}V, X \rangle\,(x)$ for any tangent vector $X_x \in T_x M$. Therefore, the invariant set coincides with the isolated solution of $\mathrm{d}V(x) = 0$, which is $x_0$, thanks to equation (5.2).

More refined tests are discussed in Section 10.2 in [78]. We summarize the previous discussion as follows.

**Lemma 5.1.** *Consider the nonlinear control system* (5.1) *with $x$ taking values on a smooth manifold $M$ and let $x_0$ be an equilibrium point. Assume the function $V$ and the feedback law $u(x)$ satisfy the conditions in* (5.2) *and* (5.3). *The point $x_0$ is locally asymptotically stable if the rank condition* (5.4) *holds.*

### Linearized Analysis

Next we examine the stability properties of the linearization of the control system (5.1). This analysis leads to a stronger stability result for the original nonlinear system.

Consider a local chart about the point $x_0$. With no loss in generality we let $x \in \mathbb{R}^n$ denote a coordinate system about the point $x_0 = 0$. In addition, we let $f, g_i, V$ and so forth denote the corresponding quantities in the coordinate system. The first observation is that the rank condition in equation (5.4) correspond exactly to the so-called linear controllability test. In other words, if condition (5.4) holds, then the nonlinear control system (5.1) is linearly controllable at the point $x_0$; see Section 3.1 in [78].

To linearize the system in equation (5.1) and the feedback in equation (5.3), we introduce the symbol $O(x^k)$ to denote a quantity that is of the same order as $\|x\|^k$. We compute the necessary Taylor series and employ the following standard notation:

$$\begin{aligned} f(x) &= Ax + O(x^2), \\ g_i(x) &= b_i + O(x), \\ V(x) &= \frac{1}{2} x^T P x + O(x^3). \end{aligned}$$

Accordingly, we compute

$$\mathcal{L}_f V(x) = \mathcal{L}_{Ax}\left(\frac{1}{2} x^T P x\right) + O(x^3), \tag{5.5}$$

$$\mathcal{L}_{g_i} V(x) = \mathcal{L}_{b_i}\left(\frac{1}{2} x^T P x\right) + O(x^2), \tag{5.6}$$

and we can now state the following result.

**Lemma 5.2.** *Consider the nonlinear control system* (5.1) *with* $x \in \mathbb{R}^n$ *and let* 0 *be an equilibrium point. Assume the conditions in equations* (5.2), (5.3) *and* (5.4). *If the second variation of* $V$ *at* $x = 0$ *is positive definite, i.e., if*

$$\frac{\partial^2 V}{\partial x \partial x}(0) = P > 0, \tag{5.7}$$

*then the point* $x = 0$ *is locally exponentially stable.*

*Proof.* We claim that the point $x = 0$ is asymptotically stable for the linear system $\dot{x} = Ax + \sum b_i u_i$. But, because the system is linear, the convergence is exponential and therefore $x = 0$ is an exponentially stable point for the original nonlinear system.

To prove that $x = 0$ is an asymptotically stable point for the linear system $\dot{x} = Ax + \sum b_i u_i$, we need to show that the triplet $(A, b_i, P)$ satisfies the assumptions in the previous lemma:

(i) The condition in equation (5.2) on $\frac{1}{2}x^T P x$ being positive definite is explicitly assumed as equation (5.7).

(ii) The two equalities in equation (5.3) become

$$0 = \mathcal{L}_{Ax}\left(\frac{1}{2}x^T P x\right), \qquad \text{and} \qquad \tilde{u}_i = \mathcal{L}_{b_i}\left(\frac{1}{2}x^T P x\right),$$

where $\tilde{u}_i$ is now the linearization of the input for the nonlinear system $u_i = \mathcal{L}_{g_i} V(x)$. Both these equalities are consequences of equations (5.5) and (5.6).

(iii) Regarding the condition in equation (5.4), it is a well-known fact that $\mathrm{ad}_f^k g_i(x_0) = (-1)^k A^k b_i$ when $A$ and $b_i$ are defined as above; see [78].

□

*Remark 5.3 (On exponential versus asymptotic stability).* Exponential stability is a much stronger property than asymptotic stability, since an exponentially stable system automatically enjoys various robustness and optimality properties; see for example the treatment in Chapter 4 in [51].

A specific result we will need later is the following. Consider an interconnected system of the form

$$\begin{aligned} \dot{x} &= f(x) + yg(x, y) \\ \dot{y} &= h(y), \end{aligned}$$

where $x \in \mathbb{R}^n, y \in \mathbb{R}$, and $f, g, h$ are smooth vector fields of the appropriate dimensions. If $x = 0$ is an exponentially stable equilibrium point for $f$ and similarly $y = 0$ is an exponentially stable equilibrium point for $h$, then the point $(x, y) = (0, 0)$ is exponentially stable for the interconnected system above. The direct proof is based on linearizing both vector fields and recalling that the eigenvalue of a matrix in upper block triangular form coincides with the eigenvalues of the diagonal blocks.

## 5.2 Mechanical Systems with Abelian Symmetries

Consider a simple mechanical control system with equations of motion

$$M_q \nabla_{\dot{q}} \dot{q} \;=\; -\mathrm{d}V(q) + \sum_{k=1}^{m} F^k(q) u_k. \tag{5.8}$$

Roughly speaking, a symmetry of the mechanical system is a group action that leaves kinetic and potential energy invariant. We refer to [52, 72] for the most general definition of group action and principal fiber bundle. In what follows, we present a simplified treatment for the trivial one-dimensional case.

The mechanical system (5.8) is said to have a *trivial Abelian symmetry* if the following two fact hold. First, the manifold $Q$ can be written as $Q = R \times G$, where $(G, +)$ is either the torus or the real line. Correspondingly, the configuration is $q = (r, x) \in R \times G$, and the smooth diffeomorphism of $Q$ defined by $(y, (r, x)) = (r, x + y)$ is called *group action*. Second, the kinetic energy $\langle M_q \dot{q}, \dot{q} \rangle$ and potential energy $V(q)$ are *invariant* under the action of $G$, that is

$$\pounds_{\frac{\partial}{\partial x}} V = 0, \qquad \text{and} \qquad \pounds_{\frac{\partial}{\partial x}} M = 0.$$

The vector field $\partial/\partial x$ is called an infinitesimal isometry or the infinitesimal generator of the group action.

Whenever a symmetry is present, the *momentum map* $\mu$ is defined as a one-form, that is a map $TQ \to \mathbb{R}$, that satisfies

$$\mu(X_q) \triangleq \langle\!\langle X_q \,,\, \frac{\partial}{\partial x} \rangle\!\rangle \qquad X_q \in T_q Q.$$

The well-known Noether's theorem states that the value of the momentum map is constant along the solutions to the unforced mechanical system.

**Theorem 5.4.** *Consider the mechanical control system in equation* (5.8) *with a Abelian symmetry. It holds*

$$\frac{d}{dt}\mu(\dot{q}) = \sum_{k=1}^{m} \langle F^k \,,\, \frac{\partial}{\partial x} \rangle u_k. \tag{5.9}$$

*Proof.* As described in [35], the vector field $\partial/\partial x$ enjoys the so-called Killing property

$$\langle\!\langle X_q \,,\, \nabla_{X_q} \frac{\partial}{\partial x} \rangle\!\rangle = 0, \qquad \forall X_q \in T_q Q.$$

Using this property and some equalities described in Section 2.3, we compute:

$$\begin{aligned}
\frac{d}{dt}\mu(\dot{q}) = \nabla_{\dot{q}}\mu(\dot{q}) &= \nabla_{\dot{q}} \langle\!\langle \dot{q} \,,\, \frac{\partial}{\partial x} \rangle\!\rangle = \langle\!\langle \nabla_{\dot{q}} \dot{q} \,,\, \frac{\partial}{\partial x} \rangle\!\rangle + \langle\!\langle \dot{q} \,,\, \nabla_{\dot{q}} \frac{\partial}{\partial x} \rangle\!\rangle \\
&= \langle\!\langle M_q^{-1} \big( -\mathrm{d}V(q) + \sum_{k=1}^{m} F^k u_k \big) \,,\, \frac{\partial}{\partial x} \rangle\!\rangle \\
&= -\langle \mathrm{d}V(q) \,,\, \frac{\partial}{\partial x} \rangle + \sum_{k=1}^{m} \langle F^k \,,\, \frac{\partial}{\partial x} \rangle u_k.
\end{aligned}$$

The result follows from $\partial V/\partial x = 0$. □

Given $\mu_0 \in \mathbb{R}$, we define the *locked inertia* $I(r)$ and the *amended potential* $V_{\mu_0}(r)$ as

$$I(r) = \langle\!\langle \frac{\partial}{\partial x}, \frac{\partial}{\partial x} \rangle\!\rangle,$$
$$V_{\mu_0}(r) = V(r) + \frac{1}{2} I(r)^{-1} \mu_0^2,$$

where we write $V(q) = V(r)$ thanks to $\partial V / \partial x = 0$. A *relative equilibrium* is a pair $(\mu_0, r_0)$, where $\mu_0 \in \mathbb{R}$ and $r_0 \in R$ is a critical point of $V_{\mu_0}$, i.e., a point such that $\mathrm{d}V_{\mu_0}(r_0)$ vanishes. Notice that, while this definition differs from the one presented in Chapter 3, the two can be reconciled within the more general framework presented in [72].

If $(\mu_0, r_0)$ is a relative equilibrium, then any curve of the form $\{(r(t), x(t)) \in Q \,|\, r(t) = r_0,\ \dot{x}(t) = \mu_0 / I(r_0),\ t \in \mathbb{R}\}$ is a solution to the unforced mechanical system (i.e., equation (5.8) with $u_k = 0$). In other words, a relative equilibrium is an "equilibrium solution" in the reduced space $R \times G$ that corresponds to a family of solutions in the full phase space.

**Horizontal and Vertical Codistributions**

Finally, we introduce the notion of momentum preserving forces. We define the *horizontal codistribution* $\mathrm{hor}_q$ as the annihilator of the distribution spanned by $\partial / \partial x$, that is:

$$\mathrm{hor}_q = \mathrm{Ker}\, \mathrm{span}_{C^\infty(Q)} \{ \frac{\partial}{\partial x} \}.$$

According to equation (5.9), a force $F$ is horizontal, i.e., it takes values in $\mathrm{hor}_q$, if and only if it preserves the momentum $\mu$. Next, we let $\mathrm{hor}_q \mathcal{F}$ denote the largest horizontal subspace (subbundle) of $\mathcal{F}$. The dimension of this subspace is either $m - 1$ or $m$, depending on whether the external forces affect the momentum or not.

## 5.3 Exponential Stabilization of Relative Equilibria

In this section we set up and solve a stabilization problem for an underactuated mechanical system moving along a relative equilibrium.

### 5.3.1 Problem Statement and Control Design

In what follows we let $(\mu_0, r_0)$ be a relative equilibrium for the mechanical system with Abelian symmetry in equation (5.8). We loosely state the control objective as follows:

**Problem 5.5.** Design a feedback law $u = u(q, \dot{q})$ such that $\big(\mu(\dot{q}(t)), r(t)\big)$ converges exponentially fast to $(\mu_0, r_0)$.

We devise our control strategy on the basis of the following assumptions. First, we assume that the horizontal input codistribution is $(m-1)$-dimensional and integrable, i.e., we assume that there exist $m - 1$ functions $\phi^i : R \to \mathbb{R}$ such that

$$\mathrm{hor}_q \mathcal{F} = \mathrm{span}_{C^\infty(Q)} \{ \mathrm{d}\phi^1, \ldots, \mathrm{d}\phi^{m-1} \}. \tag{A1}$$

The dimensionality assumption implies that there exists a covector field $F^{\mathrm{ver}}$ that completes $\mathcal{F}$ and such that in a neighborhood of $r_0$ the following holds

$$\langle F^{\mathrm{ver}}, \frac{\partial}{\partial x} \rangle (r) = 1. \tag{5.10}$$

Therefore we have decomposed the set of inputs $\mathcal{F}$ into horizontal forces (momentum preserving) and a complementary force acting on the momentum. Accordingly, we re-parameterize the input force as

$$\sum_{k=1}^{m} F^k u_k = F^{\text{ver}} u_{\text{ver}} + \sum_{i=1}^{m-1} \mathrm{d}\phi^i \, u_{\text{horiz},i},$$

so that the following holds

$$\dot{\mu} = u_{\text{ver}}. \tag{5.11}$$

Condition (A1) implies that the set of allowable inputs $\mathcal{F}$ can exert a force of the form $\mathrm{d}V_{\text{fdbk}}$, for any function $V_{\text{fdbk}} = V_{\text{fdbk}}(\phi^1, \ldots, \phi^{m-1})$. Notice that this is a different requirement than asking for $\mathcal{F}$ itself to be integrable.

Next, we require the second variation of the amended potential $V_{\mu_0}(r)$ to be positive definite over the "uncontrolled" subspace $\text{Ker}\{\text{hor}_q \mathcal{F}\} \subset T_r R$. More precisely, we require that

$$\left( \frac{\partial^2 V_{\mu_0}}{\partial r^i \partial r^j}(r_0) \right) > 0, \tag{A2}$$

when restricted to the subspace

$$\text{Ker}\, \text{span}_{C^\infty(Q)}\{\mathrm{d}\phi^1(r_0), \ldots, \mathrm{d}\phi^{m-1}(r_0)\} \subset T_{r_0} R.$$

This requirement is closely related to the condition given in [86] for the notion of orbital stability of a relative equilibrium. Additionally, this requirement is the translation to the present setting of the condition in Proposition 2.3 of [98]. As in the latter reference, this property allows us to render positive definite the (amended) potential and to prove Lyapunov stability.

We are designing a Lyapunov function for the closed loop system which is positive definite in *all* $(n-1)$ directions (one less than the dimension of the configuration space: it is the symmetry direction). In the language employed in [60], all symmetries of the mechanical system are broken and neither drift nor any constant final error is allowed.

Finally, we require the following controllability condition. Set $u_{\text{ver}} = 0$ (i.e., only horizontal forces are allowed) and let $(A, B_{\text{horiz}})$ denote the linearization about the point $(r, \dot{r}, \mu) = (r_0, 0, \mu_0)$ of the mechanical system in equation (5.8). We say that the horizontal forces have full linear controllability rank if

$$\text{rank} \begin{bmatrix} B_{\text{horiz}} & AB_{\text{horiz}} & \cdots & A^{2(n-1)} B_{\text{horiz}} \end{bmatrix} = 2(n-1). \tag{A3}$$

This condition allows us to prove asymptotic and exponential stability. A similar statement can be expressed in terms of an involutivity condition of certain Poisson brackets, see [98], or in terms of the notion of zero-output detectability, see [30]. Our version is motivated by the treatment in [78, Chapter 3]. Note that in assuming (A1) and (A3) we are excluding single input $(m = 1)$ systems.

Finally, we state the main result.

**Theorem 5.6.** *Consider the simple mechanical control system in equation* (5.8) *and let* $(\mu_0, r_0)$ *be a relative equilibrium. Let assumptions (A1,A2,A3) hold. Then there exist* $(m-1)$

*positive constants* $k_{\mathrm{p}1}, \ldots, k_{\mathrm{p}(m-1)}$ *such that*

$$V_{\mu_0}(r) + \sum_{i=1}^{m-1} k_{\mathrm{p}i}\phi^i(r)^2 > 0,$$

*for all* $r \neq r_0$ *in a neighborhood of* $r_0$. *Let* $k_{\mathrm{ver}}$ *and* $k_{\mathrm{d}1}, \ldots, k_{\mathrm{d}(m-1)}$ *be positive constants and define*

$$\begin{aligned} u_{\mathrm{ver}} &= -k_{\mathrm{ver}}(\mu(\dot{q}) - \mu_0), \\ u_{\mathrm{horiz},i} &= -k_{\mathrm{p}i}\phi^i(r) + k_{\mathrm{d}i}\dot{\phi}_i(r,\dot{r}), \qquad \forall i = 1, \ldots, m-1. \end{aligned}$$

*Then* $(\mu_0, r_0)$ *is locally exponentially stable.*

*Proof.* The proof is organized in two steps. First we examine the evolution of the momentum $\mu$. From assumptions (A1), equation (5.11), and the definition of $u_{\mathrm{ver}}$, the closed loop system is given by

$$\dot{\mu} = -k_{\mathrm{ver}}(\mu - \mu_0),$$

and therefore $\mu$ converges exponentially fast to $\mu_0$.

Next we examine the evolution of the variable $r$ under the assumption of constant momentum $\mu(0) = \mu(t) = \mu_0$. Because of the symmetry we can perform the so-called Hamiltonian reduction procedure and from the full system in equation (5.8) we obtain a mechanical system defined on the manifold $R$. This procedure is described in detail for example in Chapter 4 in [1]. According to this treatment, there exists a Riemannian metric $M_r'$ on the manifold $R$ such that the following quantity, called the *reduced Hamiltonian*, is a constant of motion:

$$H_\mu(r,\dot{r}) = \frac{1}{2}\|\dot{r}\|^2_{M_r'} + V_{\mu_0}(r).$$

In addition, the unforced system has equations of motion of the form

$$M_r' \nabla'_{\dot{r}}\dot{r} = -\mathrm{d}V_{\mu_0} + \beta_{\mu_0}(\dot{r}), \tag{5.12}$$

where the (gyroscopic) force $\beta_{\mu_0}$ is a tensor field $T_rR \to T^*R$ and depends linearly on $\mu_0$. Similarly, the closed loop reduced system can be written as

$$M_r' \nabla'_{\dot{r}}\dot{r} = -\mathrm{d}V_{\mu_0} + \beta_{\mu_0}(\dot{r}) - \sum_{i=1}^{m-1}\left(k_{\mathrm{p}i}\phi^i + k_{\mathrm{d}i}\dot{\phi}_i\right)\mathrm{d}\phi^i. \tag{5.13}$$

At $k_{\mathrm{d}i} = 0$, this reduced system admits the conserved quantity $H_\mu(r,\dot{r}) + \frac{1}{2}\sum k_{\mathrm{p}i}(\phi^i)^2$. Due to assumption (A2) and Proposition 2.3 in [98], there exist sufficiently large $k_{\mathrm{p}i}$ such that this conserved quantity is a positive definite function (i.e., it satisfies equation (5.2)). This is the first statement in the theorem above.

Setting $k_{\mathrm{d}i} > 0$ the system is a Hamiltonian system with dissipation and also the relationship in equation (5.3) holds. Next, due to the controllability assumption (A3), the result in Lemma 5.1 applies to the closed loop system in equation (5.13) and $(r_0, 0)$ is an asymptotically stable equilibrium point. This is the same analysis in [98] and [47]. Local exponential stability can be proven because the reduced Hamiltonian (plus potential shaping) is a quadratic Lyapunov function; see Lemma 5.2.

Finally, since $\mu(\dot{q}(0)) \neq \mu_0$, the full system consists of an exponentially stable subsystem

forced by an exponentially decaying perturbation. To prove local exponential stability, we recall the discussion at the end of Section 5.1, with $x = (r, \dot{r})$ and $y = \mu - \mu_0$. That discussion applies because the perturbation to the reduced Hamiltonian system is of order at least linear on $\mu - \mu_0$. □

### 5.3.2 Remarks

There are two advantages of the controller described in the previous theorem over a standard linear controller based on linearization: First, by investigating the amended potential $V_{\mu_0}$, we can establish the region of attraction of our controller. Second, our design is independent of the exact knowledge of the inertia coefficients, leading to robustness to parameter uncertainty.

The assumption that the amended potential be positive definite over the "uncontrolled subspace" is quite strong. In some examples our requirement is that the unforced system has an "orbitally stable" (roughly the equivalent of Lyapunov stable) relative equilibria; for more details see [86]. Should this condition fail, we refer the reader to the "controlled Lagrangians" methodology introduced in [11].

In the models of mechanical systems described so far, we have always neglected dissipative effects. In fact, it would not be difficult to include them into the analysis in Theorem 5.6. A simple strategy would consist of canceling the vertical component of the dissipative force in order to maintain the existence of the relative equilibrium. The effect of the horizontal dissipative component is stabilizing.

## 5.4 Applications to Vehicle Control

We present two design examples for models of vehicles. While both the planar body and the satellite have a full SE(2) and SO(3) symmetry, we focus on the stabilization of a one-dimensional symmetry: translation (or rotation) along the major axis for the planar body (for the satellite).

As a side comment, we emphasize that our analysis of the positive definiteness of the amended potential agrees with the results in [71], [59] and [60].

### 5.4.1 A Planar Rigid Body with Two Forces

We consider the model of a planar body moving in an idealized fluid; see [60] for more details. This is the example in Section 3.2.1 except for a different Lagrangian $L = \frac{1}{2}J\omega^2 + \frac{1}{2}m_x v_x^2 + \frac{1}{2}m_y v_y^2$ where we assume $J > 0$ and $m_x > m_y > 0$. The two control inputs consist of forces $\{f_1, f_2\}$ applied at a distance $h$ from the center of mass; see Figure 3.2 in Section 3.2.1. The equations of motion are written as:

$$\begin{aligned} \dot{\theta} &= \omega & J\dot{\omega} &= (m_x - m_y)v_x v_y - hu_2 \\ \dot{x} &= v_x\cos(\theta) - v_y\sin(\theta) & m_x\dot{v}_x &= m_y\omega v_y + u_1 \\ \dot{y} &= v_x\sin(\theta) + v_y\cos(\theta) & m_y\dot{v}_y &= -m_x\omega v_x + u_2. \end{aligned}$$

Even though the planar body has a full SE(2) symmetry, we focus on the Abelian group action $(\chi, (\theta, x, y)) \mapsto (\theta, x + \chi, y)$. According to the definitions in Section 5.2, we compute:

$$\begin{aligned} \mu &= (m_x\cos^2(\theta) + m_y\sin^2(\theta))\dot{x} + (m_x - m_y)\sin(\theta)\cos(\theta)\dot{y}, \\ I(r) &= m_x\cos^2(\theta) + m_y\sin^2(\theta), \end{aligned}$$

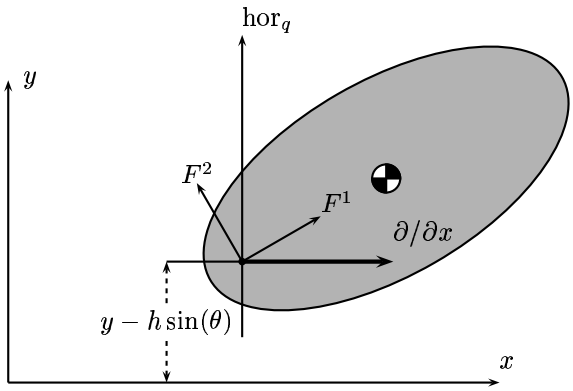


Figure 5.1: Force decomposition and integrability in the planar body example.

and $V_{\mu_0}(r) = \frac{1}{2}\mu_0^2/I(r)$. The control goal is to stabilize the relative equilibrium described by $r = (\theta, y) = (0,0)$ and $\mu = \mu_0 = m_x\dot{x}_0$.

Assumption (A1) holds because

$$\begin{aligned}\mathcal{F} &= \mathrm{span}_{C^\infty(\mathrm{SE}(2))}\{f_1, f_2\}\\ &\equiv \mathrm{span}_{C^\infty(\mathrm{SE}(2))}\{\cos(\theta)\mathrm{d}x + \sin(\theta)\mathrm{d}y\,,\ -\sin(\theta)\mathrm{d}x + \cos(\theta)\mathrm{d}y - h\mathrm{d}\theta\}\\ &= \mathrm{span}_{C^\infty(\mathrm{SE}(2))}\{\mathrm{d}y - h\cos(\theta)\mathrm{d}\theta\} + \mathrm{span}_{C^\infty(\mathrm{SE}(2))}\{\mathrm{d}x + h\sin(\theta)\mathrm{d}\theta\},\end{aligned}$$

where one can verify that $\mathrm{hor}_q\,\mathcal{F} = \mathrm{span}_{C^\infty(\mathrm{SE}(2))}\{\mathrm{d}(y - h\sin(\theta))\}$ and where we have chosen $\mathrm{d}x + h\cos(\theta)\mathrm{d}\theta$ to complete the input codistribution. Regarding (A2), we compute the second variation of $V_{\mu_0}$ as

$$\left(\frac{\partial^2 V_{\mu_0}}{\partial\theta\,\partial y}(0,0)\right) = \frac{\mu_0^2}{m_x^2}\begin{bmatrix} m_x - m_y & 0\\ 0 & 0\end{bmatrix},$$

and we verify that it is positive definite for $m_x > m_y$ and $\mu_0 \neq 0$, when restricted to the subspace $\mathrm{Ker}\,\mathrm{span}_{C^\infty(\mathrm{SE}(2))}(\mathrm{d}y - h\cos(\theta)\mathrm{d}\theta) = \mathrm{span}_{C^\infty(\mathrm{SE}(2))}\{\frac{\partial}{\partial y} + h\cos(\theta)\frac{\partial}{\partial\theta}\}$. The controllability assumption (A3) can be easily verified. Summarizing, the control law

$$\begin{bmatrix}u_1\\ u_2\end{bmatrix} = \begin{bmatrix}\cos(\theta) & -\sin(\theta)\\ \sin(\theta) & \cos(\theta)\end{bmatrix}\begin{bmatrix}-k_{\mathrm{ver}}(\mu - m_x v_0)\\ -k_p(y - h\sin(\theta)) - k_d(\dot{y} - h\omega\cos(\theta)),\end{bmatrix}$$

achieves local exponential stability, provided $\mu_0 = m_x v_0 \neq 0$.

### 5.4.2 A Satellite with Two Thrusters

We consider the model of a satellite with two thrusters described in Section 3.2.2. The attitude and the body fixed velocity are $(R, \Omega)$, the kinetic energy is $\frac{1}{2}\Omega^T\mathbb{J}\Omega$, and the two inputs consist of torques about the first and second axes. The equations of motion (3.10) are:

$$\begin{aligned}\dot{R} &= R\widehat{\Omega}\\ \mathbb{J}\dot{\Omega} &= \mathbb{J}\Omega\times\Omega \ + \mathsf{e}_1 u_1(t) + \mathsf{e}_2 u_2(t),\end{aligned} \tag{5.14}$$

where $\{\mathsf{e}_1, \mathsf{e}_2, \mathsf{e}_3\}$ denotes the standard basis on $\mathbb{R}^3$, i.e., $\mathsf{e}_1 = (1,0,0)$, $\mathsf{e}_2 = (0,1,0)$ and $\mathsf{e}_3 = (0,0,1)$. We assume $\mathbb{J} = \operatorname{diag}\{J_1, J_2, J_3\}$ with $J_1 > J_2 > J_3$.

Even though the satellite has a full SO(3) symmetry, we focus on the Abelian group action $(\chi, R) \mapsto \exp(\chi \mathsf{e}_1)R$ where the exponential map $\exp : \mathfrak{so}(3) \to \mathrm{SO}(3)$ is defined in Section 2.2.

Because the later computations are better performed in coordinates, we now choose a convenient parameterization and obtain various coordinate expressions. We write $R$ as

$$R(\alpha, \beta, \gamma) = \exp(\alpha \widehat{\mathsf{e}}_1) \exp(\beta \widehat{\mathsf{e}}_2) \exp(\gamma \widehat{\mathsf{e}}_3),$$

that is, we parameterize[1] SO(3) by a set of Euler angles $(\alpha, \beta, \gamma)$, that is singular at $\beta = \pm\pi/2$. The unusual order of rotation is well-suited to the symmetry we consider and to the set of input vector fields. The one-dimensional symmetry reads in these coordinates as $(\chi, (\alpha, \beta, \gamma)) \mapsto (\alpha + \chi, \beta, \gamma)$. The Jacobian relating Euler angles rates and body fixed velocity is

$$\Omega = \begin{bmatrix} \cos(\beta)\cos(\gamma) & \sin(\gamma) & 0 \\ -\cos(\beta)\sin(\gamma) & \cos(\gamma) & 0 \\ \sin(\beta) & 0 & 1 \end{bmatrix} \begin{bmatrix} \dot\alpha \\ \dot\beta \\ \dot\gamma \end{bmatrix},$$

and accordingly the inertia matrix $M$ (with respect to the basis $\{\frac{\partial}{\partial\alpha}, \frac{\partial}{\partial\beta}, \frac{\partial}{\partial\gamma}\}$) is:

$$\begin{bmatrix} J_3\sin^2(\beta) + \cos^2(\beta)(J_1\cos^2(\gamma) + J_2\sin^2(\gamma)) & (J_1 - J_2)\cos(\beta)\cos(\gamma)\sin(\gamma) & J_3\sin(\beta) \\ (J_1 - J_2)\cos(\beta)\cos(\gamma)\sin(\gamma) & J_2\cos^2(\gamma) + J_1\sin^2(\gamma) & 0 \\ J_3\sin(\beta) & 0 & J_3 \end{bmatrix}.$$

The one-dimensional symmetry is illustrated by $\partial M/\partial\alpha = 0$. One way to write the two input one-forms with respect to the basis $\{\mathrm{d}\alpha, \mathrm{d}\beta, \mathrm{d}\gamma\}$ is to exploit the notion of "work." This way it is possible to show that:

$$\begin{aligned} f^1 &= (\cos(\beta)\cos(\gamma))\mathrm{d}\alpha + \sin(\gamma)\mathrm{d}\beta \\ f^2 &= (-\cos(\beta)\sin(\gamma))\mathrm{d}\alpha + \cos(\gamma)\mathrm{d}\beta. \end{aligned}$$

According to the definitions in Section 5.2, we compute:

$$\begin{aligned} \mu &= \left(J_3\sin(\beta)^2 + \cos(\beta)^2(J_1\cos(\gamma)^2 + J_2\sin(\gamma)^2)\right)\dot\alpha \\ &\quad + \tfrac{1}{2}(J_1 - J_2)\cos(\beta)\sin(2\gamma)\dot\beta + J_3\sin(\beta)\dot\gamma, \\ I(r) &= J_1\cos^2(\beta)\cos^2(\gamma) + J_3\sin^2(\beta) + J_2\cos^2(\beta)\sin^2(\gamma), \end{aligned}$$

and $V_{\mu_0}(r) = \frac{1}{2}\mu_0^2/I(r)$. The control goal is to stabilize the relative equilibrium described by $r = (\beta, \gamma) = (0,0)$ and $\mu = J_1\dot\alpha_0$. This problem is often referred to as "spin axis stabilization."

Assumption (A1) holds because

$$\begin{aligned} \mathcal{F} &= \operatorname{span}_{C^\infty(\mathrm{SO}(3))}\{f_1, f_2\} \\ &\equiv \operatorname{span}_{C^\infty(\mathrm{SO}(3))}\{(\cos(\beta)\cos(\gamma))\mathrm{d}\alpha + \sin(\gamma)\mathrm{d}\beta,\ (-\cos(\beta)\sin(\gamma))\mathrm{d}\alpha + \cos(\gamma)\mathrm{d}\beta\} \\ &= \operatorname{span}_{C^\infty(\mathrm{SO}(3))}\{\mathrm{d}\beta\} + \operatorname{span}_{C^\infty(\mathrm{SO}(3))}\{\mathrm{d}\alpha\}, \end{aligned}$$

[1] This local chart of SO(3), obtained via repeated single exponentials, is referred to as "exponential coordinates of the second kind."

where one can verify that $\mathrm{hor}_q \mathcal{F} = \mathrm{span}_{C^\infty(\mathrm{SO}(3))}\{\mathrm{d}\beta\}$ and where we have chosen $\mathrm{d}\alpha$ to complete the input codistribution. Regarding (A2), we compute the second variation of $V_{\mu_0}$ as

$$\left(\frac{\partial^2 V_{\mu_0}}{\partial\beta\,\partial\gamma}(0,0)\right) = \frac{\mu_0^2}{J_1^2}\begin{bmatrix} J_1 - J_3 & 0 \\ 0 & J_1 - J_2 \end{bmatrix},$$

and we verify that it is positive definite for $J_1 > J_2$ and $\mu_0 \neq 0$, when restricted to the subspace $\mathrm{Ker}\,\mathrm{span}_{C^\infty(\mathrm{SO}(3))}(\mathrm{d}\beta) = \mathrm{span}_{C^\infty(\mathrm{SO}(3))}\{\frac{\partial}{\partial\gamma}\}$. The controllability assumption (A3) can be easily verified. Summarizing, the control law

$$\begin{bmatrix} u_1 \\ u_2 \end{bmatrix} = \begin{bmatrix} \cos(\gamma) & -\sin(\gamma) \\ \sin(\gamma) & \cos(\gamma) \end{bmatrix} \begin{bmatrix} -k_{\mathrm{ver}}(\mu - J_1\omega_0)/\cos(\beta) \\ -k_p\beta - k_d\dot{\beta}, \end{bmatrix}$$

achieves local exponential stability, provided $\mu_0 = J_1\dot{\alpha}_0 \neq 0$.

# Chapter 6

# Controllability of Underactuated Systems

In this chapter we investigate the local controllability properties of underactuated mechanical systems starting at rest and present various tests for controllability of these systems. We also present numerous examples that provide insight into these controllability results.

The chapter is organized as follows. In Section 6.1 we review the notions of local controllability following Sussmann [93] and Kawski [48], and in Section 6.2, we review the notion of local configuration controllability originally developed by Lewis and Murray [67]. Section 6.3 presents an extension to systems on Lie groups and Section 6.4 is dedicated to systems with impacts. The results on controllability on Lie groups are joint work with Andrew Lewis; the results on systems with impacts are joint work with Miloš Žerfan. These results were originally presented in [24, 29].

## 6.1 Review of Local Controllability Theory for Nonlinear Systems

In this section we review some local nonlinear controllability tests as presented in [48]. For the more basic aspects we refer to [78]. Consider the nonlinear control system

$$\dot{q} = X(q) + \sum_{j=1}^{m} Y_j(q)u_j, \tag{6.1}$$

where $q$ takes values in the $n$ dimensional manifold $Q$, the vector fields $\{X, Y_1, \ldots, Y_m\}$ are analytic, the controls $u$ are bounded and measurable, and $q(0) = q_0$ is an equilibrium point, i.e., $X(q_0) = 0$. We let $\mathcal{Y} = (Y_1, \ldots, Y_m)$ denote the family of input vector fields.

For $T > 0$, a *solution of a control system* of the system (6.1) is a pair of piecewise curves $\{(q, u)(t), t \in [0, T]\}$ that satisfy the equation (6.1). Let $V \subset Q$ be a neighborhood of $q_0$, and define the set of reachable states as

$$\mathcal{R}_Q^V(q_0, \leq T) = \bigcup_{0 \leq t \leq T} \{q_1 \in Q \mid \exists\, (q, u)(\tau) \text{ solution to (6.1) such that } q(0) = q_0,\ q(\tau) \in V \text{ for } \tau \in [0, t] \text{ and } q(t) = q_1\}.$$

The system (6.1) is small time *locally accessible* from $q_0$ if the set $\mathcal{R}_Q^V(q_0, \leq T)$ has a nonempty interior for every $T > 0$. The system (6.1) is *small time locally controllable* (STLC) from $q_0$ if it is accessible and if $q_0$ belong to the interior of $\mathcal{R}_Q^V(q_0, \leq T)$ for every $T > 0$.

Recall the definition of Lie bracket in equation (2.1) and define the *involutive closure* $\text{Lie}(X, \mathcal{Y})$ as the family of vector fields obtained by taking iterated Lie bracket of vector

fields in $\{X, \mathcal{Y}\}$. Chow's theorem leads to the following characterization: the system (6.1) is locally accessible from $q_0$ if and only if

$$\dim \mathrm{Lie}(X, \mathcal{Y})(q_0) = n.$$

This is the so-called Lie algebra rank condition (LARC).

Only sufficient conditions for local controllability are currently known and they require a much more refined approach. In particular, we need the following two definitions. Given the $(m+1)$tuple of non-negative integers $(k, l_1, \ldots, l_m) = (k, l)$, let the distribution $\mathrm{Lie}^{(k,l)}(X, \mathcal{Y})$ be the linear span of all the Lie brackets that contain the $X$ factor[1] $k$ times and the $Y_j$ factor $l_j$ times for all $j$. Given a weight $\theta \in [0, 1]$, and two $(m+1)$tuples of non-negative integers $(k, l)$ and $(k', l')$, define the ordering $(k, l) \prec_\theta (k', l')$ whenever $\theta k + \sum_j l_j < \theta k' + \sum_j l'_j$.

**Theorem 6.1 (Sussmann [93]).** *The system* (6.1) *is STLC from $q_0$ if it is accessible from $q_0$ and if there exists a weight $\theta \in [0, 1]$ such that whenever $k$ is odd and $l_1, \ldots, l_m$ are all even, then*

$$\mathrm{Lie}^{(k,l)}(X, \mathcal{Y})(q_0) \subseteq \sum_{(k',l') \prec_\theta (k,l)} \mathrm{Lie}^{(k',l')}(X, \mathcal{Y})(q_0).$$

Two important examples are particular cases of the theorem:

(i) By setting $\theta$ equal to zero and considering brackets with only one factor from $\mathcal{Y}$, i.e., brackets with $\sum_j l_j = 1$, one can recover the fact that linearly controllable systems are STLC.

(ii) For *driftless systems*, i.e., systems with $X(q) \equiv 0$, local accessibility is equivalent to STLC since in the theorem $k$ is always necessarily zero (hence never odd).

*Remark 6.2 (Good versus bad brackets).* This condition for controllability can be equivalently stated as follows. We say that a Lie bracket is *bad* if it contains an odd number of $X$ factors and an even number of each $Y_j$ factors. Otherwise we say it is *good*. The system (6.1) is STLC from $q_0$ if there exists a weight $\theta$ such that every bad Lie bracket is a linear combination of lower order good Lie brackets, where the order of a bracket is $\theta k + \sum_j l_j$.

## 6.2 Controllability of Mechanical Control Systems

In this section we investigate the controllability properties of a control system described by an affine connection. Given a manifold $Q$, an affine connection $\nabla$ and a family of input vector fields $\mathcal{Y} = \{Y_1, \ldots, Y_m\}$, the (generalized Euler-Lagrange) equations of motion are

$$\nabla_{\dot{q}} \dot{q} = \sum_{j=1}^{m} Y_j(q) u_j. \tag{6.2}$$

In what follows, we consider initial states that have zero velocity, and we focus on the evolution of the configuration variables as opposed to the full state. In other words, one question of interest is how to characterize the set of reachable configurations when the initial velocity of the system is zero.

[1] This heuristic definition can be made precise via the notion of free Lie algebra, see [93].

For $T > 0$, a *solution* of the system (6.2), is a pair $(q, u)$, where $q : [0, T] \to Q$ is a piecewise smooth curve on $Q$, $u : [0, T] \to \mathbb{R}^m$ is an admissible input in $\mathcal{U}^m$ and $(q(t), u(t))$ is a solution to the equations (6.2). Let $q_0 \in Q$, let $V \subset Q$ be a neighborhood of $q_0$ and let $W \subset TQ$ be a neighborhood of $(q_0, 0)$, where 0 here denotes the zero vector in $T_{q_0}Q$. For $T > 0$, define the set of reachable configurations as

$$\mathcal{R}_Q^V(q_0, \leq T) = \bigcup_{0 \leq t \leq T} \{q_1 \in Q \mid \exists\, (q, u)(\tau) \text{ solution to (6.2) such that } (q, \dot{q})(0) = (q_0, 0),\ q(\tau) \in V \text{ for } \tau \in [0, t] \text{ and } q(t) = q_1\}.$$

Similarly, define the set of reachable states as

$$\mathcal{R}_{TQ}^W(q_0, \leq T) = \bigcup_{0 \leq t \leq T} \{(q_1, \dot{q}_1) \in TQ \mid \exists\, (q, u)(\tau) \text{ solution to (6.2) such that } (q, \dot{q})(0) = (q_0, 0),\ (q, \dot{q})(\tau) \in W \text{ for } \tau \in [0, t] \text{ and } (q, \dot{q})(t) = (q_1, \dot{q}_1)\}.$$

The following two definitions characterize different notions of accessibility for mechanical systems:

**Definition 6.3.** The system (6.2) is *small-time locally accessible at $q_0$ and zero velocity* if $\mathcal{R}_{TQ}^W(q_0, \leq T)$ contains a non-empty open subset of $TQ$ for all $T > 0$ and for all neighborhoods $W$ of $(q_0, 0)$.

**Definition 6.4.** The system (6.2) is *small-time locally configuration accessible at $q_0$* if $\mathcal{R}_Q^V(q_0, \leq T)$ contains a non-empty open subset of $Q$ for all $T > 0$ and for all neighborhoods $V$ of $q_0$.

Recall from the previous section that, corresponding to the operation of Lie bracket between vector fields, we defined the *involutive closure* of $\mathcal{X}$, denoted by $\mathrm{Lie}(\mathcal{X})$, as the family of vector fields obtained by taking iterated Lie brackets of the fields in $\mathcal{X}$. Now we perform the equivalent construction for the symmetric product. The latter was defined in equation (2.6) as

$$\langle X : Y \rangle = \nabla_X Y + \nabla_Y X.$$

We define the *symmetric closure* of $\mathcal{X}$, denoted by $\mathrm{Sym}(\mathcal{X})$, as the family of vectors obtained by taking iterated symmetric products of the fields $\{X_1, \ldots, X_m\}$.

**Theorem 6.5 (Lewis and Murray [67]).** *Consider the system in equation* (6.2) *and let* $\mathcal{Y} = \{Y_1, \ldots, Y_m\}$.

*(i) The system is locally accessible at $q_0$ and at zero velocity if and only if*

$$\dim \mathrm{Sym}(\mathcal{Y})(q_0) = n.$$

*(ii) The system is locally configuration accessible at $q_0$ if and only if*

$$\dim \mathrm{Lie}(\mathrm{Sym}(\mathcal{Y}))(q_0) = n.$$

Next, we present three notions of controllability for the mechanical system (6.2). In addition to the "classic" small-time local controllability, we also consider two weaker versions called small-time local configuration controllability and equilibrium controllability. Notice that the latter property is not a local notion.

**Definition 6.6.** The system (6.2) is *small-time locally controllable at $q_0$ and at zero velocity* if, for all $T > 0$ and for all neighborhoods $W$ of $(q_0, 0)$, the set of reachable states $\mathcal{R}^W_{TQ}(q_0, \leq T)$ contains a non-empty open set and if $(q_0, 0)$ belongs to this set.

The system (6.2) is *small-time locally configuration controllable at $q_0$* (STLCC) if, for all $T > 0$ and for all neighborhoods $V$ of $q_0$, the set of reachable configurations $\mathcal{R}^V_Q(q_0, \leq T)$ contains a non-empty open set and if $q_0$ belongs to this set.

The system (6.2) is *equilibrium controllable* on $V \subset Q$, if, for $q_1, q_2 \in V$, there exists an input $\{u(t), t \in [0,T]\}$ and a solution $\{q(t), t \in [0,T]\}$ such that $q(0) = q_1$, $q(T) = q_2$, $q(t) \in V$ for all $t \in [0,T]$, and $\dot{q}(0) = 0$, $\dot{q}(T) = 0$.

Similarly to the STLC treatment in the previous section, we establish sufficient conditions for controllability via two additional notions. Given an $m$-tuple of non-negative integers $l = (l_1, \ldots, l_m)$, let the distribution $\mathrm{Sym}^{(l)}(\mathcal{Y})$ be the linear span of all the symmetric products that contain the $Y_j$ factor $l_j$ times for all $j$[2]. Given two $m$tuples of non-negative integers $l$ and $l'$, define the ordering $l \prec l'$ whenever $\sum_j l_j < \sum_j l'_j$.

**Theorem 6.7 (Lewis and Murray [67]).** *Consider the system* (6.2)*:*

*(i) The system is STLC (or STLCC) from $q_0$ if it is locally accessible from $q_0$ (respectively locally configuration accessible) and if whenever $l_1, \ldots, l_m$ are all even then*

$$\mathrm{Sym}^{(l)}(\mathcal{Y})(q_0) \subseteq \sum_{l' \prec l} \mathrm{Sym}^{(l')}(\mathcal{Y})(q_0).$$

*(ii) The system is equilibrium controllable on $V$, if it is STLCC at each $q$.*

The statements in Theorem 6.5 and 6.7 are direct consequences of the results in [93] and [67]. Notice that these tests are performed on a reduced space, i.e., on $Q$ as opposed to $TQ$. Additionally, they have have a simple interpretation; symmetric products of input vectors identify which velocities are reachable, whereas Lie brackets of reachable velocities identify which configurations are reachable.

Single-input systems (with $n > m = 1$) always fail the sufficient condition for both controllability notions. Indeed, if only one input $Y$ vector is available, then accessibility implies $\mathrm{span}\{Y\} \subset \mathrm{Sym}^{(2)}(Y)$ and this violates the sufficient condition from the theorem: $\mathrm{Sym}^{(2)}(Y) \subseteq \mathrm{Sym}^{(1)}(Y) \equiv \mathrm{span}\{Y\}$. Further, it can be proven that single-input systems are neither STLC at zero velocity nor STLCC, see [65]. Incidentally, notice that more general single-input systems (e.g., an inverted pendulum on a cart) are possibly linearly controllable and therefore STLC.

### Bad versus Good Symmetric Products

This condition for controllability can be stated equivalently as follows. The *order* of an iterated symmetric product of factors from $\mathrm{Sym}(\mathcal{X})$ is the total number of factors. We say that a symmetric product from $\mathrm{Sym}(\mathcal{X})$ is *bad* if it contains an even number of each of the vector fields in $\mathcal{X}$. Otherwise, we say that the symmetric product is *good*. For example, the symmetric product $\langle\langle Y_1 : Y_2\rangle : Y_1\rangle$ has order three and it is good; the symmetric product $\langle\langle\langle Y_1 : Y_2\rangle : Y_2\rangle : Y_1\rangle$ has order four and it is bad.

Finally, the system (6.2) is STLC (or STLCC) from $q_0$ if it is locally accessible (respectively locally configuration accessible) and if every bad symmetric product is a linear combination of lower-order good symmetric products.

[2]This heuristic definition can be made precise via the notion of symmetric algebra, see [67].

## 6.3 Controllability of Mechanical Control Systems on Lie Groups

This section deals with the controllability properties of mechanical systems on Lie groups as described in Section 3.2. For the sake of brevity, we present directly the controllability results, and the corresponding accessibility results are obvious. Given a Lie group $G$ and corresponding algebra $\mathfrak{g}$, an inertia tensor $\mathbb{I}$ and a set of input vectors, the Euler-Poincaré equations of motion are:

$$\begin{aligned} \dot{g} &= g \cdot \xi \\ \dot{\xi} &= \mathbb{I}^{-1}\mathrm{ad}^*_\xi \mathbb{I}\xi + \sum_{j=1}^{m} b_j u_j(t), \end{aligned} \tag{6.3}$$

where $\xi$ is the body fixed velocity and takes values on the Lie algebra $\mathfrak{g}$.

As discussed in Chapter 2, the equations (6.3) are of the form of equations (6.2). Therefore, the controllability definitions and tests from the previous section apply to the new setting unchanged. However, some important simplifications take place. In particular, recall that the input vector fields and the inertia metric are left invariant and that all of the relevant computations can be performed on the Lie algebra $\mathfrak{g}$. For example, from equation (2.13) the symmetric product between vectors in $\mathfrak{g}$ is

$$\langle \xi : \eta \rangle \triangleq -\mathbb{I}^{-1}\big(\mathrm{ad}^*_\xi \mathbb{I}\eta + \mathrm{ad}^*_\eta \mathbb{I}\xi\big).$$

Therefore, symmetric and involutive closures can be computed by algebraic means on $\mathfrak{g}$.

We present the tests in terms of the notion of bad and good symmetric product. Given a family $\mathcal{B}$ of vectors in $\mathfrak{g}$, we denote by $\mathrm{Lie}_{\mathfrak{g}}(\mathcal{B})$ and by $\mathrm{Sym}_{\mathfrak{g}}(\mathcal{B})$ the involutive and symmetric closure of $\mathcal{B}$ in $\mathfrak{g}$. The *order* of a symmetric product from $\mathrm{Sym}_{\mathfrak{g}}(\mathcal{B})$ is the total number of factors, and a symmetric product is *bad* if it contains an even number of each of the vectors in $\mathcal{B}$; otherwise, it is *good*. We can now state a stronger version of Theorem 6.7:

**Proposition 6.8.** *Consider the system* (6.3)*:*

*(i) The system is STLC at zero velocity if the subspace defined by* $\mathrm{Sym}_{\mathfrak{g}}(\mathcal{B})$ *has full rank and every bad symmetric product is a linear combination of lower-order good symmetric products.*

*(ii) The system is both STLCC and equilibrium controllable if the subspace defined by* $\mathrm{Lie}_{\mathfrak{g}}(\mathrm{Sym}_{\mathfrak{g}}(\mathcal{B}))$ *has full rank and every bad symmetric product is a linear combination of lower-order good symmetric products.*

*Proof.* The proof is a straightforward translation of the results in Theorems 6.5 and 6.7 to the setting of invariant affine connections. □

Notice that the various controllability conditions are now expressed in a purely algebraic way (no differentiation is required). This is remarkable since the system of equations (6.3) presents strong nonlinearities. Additionally, the controllability conditions in the theorem are independent of the base point $g \in G$, as the invariance of the original system suggests.

*Remark 6.9 (Comparison with literature).* It is instructive to remark similarities and differences of our analysis with respect to the works in [12], [33] and [70]: while the accessibility computations turn out to be similar, the key difference lies in our interest in the local configuration controllability properties (as opposed to global full-state controllability).

We conclude this section by investigating the controllability properties of the various examples introduced in Section 3.2. We label various instructive choices of systems and input forces and provide a catalog of accessible, controllable and configuration controllable systems.

### 6.3.1 Planar Rigid Bodies with Combinations of Forces

Consider the planar rigid body described in Section 3.2.1 with input vectors $b_1 = \frac{1}{m}\mathsf{e}_2$ and $b_2 = \frac{-h}{J}\mathsf{e}_1 + \frac{1}{m}\mathsf{e}_3$. The relevant symmetric products are computed as follows:

$$\begin{aligned} \langle b_1 : b_1 \rangle &= 0, \\ \langle b_1 : b_2 \rangle &= \frac{-h}{Jm}\mathsf{e}_3, \\ \langle b_2 : b_2 \rangle &= \frac{2h}{Jm}\mathsf{e}_2, \\ \langle b_2 : \langle b_2 : b_2 \rangle \rangle &= \frac{-2h}{J^2 m}\mathsf{e}_3. \end{aligned}$$

We distinguish the following cases which depend on the availability of the two input vectors:

[PRB1] $\mathcal{B} = \{b_1\}$: the system is neither accessible at zero velocity nor configuration accessible, as all symmetric products and Lie brackets vanish. An interpretation of this result is that, for all possible inputs, the body is only allowed to translate parallel to the body fixed $x$-axis.

[PRB2] $\mathcal{B} = \{b_2\}$: the system is (small-time locally) accessible at zero velocity since the subspace generated by the vectors $\{b_2, \langle b_2 : b_2 \rangle, \langle b_2 : \langle b_2 : b_2 \rangle \rangle\}$ has full rank. However, the sufficient condition for controllability fails to hold, as $\langle b_2 : b_2 \rangle$ is a bad symmetric product and it is not a multiple of any lower-order symmetric product ($b_2$ is the only one). Additionally, as mentioned above, the results in [65] show that the system is neither STLC at zero velocity nor STLCC.

[PRB3] $\mathcal{B} = \{b_1, b_2\}$: the system is STLC at zero velocity, since the subspace generated by the vectors $\{b_1, b_2, \langle b_1 : b_2 \rangle\}$ has full rank and the bad symmetric product $\langle b_2 : b_2 \rangle$ is a linear combination of lower-order good symmetric products: $b_2 = -2b_1$.

### 6.3.2 A Satellite with Two Thrusters or with Two Rotors

Consider the satellite with thrusters described in Section 3.2.2. The input vectors are $b_1 = \frac{1}{J_1}\mathsf{e}_1$ and $b_2 = \frac{1}{J_2}\mathsf{e}_2$. The relevant symmetric products and Lie brackets are computed as

$$\begin{aligned} \langle b_1 : b_1 \rangle = \langle b_2 : b_2 \rangle &= 0, \\ \langle b_1 : b_2 \rangle &= \frac{J_2 - J_1}{J_1 J_2 J_3}\mathsf{e}_3, \\ [b_1, b_2] &= \frac{1}{J_1 J_2}\mathsf{e}_3. \end{aligned}$$

The controllability properties are as follows:

[ST] $\mathcal{B} = \{b_1, b_2\}$ and $J_1 \neq J_2$: if the satellite is not axisymmetric, then the rank of $\{b_1, b_2, \langle b_1 : b_2 \rangle\}$ is full and there are no bad symmetric products. Therefore, the system is STLC at zero velocity. If the satellite is axisymmetric, i.e., $J_1 = J_2$, then a simple analysis shows that the system is STLCC.

Next, we consider a satellite with two rotors as introduced in Section 3.2.2. We compute symmetric products and Lie brackets as

$$\langle b_1 : b_1 \rangle = \langle b_2 : b_2 \rangle = \langle b_1 : b_2 \rangle = 0,$$

and

$$\begin{aligned}
[b_1, b_2] &= \frac{1}{(J_{\text{rot1}} - J_1)(J_{\text{rot2}} - J_2)} \mathsf{e}_3, \\
[[b_1, b_2], b_1] &= \frac{1}{(J_{\text{rot1}} - J_1)^2 (J_2 - J_{\text{rot2}})} \mathsf{e}_2, \\
[[b_1, b_2], b_2] &= \frac{1}{(J_{\text{rot1}} - J_1)(J_{\text{rot2}} - J_2)^2} \mathsf{e}_1.
\end{aligned}$$

[SR] $\mathcal{B} = \{b_1, b_2\}$: the system is not accessible at zero velocity (every symmetric product vanishes) and hence not STLC, but it is STLCC since the involutive closure has full rank.

This result was partly expected but not trivial. Since the satellite–rotors system is not subject to any external force, its total angular momentum is conserved. Therefore, it is intuitively clear that the system cannot be accessible in both configurations and velocities. However, the less trivial fact is that the system is STLCC. This means that, despite the conservation law, any configuration can be reached, that is, any orientation $R$ together with any rotor angles $(\theta_1, \theta_2)$.

### 6.3.3 An Underwater Vehicle with Three Thrusters

Consider the underwater vehicle introduced in Section 3.2.3, with the input forces depicted in Figure 3.3. We compute some good symmetric products as

$$\begin{aligned}
\langle b_1 : b_2 \rangle &= \frac{m_2 - m_1}{J_3 m_1 m_2} \mathsf{e}_3 - \frac{h}{J_3 m_2} \mathsf{e}_5, \\
\langle b_1 : b_3 \rangle &= \frac{m_1 - m_3}{J_2 m_1 m_3} \mathsf{e}_2 - \frac{h}{J_2 m_3} \mathsf{e}_6, \\
\langle b_2 : b_3 \rangle &= \frac{1}{J_1} \left( \frac{h^2}{J_3} - \frac{h^2}{J_2} - \frac{1}{m_3} + \frac{1}{m_2} \right) \mathsf{e}_1
\end{aligned}$$

and some bad ones as

$$\langle b_1 : b_1 \rangle = 0, \qquad \langle b_2 : b_2 \rangle = \frac{2h}{I_3 m_1} \mathsf{e}_4, \quad \langle b_3 : b_3 \rangle = \frac{2h}{I_2 m_1} \mathsf{e}_4.$$

[UV] $\mathcal{B} = \{b_1, b_2, b_3\}$: Consider the $6 \times 6$ matrix defined by the good symmetric products of order one and two, that is $\{b_1, b_2, b_3, \langle b_1 : b_2 \rangle, \langle b_1 : b_3 \rangle, \langle b_2 : b_3 \rangle\}$. This matrix is generically nonsingular.[3] Hence, the system is small-time locally accessible at zero velocity. Additionally, since the bad second-order symmetric products are proportional to $b_1$, they are spanned by good lower-order symmetric products ($b_1$ is a good symmetric product of order 1). Therefore, the system is generically STLC at zero velocity.

Notice that this is a 12-dimensional nonlinear system with 3 inputs, and controllability is established via a few intuitive and simple algebraic computations.

[3] The matrix is singular when $h^2 m_1 m_2 + J_3(m_1 - m_2) = 0$ or when $h^2 m_1 m_3 + J_2(m_1 - m_3) = 0$ or when $h^2(1/J_3 - 1/J_2) = 1/m_3 - 1/m_2$.

## 6.4 Controllability for Hybrid Mechanical Control Systems

In this section we provide an algebraic procedure for testing sufficient conditions for equilibrium controllability of hybrid mechanical systems, i.e., for systems with impacts as described in Section 3.4.1. We rely on the notion of equilibrium controllability and therefore only consider the case when the velocity at the impact is zero. Since the definition of equilibrium controllability 6.6 relies only on the properties of the solutions $\{q(t), t \in [0,T]\}$, the definition above is also applicable in the setting of hybrid systems.

According to the definition in equation (3.20), a hybrid mechanical control system is a finite collection of constrained mechanical control systems (CMCS) together with a set of jump transition maps. Any CMCS $\Sigma_i = \{Q, M_q, \mathcal{F}, \mathcal{D}_i\}$ (discrete regime $i$) is characterized by a connection $\nabla^i$ and an input distribution $\mathcal{Y}_i$. The equations of motion are therefore:

$$\nabla^i_{\dot{q}}\dot{q} = \sum_{k=1}^{m} Y^i_k u_k(t). \tag{6.4}$$

where $\{Y^i_1, \ldots, Y^i_m\}$ is a base for $\mathcal{Y}_i$.

For each discrete regime $i$, we can repeat the construction in the previous sections and introduce the notion of symmetric closure, of bad and good product, and of order of a product. Given the family of input vector fields $\mathcal{Y}_i$, we let $\mathrm{Sym}_i(\mathcal{Y}_i)$ denote its symmetric closure. The index denotes that when computing symmetric closures, the connection $\nabla^i$ (different for different regimes $i$) must be used.

**Proposition 6.10.** *The hybrid mechanical control system* (3.20) *is equilibrium controllable on an open set $W$ if the following two conditions hold:*

*(i) in each discrete regime $i$, every bad symmetric product is a linear combination of lower order good symmetric products*

*(ii) the rank of* $\mathrm{Lie}(\sum_{i\in I} \mathrm{Sym}_i(\mathcal{Y}_i))(q)$ *is full for all $q \in W$.*

The two conditions have the following interpretation. Condition (ii) guarantees that by combining subsequent motions that are feasible in different regimes, a full neighborhood of the initial point is accessible. Condition (i) is the functional equivalent of the usual bad versus good Lie bracket condition and guarantees that the system is controllable as opposed to accessible.

*Proof.* We start by examining the set of configurations reachable at zero velocity for the $i$th constrained system. For any point $q_0 \in W$, consider the distribution $\mathrm{Lie}(\mathrm{Sym}_i(Y^i_1, \ldots, Y^i_m))$, and let $N_i \subset Q$ be its maximal integral manifold through the point $q_0$. Consider the trajectories of the control system in equation (6.4) starting from point $q_0$ at zero velocity; they are constrained to remain on $N_i$ (see Theorem 6.5 on configuration accessibility). Additionally, because each bad symmetric product is compensated by a lower order, good symmetric product, each configuration on $N_i \cap W$ is reachable at zero velocity; see Theorem 6.7.

By relying on configuration controllability and thereby exploring the fact that any configuration can be reached at zero velocity, we essentially reduced the computation of the reachable configurations for a second order control system (with drift) to those for a fisrt order (kinematic) control system (without drift). More precisely, the set of configurations that can be reached starting and finishing at rest for the control system

$$\nabla^i_{\dot{q}}\dot{q} = Y^i_1 u^i_1 + \ldots + Y^i_m u^i_m, \tag{6.5}$$

is equal to the set of configurations that can be reached for the control system

$$\dot{q} = X_1^i v_1^i + \ldots + X_p^i v_p^i, \tag{6.6}$$

where the family of vector fields $\{X_1^i, \ldots, X_p^i\}$ spans the distribution $\text{Lie}(\text{Sym}_i(Y_1^i, \ldots, Y_m^i))$. Remarkably, equation(6.5) evolves on $TQ$ while equation (6.6) evolves on $Q$.

In the second half of the proof, consider the first order control system

$$\dot{q} = \sum_{i \in I} (X_1^i v_1^i + \ldots + X_p^i v_p^i), \tag{6.7}$$

where vector fields from all regimes $i \in I$ are present. Since

$$\text{Lie}(\cup_i \text{Lie}(\text{Sym}_i(Y_1^i, \ldots, Y_m^i))) = \text{Lie}(\cup_i \text{Sym}_i(Y_1^i, \ldots, Y_m^i)),$$

and since $\text{Lie}(\cup_i \text{Sym}_i(Y_1^i, \ldots, Y_m^i))$ is full rank by assumption, the system in equation (6.7) is locally controllable by Chow's theorem. Therefore, for any point $q_1 \in W$, there exist piecewise constant inputs $\{v_k^j(t)\}$ that steer the state of the previous control system from $q_0$ to $q_1$. Specifically, there exist a sequence of vector fields $X_{\alpha_k}$ belonging to $\cup_i \text{Lie}(\text{Sym}_i(Y_1^i, \ldots, Y_m^i))$ and positive scalar values $\epsilon_k$ such that

$$q_1 = \Phi_{\epsilon_1}^{X_{\alpha_1}} \circ \cdots \circ \Phi_{\epsilon_N}^{X_{\alpha_N}}(q_0),$$

where $\Phi_\epsilon^{X_\alpha}(q)$ denotes the flow along the vector field $X_\alpha$ for time $\epsilon$ starting from point $q$.

The following two observations then complete the proof. First, each flow $\Phi_\epsilon^{X_\alpha}(q)$ of the kinematic system (6.7) can be realized by the dynamic system (6.5), as discussed above. Second, since we assume $V_{ij} \neq \emptyset$ in point (iv) of the definition of HMCS, system (6.5) can switch at any time from each smooth regime to any other regime and therefore it can flow along the sequence of regimes $\{\alpha_k\}$. □

This result can be interpreted as follows. Because of condition $(i)$ each regime is equilibrium controllable when restricted to the integral manifold of $\text{Lie}(\text{Sym}_i(\mathcal{Y}_i))$. Hence, if we can reach a certain configuration, then we can reach it at zero velocity. Finally, since we can switch at zero velocity and at any desired point in time and configuration, we can combine the flows on each regime. But combining flows is equivalent to computing the involutive closure in the ambient space.

### 6.4.1 A Sliding and Clamping Device

We now have the tools to check for equilibrium controllability of the device described in Section 3.4.2. In particular, we perform the operation of symmetric closure on the three regimes: $\text{Sym}_i(Y_i)$ for $i = 0, 1, 2$. It holds that for all $i$, we have

$$\langle Y_i : Y_i \rangle_i = 2\nabla_{Y_i}^i Y_i \in \text{span}\{Y_i\}.$$

Therefore, in each regime all (good and bad) symmetric products are linear combination of lower order symmetric products. Next we look at the Lie brackets computations on the manifold $Q$. The brackets are not reported here for the sake of brevity. It is straightforward to compute that

$$\text{rank}\,\{\text{Lie}(Y_0, Y_1)(q)\} = \text{rank}\,\{Y_0, Y_1, [Y_0, Y_1], [Y_0, [Y_0, Y_1]]\}\,(q) = 4,$$

in a neighborhood of the point $(\theta_1, \theta_2, x_{\text{CM}}, y_{\text{CM}}) = (0, 0, 0, 0)$. Regarding the second constrained regime, one can show that if $l_1 = l_2$

$$\text{rank}\,\{\text{Lie}(Y_0, Y_2)(q)\} < 4, \qquad \forall q \in Q.$$

Incidentally, the involutive closure of $\{Y_0, Y_2\}$ cannot have full rank since it holds $\text{d}(\theta_1 + \theta_2) \cdot Y_0 = \text{d}(\theta_1 + \theta_2) \cdot Y_2 = 0$, and therefore $(\theta_1 + \theta_2)$ is a conserved quantity for the control system $\Sigma = \{\Sigma_0, \Sigma_2\}$. Since the tests presented in Section 6.4 are only sufficient, we can only state that the hybrid mechanical control systems $\Sigma = \{\Sigma_0, \Sigma_1\}$ and $\Sigma = \{\Sigma_0, \Sigma_1, \Sigma_2\}$ are equilibrium controllable.

# Chapter 7

# Motion Algorithms for Underactuated Systems on Lie Groups

In this chapter we design motion algorithms for underactuated mechanical systems on Lie groups. We rely on the controllability analysis in the previous chapter and design global algorithms based on local motion primitives of motion.

The chapter is organized as follows. In Section 7.1 we compute approximate expansions that describe the evolution of a mechanical system forced by small amplitude forcing. Numerous examples provide intuition about the expansions. Then, on the basis of a controllability assumption, we design two basic motion primitives for maintaining and changing the velocity of a system. Finally, in Section 7.2 we combine the motion primitives to obtain control algorithms. The treatment in this chapter is joint work with Naomi Ehrich Leonard, see [22, 23, 24].

## 7.1 Small-Amplitude Forcing and Approximate Solutions

In this section we study the behavior of system

$$\dot{g} = g \cdot \xi \tag{7.1}$$

$$\mathbb{I}\dot{\xi} = \mathrm{ad}^*_\xi \mathbb{I}\xi + \sum_{i=1}^{m} f_i u_i(t), \tag{7.2}$$

under small-amplitude forcing. The key analysis tool is the standard perturbation method as described, for example, in [51]. Assuming a small-amplitude input (say of order $\epsilon$, for $0 < \epsilon \ll 1$), this method provides us with a solution to system (7.1)–(7.2) in the form of a Taylor series in $\epsilon$. Since the computation of only a few terms in the series is tractable, we obtain an approximate expansion. However, this estimate illustrates the role of symmetric products and Lie brackets in determining the solution of the forced system (7.1)–(7.2). Therefore, this estimate provides insight into the controllability tests introduced in the previous chapter and, as we shall see, it is instrumental in designing the motion algorithms of the next section.

### 7.1.1 Notation and Results

We introduce the following notation. Given a possibly vector-valued function $h(t)$ with $t \in \mathbb{R}_+$, define its first integral function $\overline{h}(t)$ with $t \in \mathbb{R}_+$, as the finite integral from 0 to $t$

$$\overline{h}(t) \triangleq \int_0^t h(\tau) d\tau.$$

Higher-order integrals, as for example $\overline{\overline{h}}(t)$, are defined recursively. In the following, we consider inputs of the form

$$u_i(t,\epsilon) = \epsilon u_i^1(t) + \epsilon^2 u_i^2(t),$$

where $0 < \epsilon \ll 1$ and where $u_i^1, u_i^2$ are $O(1)$. Accordingly, we write the resultant forcing $\sum_i b_i u_i(t,\epsilon)$ as the sum of two terms of different order in $\epsilon$

$$\begin{aligned} \sum_{i=1}^m b_i u_i(t,\epsilon) &= \sum_{i=1}^m b_i \left(\epsilon u_i^1(t) + \epsilon^2 u_i^2(t)\right) \\ &= \epsilon\, b^1(t) + \epsilon^2\, b^2(t), \end{aligned} \tag{7.3}$$

where we define $b^1(t) = \sum_{i=1}^m b_i u_i^1(t)$ and $b^2(t) = \sum_{i=1}^m b_i u_i^2(t)$. In the following, given any quantity $y(\epsilon)$, we let $y^k$ denote the $k$th term in the Taylor expansion of $y(\epsilon)$ about $\epsilon = 0$; for example, we will write $\xi(t,\epsilon) = \epsilon\xi^1(t) + \epsilon^2\xi^2(t) + O(\epsilon^3)$. The following proposition describes the system's behavior when forced by small (order $\epsilon$ and order $\epsilon^2$) amplitude inputs as defined in equation (7.3).

**Proposition 7.1 (Approximate evolution).** *For $0 < \epsilon \ll 1$ and for inputs of the form in equation (7.3), let $(g(t), \xi(t))$ be the solutions of system (7.1)–(7.2). Let $x(t)$ be the exponential coordinates of $g(t)$ about the initial condition $g(0) = \mathrm{Id}$. Also, write the initial velocity as $\xi(0) = \epsilon\xi_0^1 + \epsilon^2\xi_0^2$ where $\xi_0^1$ and $\xi_0^2$ are $O(1)$.*
*Then for $t \in [0, 2\pi]$ it holds that $\xi(t,\epsilon) = \epsilon\xi^1(t) + \epsilon^2\xi^2(t) + \epsilon^3\xi^3(t) + O(\epsilon^4)$, with*

$$\begin{aligned} \xi^1(t) &= \xi_0^1 + \overline{b^1}(t), \\ \xi^2(t) &= \xi_0^2 - \left\langle \xi_0^1 : \xi_0^1 \right\rangle \frac{t}{2} - \left\langle \xi_0^1 : \overline{\overline{b^1}}(t) \right\rangle + \left(\overline{b^2 - \tfrac{1}{2}\left\langle \overline{b^1} : \overline{b^1} \right\rangle}\right)(t), \\ \xi^3(t) &= -\left\langle \xi_0^1 : \xi_0^2 \right\rangle t + \left\langle \xi_0^1 : \left\langle \xi_0^1 : \xi_0^1 \right\rangle \right\rangle \frac{t^2}{4} + \left\langle \xi_0^1 : \left\langle \xi_0^1 : \overline{\overline{b^1}}(t) \right\rangle \right\rangle \\ &\quad - \left\langle \xi_0^1 : \left(\overline{b^2 - \tfrac{1}{2}\left\langle \overline{b^1} : \overline{b^1} \right\rangle}\right)(t) \right\rangle - \left\langle \overline{\overline{b^1}}(t) : \xi_0^2 \right\rangle + \tfrac{1}{2}\overline{\left\langle \left\langle \xi_0^1 : \xi_0^1 \right\rangle t : \overline{b^1}(t) \right\rangle} \\ &\quad + \overline{\left\langle \overline{b^1} : \left\langle \xi_0^1 : \overline{\overline{b^1}} \right\rangle \right\rangle}(t) - \overline{\left\langle \overline{b^1} : \left(\overline{b^2 - \tfrac{1}{2}\left\langle \overline{b^1} : \overline{b^1} \right\rangle}\right) \right\rangle}(t), \end{aligned}$$

*and $x(t,\epsilon) = \epsilon x^1(t) + \epsilon^2 x^2(t) + O(\epsilon^3)$, with*

$$\begin{aligned} x^1(t) &= \xi_0^1 t + \overline{\overline{b^1}}(t), \\ x^2(t) &= \xi_0^2 t - \left\langle \xi_0^1 : \xi_0^1 \right\rangle \frac{t^2}{4} + \left(\overline{\overline{b^2 - \tfrac{1}{2}\left\langle \overline{b^1} : \overline{b^1} \right\rangle}}\right)(t) - \left\langle \xi_0^1 : \overline{\overline{\overline{b^1}}}(t) \right\rangle + \tfrac{1}{2}\overline{\left[\xi_0^1 + \overline{b^1}, \xi_0^1 t + \overline{\overline{b^1}}\right]}(t). \end{aligned}$$

Note that both symmetric products and Lie brackets show up in the Taylor expansions and this agrees with the controllability tests presented above. Also, note that the approx-

imations in Proposition 7.1 hold only over a finite period of time and particular care is needed in order to compute approximations valid over a time interval of order $1/\epsilon$.

*Proof.* The proof is based on the standard perturbation method as described in [51] and on the approximate solutions for the kinematic system obtained in [39]. We start by proving the validity of the expansion in $\xi(t,\epsilon)$. Consider the ordinary differential equation

$$\dot{x} = f(x) + g(t,\epsilon),$$

and let $x(t,\epsilon)$ denote the solution from initial condition $x_0(\epsilon)$. At $\epsilon = 0$, suppose that $f(x_0(0)) = g(t,0) = 0$, so that $x(t,0) = x_0(0)$ is a constant solution. We now expand $x(t,\epsilon)$ and $g(t,\epsilon)$ in a Taylor series about the value $\epsilon = 0$ and write

$$x(t,\epsilon) = \sum_{i=0}^{\infty} \epsilon^i x^i(t) \quad \text{and} \quad g(t,\epsilon) = \sum_{i=0}^{\infty} \epsilon^i g^i(t).$$

As shown in [51], the components in the expansion of $x$ satisfy the following differential equations

$$\dot{x}^n(t) = \frac{1}{n!}\frac{\partial^n}{\partial \epsilon^n}\Big|_{\epsilon=0} f(x(t,\epsilon)) + g^n(t),$$

with initial condition $x^n(0) = \frac{1}{n!}\frac{\partial^n}{\partial \epsilon^n}\Big|_{\epsilon=0} x_0(\epsilon)$.

The differential equation of interest in our case is equation (7.2), which we rewrite as

$$\dot{\xi} = -\frac{1}{2}\langle \xi : \xi \rangle \; + \; \epsilon b^1(t) + \epsilon^2 b^2(t).$$

The initial condition is $\xi(0,\epsilon) = \epsilon\xi_0^1 + \epsilon^2\xi_0^2$. The constant solution we expand about is $\xi(t,0) = \xi^0(t) = 0$.

Differentiating the function $f(\xi(\epsilon)) = -\frac{1}{2}\langle \xi : \xi \rangle$, we have

$$\begin{aligned}
\frac{\partial f}{\partial \epsilon} &= -\left\langle \xi : \frac{\partial \xi}{\partial \epsilon} \right\rangle, \\
\frac{\partial^2 f}{\partial \epsilon^2} &= -\left\langle \frac{\partial \xi}{\partial \epsilon} : \frac{\partial \xi}{\partial \epsilon} \right\rangle - \left\langle \xi : \frac{\partial^2 \xi}{\partial \epsilon^2} \right\rangle, \\
\frac{\partial^3 f}{\partial \epsilon^3} &= -3\left\langle \frac{\partial \xi}{\partial \epsilon} : \frac{\partial^2 \xi}{\partial \epsilon^2} \right\rangle - \left\langle \xi : \frac{\partial^3 \xi}{\partial \epsilon^3} \right\rangle,
\end{aligned}$$

and noting that $\frac{\partial^n}{\partial \epsilon^n}\Big|_{\epsilon=0} \xi = n!\,\xi^n$, we have

$$\begin{aligned}
\frac{\partial f}{\partial \epsilon}\Big|_{\epsilon=0} &= -\left\langle \xi^0 : \xi^1 \right\rangle, \\
\frac{\partial^2 f}{\partial \epsilon^2}\Big|_{\epsilon=0} &= -\left\langle \xi^1 : \xi^1 \right\rangle - 2\left\langle \xi^0 : \xi^2 \right\rangle, \\
\frac{\partial^3 f}{\partial \epsilon^3}\Big|_{\epsilon=0} &= -6\left\langle \xi^1 : \xi^2 \right\rangle - 6\left\langle \xi^0 : \xi^3 \right\rangle.
\end{aligned}$$

Next, we write the differential equations as described above. Recalling that $\xi^0(t) = 0$ we

have

$$\begin{aligned}\dot{\xi}^1 &= b^1,\\ \dot{\xi}^2 &= -\frac{1}{2}\left\langle \xi^1 : \xi^1 \right\rangle + b^2,\\ \dot{\xi}^3 &= -\left\langle \xi^1 : \xi^2 \right\rangle.\end{aligned}$$

Initial conditions are $\xi^1(0) = \xi_0^1$, $\xi^2(0) = \xi_0^2$, $\xi^3(0) = 0$. Finally, we employ the notation introduced in Section 7.2 to integrate the three differential equations:

$$\begin{aligned}\xi^1(t) &= \xi_0^1 + \overline{b^1}(t),\\ \xi^2(t) &= \xi_0^2 - \frac{1}{2}\overline{\left\langle \xi_0^1 + \overline{b^1}(t) : \xi_0^1 + \overline{b^1}(t) \right\rangle} + \overline{b^2}(t),\\ \xi^3(t) &= -\overline{\left\langle \xi_0^1 + \overline{b^1}(t) \quad : \quad \xi_0^2 - \frac{1}{2}\overline{\left\langle \xi_0^1 + \overline{b^1}(t) : \xi_0^1 + \overline{b^1}(t) \right\rangle} + \overline{b^2}(t) \right\rangle}.\end{aligned}$$

Expanding the terms on the right-hand side, one recovers all of the terms in the expansions of $\xi(t,\epsilon)$ in Proposition 7.1.

In the second part of the proof we prove the validity of the expansion of $x(t,\epsilon)$ by means of the approximate solutions for kinematic systems obtained in [39] and used in [62]. From these references we know that, if $\xi(t,\epsilon) = O(\epsilon)$, then

$$x(t,\epsilon) = \overline{\xi}(t) + \frac{1}{2}\overline{[\xi,\overline{\xi}]}(t) + O(\epsilon^3).$$

Substituting $\xi(t,\epsilon) = \epsilon\xi^1(t) + \epsilon^2\xi^2(t) + O(\epsilon^3)$, we have:

$$x(t,\epsilon) = \epsilon\overline{\xi^1}(t) + \epsilon^2\overline{\xi^2}(t) + \frac{1}{2}\epsilon^2\overline{\left[\xi^1,\overline{\xi^1}\right]}(t) + O(\epsilon^3).$$

And substituting the values for $\xi^1(t)$ and $\xi^2(t)$, and writing $x(t,\epsilon) = \epsilon x^1(t) + \epsilon^2 x^2(t) + O(\epsilon^3)$, we have

$$\begin{aligned}x^1(t) &= \overline{\xi_0^1 + \overline{b^1}}(t),\\ x^2(t) &= \left(\xi_0^2 t - \left\langle \xi_0^1 : \xi_0^1 \right\rangle \frac{t^2}{4} - \left\langle \xi_0^1 : \overline{\overline{b^1}} \right\rangle(t) + \left(\overline{b^2 - \tfrac{1}{2}\left\langle \overline{b^1} : \overline{b^1} \right\rangle}\right)(t)\right)\\ &\quad + \frac{1}{2}\overline{\left[\xi_0^1 + \overline{b^1}, \overline{\xi_0^1 + \overline{b^1}}\right]}(t).\end{aligned}$$

Expanding the terms on the right-hand side, one recovers all of the terms in the expansions of $x(t,\epsilon)$ in Proposition 7.1. □

### 7.1.2 Examples and Remarks

We now relate the approximations above to the controllability tests of the previous section. To simplify the expansions above and to investigate the nonlinear second-order effects of the inputs, we let the initial velocity vanish, $\xi(0) = 0_{\mathfrak{g}}$, and the first order input $b^1(t)$ verify

Figure 7.1: Planar rigid body with single input: PRB1 and PRB2.

$\overline{b^1}(2\pi) = \overline{\overline{b^1}}(2\pi) = 0_{\mathfrak{g}}$. It holds that

$$\xi(2\pi) \approx \epsilon^2 \left(\overline{b^2 - \tfrac{1}{2}\left\langle \overline{b^1} : \overline{b^1} \right\rangle}\right)(2\pi), \quad \text{and} \quad x(2\pi) \approx \epsilon^2 \left(\overline{\overline{b^2} - \tfrac{1}{2}\overline{\left\langle \overline{b^1} : \overline{b^1} \right\rangle}} + \tfrac{1}{2}\overline{\left[\overline{\overline{b^1}}, \overline{b^1}\right]}\right)(2\pi), \tag{7.4}$$

where, for the remainder of this section, the symbol $\approx$ denotes an equality up to a third order error in $\epsilon$. Also, if we set $b^2(t) = 0_{\mathfrak{g}}$, it holds that

$$\xi(2\pi) \approx -\tfrac{1}{2}\epsilon^2 \overline{\left\langle \overline{b^1} : \overline{b^1} \right\rangle}(2\pi), \quad \text{and} \quad x(2\pi) \approx -\tfrac{1}{2}\epsilon^2 \left(\overline{\overline{\left\langle \overline{b^1} : \overline{b^1} \right\rangle}} + \overline{\left[\overline{\overline{b^1}}, \overline{b^1}\right]}\right)(2\pi). \tag{7.5}$$

Up to a higher-order error in $\epsilon$, the final velocity $\xi(2\pi)$ is determined by certain symmetric products and the final configuration variable $x(2\pi)$ is determined by certain symmetric products and Lie brackets. Next, we study in more detail these remaining terms to gain some insight into what terms are "good," what are "bad" and which ones we can exploit to design motion algorithms.

### Single-Input Systems: Relative Equilibria and Bad Symmetric Products

Both examples of planar rigid bodies, [PRB1] and [PRB2], are single-input systems. Recall that [PRB1] denotes the system with a single force $b_1$ with the line of action through the center of mass, and [PRB2] denotes the system with the single force $b_2$ applied at a point a distance $h$ from the center of mass and perpendicular to $b_1$, as shown in Figure 7.1.

Let $b_{\mathrm{si}}$ denote the single input vector, e.g., $b_{\mathrm{si}} = b_1$ in [PRB1] and $b_{\mathrm{si}} = b_2$ in [PRB2]. If the symmetric product $\langle b_{\mathrm{si}} : b_{\mathrm{si}} \rangle$ vanishes, see the [PRB1] example, the system is neither accessible nor configuration accessibility, and the final state $(x, \xi)(2\pi)$ vanishes. Recall from Section 3.2 that for any vector $\eta$ such that $\langle \eta : \eta \rangle \equiv \mathrm{ad}^*_\eta \mathbb{I}\eta = 0$, the curve $t \in \mathbb{R} \mapsto (\exp(t\eta), \eta)$ is a relative equilibria, i.e., a motion corresponding to constant body-fixed velocity. Thus, an actuator $b_{\mathrm{si}}$ aligned with a relative equilibria has vanishing bad symmetric product $\langle b_{\mathrm{si}} : b_{\mathrm{si}} \rangle$.

Also instructive is the case in which the bad symmetric product $\langle b_{\mathrm{si}} : b_{\mathrm{si}} \rangle$ does not vanish, e.g., the [PRB2] system. Assuming $b^1(t) = b_{\mathrm{si}}\phi(t)$ and $\overline{\phi}(2\pi) = \overline{\overline{\phi}}(2\pi) = 0$, equations (7.5) lead to

$$\xi(2\pi) \approx -\tfrac{1}{2}\epsilon^2 \int_0^{2\pi} \overline{\phi}^2 dt \, \langle b_{\mathrm{si}} : b_{\mathrm{si}} \rangle, \quad \text{and} \quad x(2\pi) \approx -\tfrac{1}{2}\epsilon^2 \int_0^{2\pi} \int_0^s \overline{\phi}^2 ds dt \, \langle b_{\mathrm{si}} : b_{\mathrm{si}} \rangle. \tag{7.6}$$

As already mentioned, configuration and velocity change an amount proportional to $\epsilon^2$ along

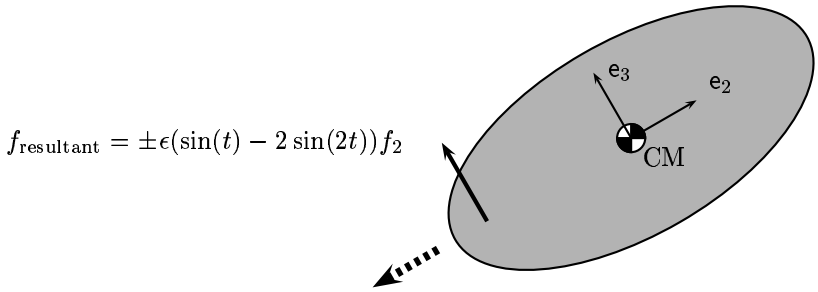


Figure 7.2: Planar rigid body with single forcing [PRB2]. With a periodic resultant external force and after a period $2\pi$, the body has moved to the left of the initial configuration.

the direction $\langle b_{\text{si}} : b_{\text{si}} \rangle$. Additionally, notice that it is impossible to change the sign of the motion, which will always be along $-\langle b_{\text{si}} : b_{\text{si}} \rangle$. For example, the [PRB2] system with forcing amplitude $\pm\epsilon\cos(t)$ always moves in the direction $-\mathsf{e}_2$, i.e., to the left (see Figure 7.2). This phenomenon suggests that the system is not locally controllable, as certain configurations appear to be not reachable. However, equation (7.6) does not prove this claim as it only specifies the final value $x(2\pi)$. The sharper analysis in [65] is needed to show that single-input systems are neither STLC at zero velocity nor STLCC.

### Multi-Input Systems with No Bad Symmetric Products

Next we examine systems with (at least) two input forces. We focus on an example with two input vectors $b_1$ and $b_2$ that have vanishing bad symmetric products $\langle b_1 : b_1 \rangle = \langle b_2 : b_2 \rangle = 0$ and either non-zero good symmetric product $\langle b_1 : b_2 \rangle \neq 0$ or non-zero Lie bracket $[b_1, b_2] \neq 0$. The satellite with two thrusters [ST] and the satellite with two rotors [SR] are such examples. Plugging $b^1(t) = b_1 u_1(t) + b_2 u_2(t)$ into equations (7.5), we have

$$\begin{aligned}\xi(2\pi) &\approx -\tfrac{1}{2}\epsilon^2 \overline{\langle \overline{u_1 b_1 + u_2 b_2} : \overline{u_1 b_1 + u_2 b_2} \rangle}(2\pi) \\ &= -\epsilon^2 \langle b_1 : b_2 \rangle \overline{u_1}\ \overline{u_2}(2\pi),\end{aligned}$$

and

$$\begin{aligned}x(2\pi) &\approx -\tfrac{1}{2}\epsilon^2 \left( \overline{\left\langle \overline{b^1} : \overline{b^1} \right\rangle} + \overline{\left[ \overline{\overline{b^1}}, \overline{b^1} \right]} \right)(2\pi) \\ &= -\epsilon^2 \langle b_1 : b_2 \rangle \overline{\overline{u_1}\ \overline{u_2}}(2\pi) - \epsilon^2 [b_1, b_2] \overline{\overline{u_1}\ \overline{u_2} - \overline{u_1}\ \overline{u_2}}(2\pi).\end{aligned}$$

We interpret the operations performed on the input signals $u_1(t)$ and $u_2(t)$ as follows: $\overline{u_1}\ \overline{u_2}(2\pi)$ is the inner product in the $L_2[0, 2\pi]$ function space between $\overline{u_1}(t)$ and $\overline{u_2}(t)$, whereas $\overline{\overline{u_1}\ \overline{u_2} - \overline{u_1}\ \overline{u_2}}(2\pi)$ is the area enclosed by the plot of signals $\overline{u_1}(t)$ versus $\overline{u_2}(t)$. We distinguish two cases:

- *Out-of-phase sinusoidal inputs generate motion along Lie brackets:* First, consider the satellite with rotors [SR] example that is STLCC but not STLC at zero velocity. The

symmetric product $\langle b_1 : b_2 \rangle$ vanishes, so that we have from equation (7.5)

$$\xi(2\pi) \approx 0 \quad \text{and} \quad x(2\pi) \approx -\epsilon^2 [b_1, b_2] \overline{\overline{u_1}\,\overline{u_2} - \overline{u_1}\,\overline{u_2}}(2\pi).$$

If we want to steer the configuration $x(2\pi)$ in the direction $[b_1, b_2]$, sinusoidal signals at the same frequency and *out-of-phase* are a simple standard choice. This is one of the basic ideas behind the algorithms presented in [62] and other literature on motion planning for driftless control systems.

- *In-phase sinusoidal inputs generate motion along good symmetric products:* Second, consider the satellite with thrusters example [ST] that is STLC at zero velocity since the symmetric product $\langle b_1 : b_2 \rangle \neq 0$. If we pick sinusoidal inputs at the same frequency and *in-phase*, e.g., $u_1(t) = u_2(t) = \cos(t)$, the contribution proportional to the Lie bracket $[b_1, b_2]$ vanishes, since the area included by two identical signal is zero. Further, it holds that

$$\xi(2\pi) \approx -\epsilon^2 \langle b_1 : b_2 \rangle \overline{(\overline{u_1})^2}(2\pi) \quad \text{and} \quad x(2\pi) \approx -\epsilon^2 \langle b_1 : b_2 \rangle \overline{\overline{(\overline{u_1})^2}}(2\pi),$$

and both velocity and configuration variables vary along $-\langle b_1 : b_2 \rangle$. Motion in the symmetric product direction is generated with sinusoidal inputs at the same frequency and *in-phase*. This is in contrast with the previous case and it is reminiscent of some results on gait selection for locomotion systems with drift, see the 1:1 gait in [80].

**Multi-Input Systems with Bad Symmetric Products**

Finally, we examine systems with non-vanishing bad symmetric products. We focus on the planar rigid body with two forces applied at a point distant from the center of mass [PRB3]. Recall that this system is STLC at zero velocity since the subspace $\{b_1, b_2, \langle b_1 : b_2 \rangle\}$ has full rank and since the good/bad products condition is verified by the equality $\langle b_2 : b_2 \rangle = \frac{2h}{J} b_1$. Setting $b^1 = b_1 u_1(t) + b_2 u_2(t)$ as above, the existence of a non-vanishing bad symmetric product causes

$$-\tfrac{1}{2}\epsilon^2 \overline{\left\langle \overline{b^1} : \overline{b^1} \right\rangle}(2\pi) = -\epsilon^2 \langle b_1 : b_2 \rangle \overline{\overline{u_1}\,\overline{u_2}}(2\pi) - \tfrac{1}{2}\epsilon^2 \langle b_2 : b_2 \rangle \overline{\overline{u_2}^2}(2\pi),$$

where the sign of the second term is independent of $u_2(t)$. However, motion in the $\langle b_2 : b_2 \rangle$ direction can be affected by a second-order input along $b_1$. In particular, by setting

$$b^2(t) = \frac{h}{2\pi J} \overline{\overline{u_2}^2}(2\pi) b_1,$$

we obtain from equation (7.4)

$$\xi(2\pi) \approx -\epsilon^2 \langle b_1 : b_2 \rangle \overline{\overline{u_1}\,\overline{u_2}}(2\pi),$$

recovering this way the result for the case without bad symmetric products. In other words, the "bad" contribution due to $\langle b_2 : b_2 \rangle$ is "annihilated" by means of the second-order input $b^2(t)$, and this is possible only because the good/bad products condition is verified.

### 7.1.3 Inversion Algorithm for Systems Controllable with Second-Order Symmetric Products

In this section we build on previous analysis and investigate ways of determining the final velocity of a forced mechanical system undergoing small amplitude forcing. The expansions

above provide an approximation of the function that maps the time evolution of the force to the final displacement. Our goal is to focus on this "force to displacement map" and invert it.

Motivated by the heuristic analysis in the last two examples and by the controllability analysis in the previuos chapter, we introduce an additional definition. A system is *STLC at zero velocity with second-order symmetric products* if it satisfies the following property:

> The subspace $\text{span}\{b_i, \langle b_j : b_k \rangle, 1 \le i \le m, 1 \le j < k \le m\}$ has full rank and each bad symmetric product $\langle b_i : b_i \rangle$ is a linear combination of the vectors $\{b_1, \ldots, b_m\}$. (A3)

The planar rigid body with two forces [PRB3], the satellite with two thrusters [ST] and the underwater vehicle [UV] satisfy this controllability condition. On the basis of this assumption, we design inputs $\big(b^1(t), b^2(t)\big)$, that allow us to simplify the approximations in Proposition 7.1 and steer the velocity of the system to an arbitrary value.

**Lemma 7.2 (Inversion Algorithm).** *Let the assumption* (A3) *hold and let* $\eta$ *be an arbitrary element in* $\mathfrak{g}$. *Define the input functions* $\big(b^1(t),\ b^2(t)\big)$ *as follows:*

*(i) Set* $N = m(m-1)/2$ *and let* $P$ *denote the set of ordered pairs* $\{(j,k) \mid 1 \le j < k \le m\}$. *Identify the elements in* $P$ *with the set of integers* $1, \ldots, N$, *and let* $a(j,k)$ *be the integer associated with the pair* $(j,k)$. *In other words,* $a : P \mapsto \{1, \ldots, N\}$ *is a enumeration of* $P$. *For* $\alpha = 1, \ldots, N$, *define the scalar functions*

$$\psi_\alpha(t) = \tfrac{1}{\sqrt{2\pi}}\Big(\alpha \sin(\alpha t) - (\alpha + N)\sin\big((\alpha + N)t\big)\Big).$$

*(ii) Given the assumption* (A3), *the matrix with columns* $b_i, 1 \le i \le m$, *and* $\langle b_j : b_k \rangle, 1 \le j < k \le m$, *has full rank. By means of its pseudo-inverse, compute* $(m + N)$ *real numbers* $z_i$ *and* $z_{jk}$ *such that*

$$\eta = \sum_{1 \le i \le m} z_i b_i + \sum_{1 \le j < k \le m} z_{jk} \langle b_j : b_k \rangle .$$

*(iii) Finally, set*

$$b^1(t) = \sum_{1 \le j < k \le m} \sqrt{|z_{jk}|}\Big(b_j - \text{sign}\,(z_{jk}) b_k\Big)\psi_{a(j,k)}(t), \tag{7.7}$$

$$b^2(t) \equiv b^2 = \frac{1}{2\pi}\sum_{1 \le i \le m} z_i b_i + \frac{1}{4\pi}\sum_{1 \le j < k \le m} |z_{jk}|\Big(\langle b_j : b_j \rangle + \langle b_k : b_k \rangle\Big). \tag{7.8}$$

*The input functions* $(b^1(t), b^2(t))$ *designed in equation* (7.7) *and* (7.8) *verify*

$$\Big(\overline{b^2 - \tfrac{1}{2}\langle \overline{b^1} : \overline{b^1} \rangle}\Big)(2\pi) = \eta. \tag{7.9}$$

*Proof.* Start by studying the properties of the functions $\psi_a(t)$. A direct computation shows

that for all $a, b, c$

$$\overline{\psi_a}(2\pi) = \overline{\overline{\psi_a}}(2\pi) = \overline{\overline{\overline{\psi_a}}}(2\pi) = 0, \tag{7.10}$$

$$\overline{\overline{\psi_a}\,\overline{\psi_b}}(t) = \frac{\delta_{ab}}{2\pi}t + r_{ab}(t), \qquad \text{where} \qquad r_{ab}(2\pi) = \overline{r_{ab}}(2\pi) = 0, \tag{7.11}$$

$$\overline{\overline{\psi_a}\,t}\,(2\pi) = \overline{\overline{\overline{\psi_a}}\,\overline{\psi_b}}(2\pi) = \overline{\overline{\psi_a}\,r_{bc}}(2\pi) = 0, \tag{7.12}$$

where $\delta_{ab}$ is the Kronecker delta function. The proof of these properties is straightforward but tedious. Next, we prove the claim in equation (7.9). Given the definition in equation (7.7) and the property (7.11) of the functions $\psi_a(t)$, we compute:

$$\begin{aligned}
\overline{\left\langle \overline{b^1} : \overline{b^1} \right\rangle}(2\pi) &= \sum_{1\le j<k\le m} \sum_{1\le p<q\le m} \sqrt{|z_{jk}z_{pq}|} \\
&\qquad \left\langle \left(b_j - \operatorname{sign}(z_{jk})b_k\right) : \left(b_p - \operatorname{sign}(z_{pq})b_q\right) \right\rangle \overline{\overline{\psi_{a(j,k)}}\,\overline{\psi_{a(p,q)}}}(2\pi) \\
&= \sum_{1\le j<k\le m} |z_{jk}| \left\langle \left(b_j - \operatorname{sign}(z_{jk})b_k\right) : \left(b_j - \operatorname{sign}(z_{jk})b_k\right) \right\rangle \\
&= \sum_{1\le j<k\le m} |z_{jk}| \left( \langle b_j : b_j \rangle - 2\operatorname{sign}(z_{jk}) \langle b_j : b_k \rangle + \langle b_k : b_k \rangle \right) \\
&= -2 \sum_{1\le j<k\le m} z_{jk} \langle b_j : b_k \rangle + \sum_{1\le j<k\le m} |z_{jk}| \Big( \langle b_j : b_j \rangle + \langle b_k : b_k \rangle \Big).
\end{aligned}$$

Summing up with $\overline{b^2}(2\pi) = 2\pi b^2$, we have

$$\left( \overline{b^2 - \tfrac{1}{2}\langle \overline{b^1} : \overline{b^1} \rangle} \right)(2\pi) = \sum_{1\le i\le m} z_i b_i + \sum_{1\le j<k\le m} z_{jk} \langle b_j : b_k \rangle ,$$

which proves equation (7.9). □

In what follows, we denote the procedure described in the Inversion Algorithm with the notation:

$$\left(b^1(t), b^2(t)\right) = \texttt{Inverse}(\eta) .$$

A direct manipulation of equation (7.7) and of $b^1(t) = \sum_{i=1}^m b_i u_i^1(t)$ leads to the equivalent statement

$$u_i^1(t) = -\sum_{j=1}^{i-1} \sqrt{|z_{ji}|} \operatorname{sign}(z_{ji}) \psi_{a(j,i)}(t) + \sum_{j=i+1}^{m} \sqrt{|z_{ij}|} \psi_{a(i,j)}(t).$$

Note that motion along the good symmetric product direction $\langle b_i : b_j \rangle$ (for $i < j$) is generated by the term $\sqrt{|z_{ij}|}\psi_{a(i,j)}(t)$ in $u_i^1(t)$ and the term $-\sqrt{|z_{ij}|}\operatorname{sign}(z_{ij})\psi_{a(i,j)}(t)$ in $u_j^1(t)$. Hence the inputs $u_i^1(t)$ and $u_j^1(t)$ have the common factor $\psi_{a(i,j)}$. The other terms in the definition of $u_k^1(t)$ for all $k$ are at different frequencies. Therefore, they are orthogonal to $\psi_{a(i,j)}$ in the inner product space $L_2[0, 2\pi]$, and so do not generate motion in any other symmetric product direction. The second term in the second order input $b^2$ compensates for the motion excited along bad symmetric product directions. Its presence is a key difference with respect to the algorithms in [62] for driftless systems.

One of the drawbacks of the previous algorithm is that the input functions contain relatively high frequencies, e.g., in an $m = 3$ input system, the input functions contain sinusoids with frequency from 1 to $m(m-1) = 6$. This can be mitigated by optimizing the

design of the coefficients $\{z_i, z_{jk}\}$ and the numbering of the set $P$. For example, the design of the coefficients can be optimized by employing a weighted pseudo-inverse.

## 7.2 Control Algorithms from Motion Primitives

In this section we design motion control algorithms based on the approximations in Proposition 7.1 and the Inversion Algorithm in Lemma 7.2. Our design is based on the controllability condition (A3), and as mentioned in Chapter 2, on the assumption that the group $G$ be the Cartesian product of an arbitrary number of copies of SE(3).[1] We start by designing two primitive motion patterns, `Maintain-Velocity` and `Change-Velocity`, that provide the system with some basic motion capabilities. We then focus on more complex control algorithms to solve the point-to-point reconfiguration problem, the local exponential stabilization problem and the static interpolation problem.

### 7.2.1 Primitives of Motion

We describe two basic maneuvers that each last $2\pi$ units of time. The parameter $\sigma \ll 1$ is a small positive constant. To maintain a velocity of order $O(\sigma)$, an input of order $O(\sigma)$ suffices, while to obtain a change in velocity of order $O(\sigma)$, we employ a control input of order $O(\sqrt{\sigma})$. Each primitive is described in terms of initial configuration and velocity, input design, and final configuration and velocity.

`Maintain-Velocity`$(\sigma, \xi_{\text{ref}})$**:** keeps the body velocity $\xi(t)$ close to a reference value $\sigma\xi_{\text{ref}}$.

Initial state:
$$g(0) = g_0,$$
$$\xi(0) = \sigma\xi_{\text{ref}} + \sigma^2\xi_{\text{error}},$$

Input:
$$\epsilon = \sigma,$$
$$(b^1, b^2) = \texttt{Inverse}(\pi \langle \xi_{\text{ref}} : \xi_{\text{ref}} \rangle - \xi_{\text{error}}),$$

Final state:
$$\log(g_0^{-1} g(2\pi)) = 2\pi\sigma\xi_{\text{ref}} + \pi\sigma^2\xi_{\text{error}} + O(\sigma^3),$$
$$\xi(2\pi) = \sigma\xi_{\text{ref}} + O(\sigma^3).$$

`Change-Velocity`$(\sigma, \xi_{\text{final}})$**:** steer the body velocity $\xi(t)$ to a final value $\sigma\xi_{\text{final}}$.

Initial state:
$$g(0) = g_0,$$
$$\xi(0) = \sigma\xi_0,$$

Input
$$\epsilon = \sqrt{\sigma},$$
$$(b^1, b^2) = \texttt{Inverse}(\xi_{\text{final}} - \xi_0),$$

Final state:
$$\log(g_0^{-1} g(2\pi)) = \pi\sigma(\xi_0 + \xi_{\text{final}}) + O(\sigma^{3/2}),$$
$$\xi(2\pi) = \sigma\xi_{\text{final}} + O(\sigma^2).$$

The statements on the final configuration and velocity of the primitives are direct extensions of the Inversion Lemma and are therefore proved in Appendix A.2. Note that the magnitude of control input is

$$\|\pi \langle \xi_{\text{ref}} : \xi_{\text{ref}} \rangle - \xi_{\text{error}}\| O(\sigma), \qquad \text{during a } \texttt{Maintain-Velocity}(\sigma, \xi_{\text{ref}}) \text{ primitive,}$$
$$\|\xi_{\text{final}} - \xi_0\| O(\sqrt{\sigma}), \qquad \text{during a } \texttt{Change-Velocity}(\sigma, \xi_{\text{final}}) \text{ primitive.}$$

We conclude this section by showing how to compute estimates of final configurations after multiple periods of control. The following result is a direct consequence of the Campbell–Baker–Hausdorff formula, see for example [85].

[1] This guarantees that the exponential map be a local diffeomorphism between the group and its algebra.

| | |
|---|---|
| **Goal:** | drive system from $(g_0, 0_{\mathfrak{g}})$ to $(g_1, 0_{\mathfrak{g}})$. |
| **Arguments:** | $(g_0, g_1, \sigma)$. |
| **Require:** | $\log(g_0^{-1} g_1)$ well defined. |
| 1: | $N \Leftarrow \text{Floor}(\|\log(g_0^{-1} g_1)\|/(2\pi\sigma))$ {Floor$(x)$ is the greatest integer less than or equal to $x$.} |
| 2: | $\xi_{\text{nom}} \Leftarrow \log(g_0^{-1} g_1)/(2\pi\sigma N)$ |
| 3: | `Change-Velocity`$(\sigma, \xi_{\text{nom}})$ {start maneuver} |
| 4: | **for** $k = 1$ to $(N-1)$ **do** |
| 5: | `Maintain-Velocity`$(\sigma, \xi_{\text{nom}})$ |
| 6: | **end for** |
| 7: | `Change-Velocity`$(\sigma, 0_{\mathfrak{g}})$ {stop maneuver} |

Table 7.1: Constant Velocity Algorithm for point-to-point reconfiguration.

**Lemma 7.3.** *Let $\sigma \ll 1$ be a positive constant and let $g_0, g_1$ be group elements. Define the exponential coordinates $y_0 = \log(g_0) \in \mathfrak{g}$ and $y_1 = \log(g_1) \in \mathfrak{g}$. If the vector $[y_0, y_1]$ is higher order in $\sigma$ than $(y_0 + y_1)$, then it holds*

$$\log(g_0 g_1) = y_0 + y_1 + O([y_0, y_1]).$$

### 7.2.2 Control Algorithms

We present three algorithms to solve various motion control problems. These algorithms combine the two motion primitives with a discrete-time feedback. This makes the approximations hold over multiple time intervals; for example, over a time interval of order $1/\sigma$.

#### Point-to-Point Reconfiguration Problem

This motion task reconfigures the system, i.e., changes its position and orientation, starting and ending at zero velocity. We assume that the initial state is $(g(0), \xi(0)) = (g_0, 0_{\mathfrak{g}})$ and the final desired state is $(g_1, 0_{\mathfrak{g}})$. For simplicity, we require $\log(g_0^{-1} g_1)$ to be well defined, even though this assumption can be removed. For example, on SO(3) the logarithm is well defined whenever the change in attitude is less than $\pi$.

The algorithm consists of three steps. Over the first time interval, we change the velocity to an appropriate reference value. We then maintain the velocity close to this constant reference value for an appropriate number of periods. Finally, we stop the system when close to the desired configuration. The details are described in Table 7.1 and the proof of the following lemma can be found in Appendix A.3.

**Lemma 7.4 (Constant Velocity Algorithm).** *Let $\sigma$ be a sufficiently small positive constant, let $(g(0), \xi(0)) = (g_0, O(\sigma^2))$, and let $g_1$ be a group element such that $\log(g_0^{-1} g_1)$ is well defined. Let $N \in \mathbb{N}$ and the inputs $(b^1, b^2)(t)$ for $t \in [0, 2(N+1)\pi]$ be determined according to the algorithm in Table 7.1. At the final time,*

$$\log\Big(g(2(N+1)\pi)^{-1} g_1\Big) = O(\sigma^{3/2}),$$
$$\xi\Big(2(N+1)\pi\Big) = O(\sigma^2).$$

The final state is not exactly as desired; instead there are errors of order $O(\sigma^{3/2})$ and $O(\sigma^2)$. This undesirable feature can be compensated for by solving the next motion problem, the point stabilization problem.

**Goal:** drive system to the state $(\mathrm{Id}, 0_{\mathfrak{g}})$ exponentially as $t \to \infty$.
**Arguments:** $\sigma$.
**Require:** $\|(\log(g(0)), \xi(0))\| \leq \sigma$.
1: **for** $k = 1$ to $+\infty$ **do**
2: $t_k \Leftarrow 4k\pi$ {$t_k$ is the current time}
3: $\sigma_k \Leftarrow \|(\log(g(t_k), \xi(t_k)))\|$
4: `Change-Velocity`$\Big(\sigma_k, -\big(\log(g(t_k)) + \pi\xi(t_k)\big)/(2\pi\sigma_k)\Big)$
5: `Change-Velocity`$(\sigma_k, 0_{\mathfrak{g}})$
6: **end for**

Table 7.2: Local Exponential Stabilization Algorithm.

### Point Stabilization Problem

This motion task asymptotically stabilizes the configuration $g(t)$ to a desired value that we assume without loss of generality to be the identity. Convergence is ensured as long as the initial condition satisfies

$$\|(\log(g(0)), \xi(0))\| \leq \sigma, \tag{7.13}$$

where $\sigma$ is a sufficiently small positive constant. Should equation (7.13) not hold, then the previous algorithm can be employed to steer the state to an admissible value.

The key idea of the algorithm is to iterate the following procedure: measure the state at time $t_k$ and design control inputs that try to steer the state to the desired value $(\mathrm{Id}, 0_{\mathfrak{g}})$ at time $t_{k+1} = t_k + 4\pi$. Since we impose two requirements, one on the final configuration and one on the final velocity, two calls to the `Change-Velocity` primitive are needed. The idea of iterating an approximate stabilization step for fast convergence can be found, for example, in [56]. The details are described in Table 7.2 and the proof of the following lemma is in Appendix A.4.

**Lemma 7.5 (Local Exponential Stabilization Algorithm).** *Let $\sigma$ be a positive constant and assume the initial condition satisfies equation (7.13). Let the inputs $(b^1(t), b^2(t))$ be determined according to the algorithm in Table 7.2 and let $t_k = 4k\pi$. Then there exists a $\lambda > 0$ such that*

$$\big\|\big(\log(g(t_k)), \xi(t_k)\big)\big\| \leq \big\|\big(\log(g(0)), \xi(0)\big)\big\|\, e^{-\lambda t_k}, \qquad \forall\, k \in \mathbb{N}.$$

*Additionally, for $t \in [4k\pi, 4(k+1)\pi]$ it holds that $\big\|\big(\log(g(t), \xi(t)\big)\big\| = O(e^{-\lambda k/2})$.*

### Static Interpolation Problem

This motion task steers the system's configuration along a path connecting the set of the ordered points $\{g_0, g_1, \ldots, g_M\}$. As above, we require $\log(g_{k-1}^{-1} g_k)$ to be well defined for $1 \leq k \leq M$. The algorithm consists of $M$ repeated constant velocity (point-to-point) maneuvers (Table 7.1), with the only difference being that when the configuration reaches the the $k$th desired value $g_k$, the velocity gets changed directly to the reference value for the next interval, i.e., without stopping. The details are described in Table 7.3. It can be shown that the configuration $g(t)$ follows a path passing through the points $\{g_0, g_1, \ldots, g_M\}$ with an error of order $\sigma$. We do not include a full proof of convergence as it is very similar to the one for Lemma 7.4.

*Remark 7.6 (Sequences of relative equilibria versus constant velocity motions).* It is of in-

**Goal:** drive system through points $\{g_0, g_1, \ldots, g_M\}$.
**Arguments:** $(g_0, g_1, \ldots, g_M, \sigma)$.
**Require:** $(g(0), \xi(0)) = (g_0, 0_{\mathfrak{g}})$ and $\log(g_i^{-1} g_i)$ well defined for $0 \leq i \leq M$.

**for** $j = 1$ to $M$ **do**
  $g_{\mathrm{tmp},j} \Leftarrow g(t)\exp(\pi\xi(t))$ {$t$ is the current time}
  $N_j \Leftarrow \mathrm{Floor}(\|\log(g_{\mathrm{tmp},j}^{-1} g_j)\|/(2\pi\sigma))$
  $\xi_{\mathrm{nom},j} \Leftarrow \log(g_{\mathrm{tmp},j}^{-1} g_j)/(2\pi\sigma N_j)$
  `Change-Velocity`$(\sigma, \xi_{\mathrm{nom},j})$
  **for** $k = 1$ to $(N_j - 1)$ **do**
    `Maintain-Velocity`$(\sigma, \xi_{\mathrm{nom},j})$
  **end for**
**end for**
`Change-Velocity`$(\sigma, 0_{\mathfrak{g}})$

Table 7.3: Static Interpolation Algorithm.

terest to compare the Constant Velocity and the Static Interpolation Algorithms, since they provide two different solutions to the reconfiguration problem. These two algorithms can be compared on the basis of an input cost of the form

$$\|u\|_{[0,T]} = \int_0^T L(u(t))dt,$$

where $T = T(\sigma)$ is the time required to complete the maneuver and $L : \mathcal{U}^m \mapsto \mathbb{R}$ is a cost on the space of input functions. In the following we let $g_i$ and $g_f$ denote initial and final (desired) configurations and we let $\mathcal{P} = \{g_0 = g_i, g_1, \ldots, g_M = g_f\}$ be a sequence of configurations such that $\log(g_{j-1}^{-1} g_j)$ is a relative equilibrium vector for all $j = 1, \ldots, M$. Recall that $\eta \in \mathfrak{g}$ is a relative equilibrium vector if $\langle \eta : \eta \rangle$ vanishes.

(i) The Constant Velocity Algorithm applied to the reconfiguration problem from $g_0$ to $g_f$ involves 2 calls to the `Change-Velocity` primitive and $(N-1)$ calls to the `Maintain-Velocity` primitive. Using notation from Table 7.1 and some of the details in Appendix A.3, the cost of the complete maneuver can be computed as

$$\|u\|_{[0,T]} = 2O(\sqrt{\sigma}) + (N-1)\| \langle \xi_{\mathrm{nom}} : \xi_{\mathrm{nom}} \rangle \| O(\sigma) = O(1),$$

since $\| \langle \xi_{\mathrm{nom}} : \xi_{\mathrm{nom}} \rangle \|$ is of order 1 and $N$ is of order $1/\sigma$.

(ii) The Static Interpolation Algorithm applied to the interpolation problem across the set of configurations $\mathcal{P}$ involves $(M+2)$ calls to the `Change-Velocity` primitive and $(\sum_{j=1}^{M} N_j)$ calls to the `Maintain-Velocity` primitive. With the notation in Table 7.3, a little algebra shows that

$$\|u\|_{[0,T]} = (M+2)O(\sqrt{\sigma}) + (\textstyle\sum_j N_j)\| \langle \xi_{\mathrm{nom},j} : \xi_{\mathrm{nom},j} \rangle \| O(\sigma).$$

Since the configuration $g(t)$ follows the path determined by the set $\mathcal{P}$ with an error of order $\sigma$, and since $\log(g_{j-1}^{-1} g_j)$ is a relative equilibrium vector, it can be shown that $\langle \xi_{\mathrm{nom},j} : \xi_{\mathrm{nom},j} \rangle = O(\sigma)$. Summarizing, the total cost is

$$\|u\|_{[0,T]} = (M+2)O(\sqrt{\sigma}) + (\textstyle\sum_j N_j)O(\sigma^2) = O(\sqrt{\sigma}).$$

We conclude that for small $\sigma$ (or equivalently, for long final times $T = O(1/\sigma)$), moving along

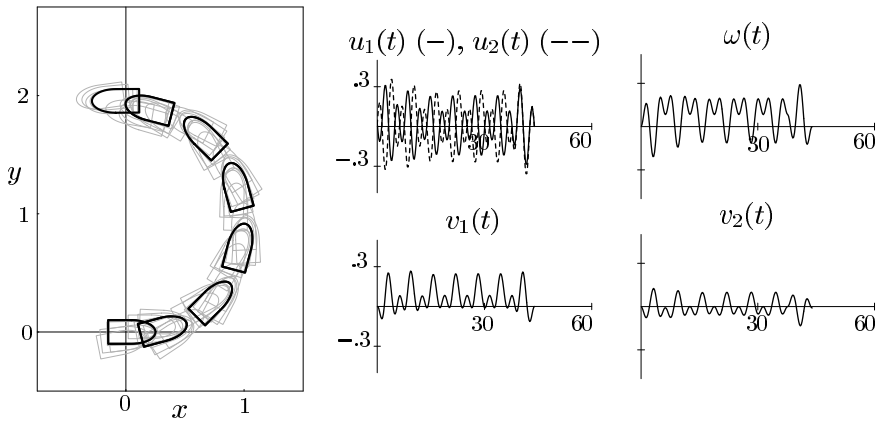


Figure 7.3: Constant Velocity Algorithm. The bullet-shaped objects drawn in the left picture represent the location of the planar body. Darker objects correspond to the location of the body at the beginning and end of a primitive. The plots on the right display the time-evolution of variables $(u_1, u_2, \omega, v_1, v_2)$.

a set of relative equilibria is a more efficient strategy than the Constant Velocity Algorithm. In other words, planning a path along relative equilibria takes into proper account the full system's dynamics and leads to some notion of optimality.

### 7.2.3 Numerical Simulations

The three algorithms introduced above have been implemented on a planar rigid body with two forces a distance $h$ from the center of mass and with two different masses along the body-fixed axes (to account for added mass when the body is in a fluid). This example is very similar to [PRB3] of Section 6.3.1. The parameter values in normalized units were chosen to be $J = 1, m_1 = .6, m_2 = 1, h = 2$. For both the Constant Velocity Algorithm and the Static Interpolation Algorithm, we let the initial configuration be the identity and the final (desired) configuration consists of a rotation of $\pi$ and a translation of 2 units along the $y$-axis, i.e., $g_{\text{initial}} = (0, 0, 0)$ and $g_{\text{final}} = (\pi, 0, 2)$. We set $\sigma = .1$. For all three algorithms, the numerical results were in agreement with the theoretical analysis presented above.

**Constant Velocity, Table 7.1:** Figure 7.3 illustrates how the velocity variables have a constant average value plus an oscillatory component. Despite the oscillations (see the light gray configurations in Figure 7.3), the configuration variables evolve along a screw motion toward the desired configuration.

**Static Interpolation, Table 7.3:** For comparison, we next present the numerical results of the Static Interpolation Algorithm. The initial and final (desired) configurations are the same as in the previous run. The set of ordered configuration points is $\{(0, 0, 0), (0, 0, 2), (\pi, 0, 2)\}$. In Figure 7.4 one can notice the path in the $x, y$ plane (consisting of a straight line and a rotation) and the various calls to the `Change-Velocity` and `Maintain-Velocity` primitives (for example, the time history of $u_1, u_2(t)$ shows peaks whenever a `Change-Velocity` maneuver occurs).

**Local Exponential Stabilization, Table 7.2:** Finally, we present the Stabilization Algorithm. Starting from the final condition of the Constant Velocity Algorithm, we

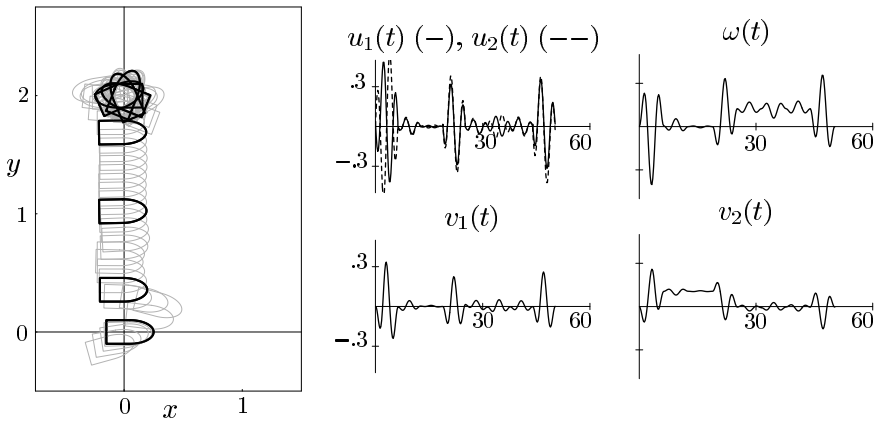


Figure 7.4: Static Interpolation Algorithm. See Figure 7.3 for an explanation of pictures. The planar body moves first along the $y$-axis (from $(0,0,0)$ to $(0,0,2)$) and then rotates to the desired final configuration $(\pi,0,2)$.

applied the local Stabilization Algorithm to steer the system exactly to the identity. Figure 7.5 illustrates how the convergence is exponential.

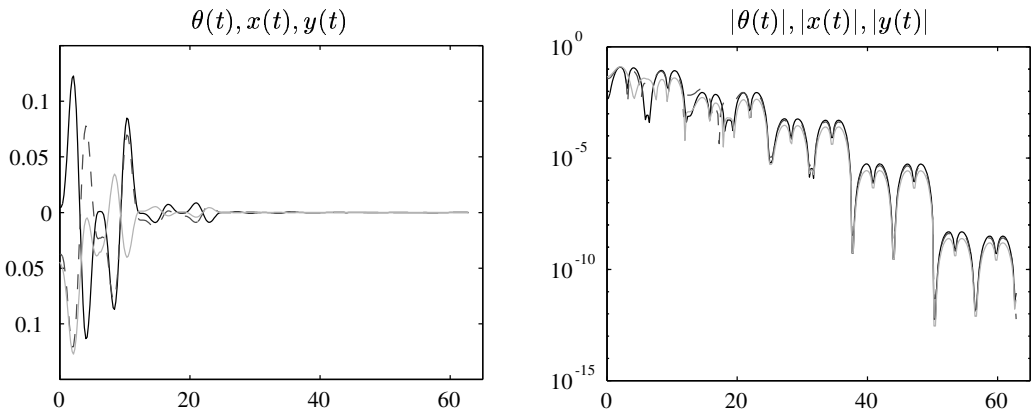


Figure 7.5: Local Stabilization Algorithm. We show only the configuration variables $\theta$ (with a solid line), $x$ (with a dashed line) and $y$ (with a light gray line). The initial condition of the simulation is the final state from the simulation of the Constant Velocity Algorithm.

# Chapter 8

# Conclusions

In this thesis we have presented a number of results in the area of nonlinear control of mechanical systems. Some of the contributions are stability type results, where the total energy of the system plays the role of a Lyapunov function, other contributions are controllability and motion planning type results, where the forced response of a mechanical system is characterized in terms of certain Lie algebra computations.

These contributions rely on various tools from nonlinear control theory and are all presented within the same modeling framework. The geometry of *affine connections* plays a central role both in the stability and in the motion planning chapters.

## 8.1 Summary

In Chapter 3 we have presented a rigorous and comprehensive framework for the study of mechanical control systems. The Euler-Lagrange equations are written in an intrinsic fashion by means of affine connections. The role of symmetry, constraints and impacts is examined in detail, leading to models useful for control purposes.

In Chapter 4 we have unveiled the geometry and the mechanics of the tracking problem for fully actuated Lagrangian systems. The design process in Section 4.2 allows us to characterize in an intrinsic way a tracking controller. The basic answered questions concern how to define configuration and velocity errors and how to compute the feed-forward control. Almost global stability and local exponential convergence are proven in full generality. Our framework successfully unifies a variety of examples: a robot manipulator on the Euclidean space $\mathbb{R}^n$, a pointing device on the two sphere $\mathbb{S}^2$, a satellite on the group of rotations SO(3) and an underwater vehicle on the group of rigid motions SE(3). Case by case, we provide new insight into previous results and introduce novel viewpoints.

In Chapter 5 we have investigated some stabilization techniques for relative equilibria of mechanical systems. We focused on one-dimensional symmetries for simplicity and in the interest of vehicle control applications. The novel contribution is the decomposition of the force codistribution onto the subspace of momentum-preserving forces and its orthogonal complement. Under specific assumptions, we prove exponential stability of the full system: the momentum converges to its desired value and all the other error variables converge to zero. The analysis in this chapter complements the results in [11, 47, 60].

In Chapter 6 and 7 we have studied motion planning and control of underactuated mechanical systems with a focus on underactuated vehicles. We have developed a geometric framework encompassing analysis and synthesis tools and showed its application to numerous examples. First, the controllability properties of these systems are characterized and their behavior under small-amplitude forcing is investigated. The perturbation method and the use of in-phase forcing turn out to play a key role. Finally, we have designed two motion

primitives to use in higher-level motion control algorithms. The latter steer the vehicle from point to point, and provide exponential stabilization of the vehicle to a desired configuration. Exponential stabilization is achieved using time-varying, continuous feedback control. The results in these chapters complement the controllability analysis of [67] and the averaging techniques of [62].

## 8.2 Future Directions

Despite the recent progresses in the study of mechanical control systems, numerous open questions of scientific and practical interest remain unanswered. For example, in the areas of autonomous vehicles and robotic locomotion, rigorous motion planning schemes for underactuated vehicles and satisfactory tools to analyze and design walking machines are not available. In what follows, we describe various promising projects, emphasizing motivations, prospects and potential rewards for each of them.

### Applications of Series Expansions for Forced Lagrangian Dynamics

A key contribution in this dissertation is the series expansion that describes the forced evolution of a mechanical system on a Lie group. In fact, this contribution raises more questions than it answers. For example, it is not yet known how to apply this methodology to mechanical systems defined on general manifold and subject perhaps to non-holonomic, dissipative or conservative forces. Such expansions would help in the study of gaits and of optimal forcing for locomotion. Also not clear is the relationship of our treatment with numerous results in averaging, vibrational stabilization and impulsive control of Lagrangian dynamics.

In these areas lots of work remains to be done and a methodic application of theoretical tools should result profitable. In particular, the theory of so-called "chronological calculus" might turn out to play a useful role, see [3] for a rigorous description and [21] for some initial results. However, some fundamental challenges and question remain in applying these expansions in new contexts (e.g., non-zero initial velocity) and with new purposes (e.g., vibrational stabilization).

### Motion Planning via Relative Equilibria for Underactuated Vehicles

As illustrated in the chapters on stability methods and in the recent literature [60, 11, 47], great progress has been made on the use of the Hamiltonian in the role of control Lyapunov function. These techniques rely on an appropriate "shaping" of the potential and kinetic energy in order to achieve stabilization of relative equilibria even though the control system is underactuated.

Despite these advances, two fundamental problems have not been tackled yet. First, no on-line method for switching from one relative equilibria to another is known. This problem is similar in its nature to the mode–switching and orbit transfer problems that arise respectively in flight control and aerospace navigation contexts. In fact, the literature on trajectory tracking for non-minimum phase systems describes some of the difficulty posed by this problem. A second shortcoming of the current techniques is that they do not apply to flight control problems with aerodynamic forces such as lift and drag. Understanding relative equilibria and their stabilization in this extended context is a difficult and potentially rewarding problem.

### Hybrid Aspects in Robotic Locomotion and Biomechanics

An area of increasing interest is modeling and control of hybrid mechanical systems, that is, locomotion and grasping devices that interact with the environment via contacts and collisions. Examples are hopping and walking robots, robots that progress by swinging arms, and devices that switch between clamped, sliding and rolling regimes.

Within this context, the engineering goal is to analyze and design systems that accomplish various tasks by means of their hybrid nature. This motivation leads to a number of problems that arise in the interaction of discontinuities, locomotion and stability. Topics of interest include stabilization via multiple Lyapunov functions, motion planning across different regimes, and numerical integrators for mechanical systems subject to impacts and forces. From a broader perspective, some of these challenges are of even deeper and independent interest because of their connection with the field of hybrid control systems.

Finally, a related interdisciplinary area is the study of biomechanics and its applications to rehabilitation engineering. Areas of current research include posture control, that is, human stability and balance, dynamic walking with and without feedback mechanisms, and stress analysis at bones and joints. An open and challenging research direction is to investigate these problem relying on the geometric understanding of motion presented in this dissertation.

### Beyond A Nonlinear Control Theory for Mechanical Systems

The topics described above are all part of a rigorous theoretical framework that encompasses mechanical control systems and their applications in various disciplines. It is the hope of the author that these themes will play a key role also in more general settings. For example, the theoretical understanding of mechanical systems turns out to be useful in the designing devices with appropriate locomotion or stability characteristics; see for example the work on underwater locomotion and on passive walking. A second way of extending these results is to investigate control problems for more general physical systems. Three important classes are aerial vehicles, micro-electromechanical systems, and distributed parameter systems.

# Appendix A

# Proofs of Some Results in Chapters 4 and 7

## A.1 The Error Function on the Rotation Group

We here study the modified trace function on SO(3) that we introduced in Section 4.4.4 and that was studied for example in [53]. Given a $3 \times 3$ symmetric matrix $K$, we define $\phi : \mathrm{SO}(3) \to \mathbb{R}_+$ as

$$\phi(R) \triangleq \frac{1}{2} \operatorname{tr}\left(K(I_3 - R)\right),$$

and, given any $3 \times 3$ matrix $A$, we defined $\operatorname{skew}(A) = \frac{1}{2}(A - A^T)$.

Recall that the linear space of $3 \times 3$ matrix $\mathbb{R}^{3\times 3}$ has an inner product given by the trace operation:

$$\langle\!\langle A\,,\, B \rangle\!\rangle = \frac{1}{2} \operatorname{tr}(A^T B).$$

With respect to this inner product, the space decomposes into the direct sum of symmetric and skew symmetric matrices $\mathfrak{so}(3)$. In particular, it holds

$$\langle\!\langle \widehat{x}\,,\, \widehat{y} \rangle\!\rangle = x^T y \qquad \text{and} \qquad \|\widehat{x}\|^2 = \|x\|^2,$$

for all $x, y$ in $\mathbb{R}^3$. Therefore, we can use this inner product to identify $\mathfrak{so}(3)$ and its dual: $\langle \alpha, \xi \rangle = \frac{1}{2} \operatorname{tr}(\alpha^T \xi)$, where $\alpha$ is in $\mathfrak{so}(3)^*$ and $\xi$ in $\mathfrak{so}(3)$.

**Lemma A.1.** *Let the eigenvalues $\{k_1, k_2, k_3\}$ of the matrix $K$ satisfy $k_i + k_j > 0$ for all $i \neq j$, and define $\mathrm{d}\phi \in \mathfrak{so}(3)^*$ such that $\dot{\phi} = \left\langle \mathrm{d}\phi, (R^T \dot{R}) \right\rangle$. It holds*

*(i)* $\phi(R) = \phi(R^T) \geq 0$ *and* $\phi(R) = 0$ *if and only if* $R = I_3$,

*(ii)* $\mathrm{d}\phi = \operatorname{skew}(KR)$, *and*

*(iii) for all* $\epsilon > 0$ *there exist* $b_1 \geq b_2 > 0$ *such that* $\phi(R) < \min_{i \neq j}(k_i + k_j) - \epsilon$ *implies* $b_1 \|\mathrm{d}\phi\|^2 \geq \phi \geq b_2 \|\mathrm{d}\phi\|^2$.

*Additionally, we have the following coordinate expressions. Let $R$ be a rotation of angle $\theta$ about the unit vector $\mathbf{k}$ and define the unit quaternion representation of $R$ by $q^T = [q_0 \;\; q_1 \;\; q_2 \;\; q_3] \equiv [q_0, \;\; \mathbf{q}_v^T]$, where*

$$q_0 = \cos(\theta/2) \quad \textit{and} \quad \mathbf{q}_v = \sin(\theta/2)\mathbf{k}.$$

*Finally define $K^{[2]}$ as the matrix with the same eigenvectors as $K$ and with eigenvalues $\{(k_2+k_3),(k_1+k_3),(k_1+k_2)\}$. Then it holds*

*(iv)* $\phi(R) = \|\mathbf{q}_v\|^2_{K^{[2]}}$, *and*

*(v)* $\mathrm{d}\phi = \frac{1}{2}\big(q_0 K^{[2]}\mathbf{q}_v - \widehat{\mathbf{q}}_v K^{[2]}\mathbf{q}_v\big)^{\widehat{}}$.

*Proof.* We start by proving (ii). It holds:

$$\dot{\phi} = \frac{1}{2}\operatorname{tr}\big(K(-\dot{R})\big) = -\frac{1}{2}\operatorname{tr}\big(KR\,R^T\dot{R}\big).$$

If we let $\operatorname{skew}(A) = \frac{1}{2}(A - A^T)$ and $\operatorname{sym}(A) = \frac{1}{2}(A + A^T)$, it holds

$$\begin{aligned}\dot{\phi} &= -\frac{1}{2}\operatorname{tr}\big(\big(\operatorname{skew}(KR) + \operatorname{sym}(KR)\big)\,(R^T\dot{R})\big)\\ &= -\frac{1}{2}\operatorname{tr}\big(\operatorname{skew}(KR)\,(R^T\dot{R})\big)\\ &= \Big\langle \operatorname{skew}(KR), (R^T\dot{R})\Big\rangle,\end{aligned}$$

where we have employed the properties of the trace pairing. This proves (ii). Next we introduce the unit quaternion representation. By Rodrigues' formula, it holds that $R = I_3 + 2q_0\widehat{\mathbf{q}}_v + 2\widehat{\mathbf{q}}_v^2$. Hence we have

$$\begin{aligned}\phi_{SO(3)} &= -\operatorname{tr}(Kq_0\mathbf{q}_v) - \operatorname{tr}(K\,\widehat{\mathbf{q}}^2)\\ &= -\operatorname{tr}(K\,\widehat{\mathbf{q}}^2) \;\equiv\; \mathbf{q}^T K^{[2]}\mathbf{q},\end{aligned}$$

where the second equality can be proved in coordinates. This proves (iv) and (v) can be verified by recalling the kinematic equation for $R$ in terms of the unit quaternion representation. Regarding (i), it is straightforward that $\phi(R) = \phi(R^T) \geq 0$. Also if $\phi(R) = 0$, then $\mathbf{q}_v$ is the zero vector and $R$ is the identity matrix.

Last, we prove the claim in (iii), that is that $\phi$ is quadratic with constant equal to the minimum eigenvalue of $K^{[2]}$. Since the two terms in the equation in (v) are orthogonal, we have

$$2\|\mathrm{d}\phi\|^2 = \|q_0 K^{[2]}\mathbf{q}_v\|^2 + \|\widehat{\mathbf{q}}_v K^{[2]}\mathbf{q}_v\|^2.$$

Since $\|\widehat{\mathbf{q}}_v K^{[2]}\mathbf{q}_v\|^2 \leq \|\mathbf{q}_v\|^2\|K^{[2]}\mathbf{q}_v\|^2 \leq \lambda_{\max}\big(K^{[2]}\big)\|\mathbf{q}_v\|^2_{K^{[2]}}$, we have

$$\begin{aligned}\phi &= \|\mathbf{q}_v\|^2_{K^{[2]}}\\ &\geq \frac{1}{2}q_0^2\|\mathbf{q}_v\|^2_{K^{[2]}} + \frac{1}{2}\|\mathbf{q}_v\|^2_{K^{[2]}}\\ &\geq \frac{1}{2}q_0^2\|\mathbf{q}_v\|^2_{K^{[2]}} + \frac{1}{2\lambda_{\max}\big(K^{[2]}\big)}\|\widehat{\mathbf{q}}_v K^{[2]}\mathbf{q}_v\|^2\\ &\geq \min\big(1, 1/\lambda_{\max}\big(K^{[2]}\big)\big)\,\|\mathrm{d}\phi\|^2.\end{aligned}$$

This proves one direction of the bound. Next, recall that we are assuming that, given an $\epsilon > 0$, we have the inequality $\phi \leq \lambda_{\min}\big(K^{[2]}\big) - \epsilon$. Hence it holds that

$$\exists \epsilon_1 > 0 \qquad \text{s.t.} \qquad \|\mathbf{q}_v\|^2 \leq 1 - \epsilon_1,$$

and this implies that

$$\exists \epsilon_1 > 0 \qquad \text{s.t.} \qquad \|q_0\|^2 \geq \epsilon_1.$$

However, it holds that $\|\mathrm{d}\phi\|^2 \geq \frac{1}{2}\|q_0 K^{[2]}\mathbf{q}_v\|^2 = \frac{1}{2}q_0^2\phi$, and therefore

$$\|\mathrm{d}\phi\|^2 \geq \frac{1}{2}\epsilon_1\phi.$$

This completes the proof of (iii) and of the whole Lemma. □

## A.2 Primitives of Motion

The statements in the description of both primitives are direct consequences of the following result.

**Proposition A.2.** *With the notation adopted in Chapter 7, let the assumptions in Proposition 7.1 hold and let* $\left(b^1(t), b^2(t)\right) = \texttt{Inverse}(\eta)$. *If* $\xi(0) = \epsilon\xi_0^1 + \epsilon^2\xi_0^2$, *we have*

$$\xi(2\pi) = \epsilon\xi_0^1 + \epsilon^2\Big(\xi_0^2 - \pi\left\langle \xi_0^1 : \xi_0^1\right\rangle + \eta\Big) + \epsilon^3\pi\Big(\pi\left\langle \xi_0^1 : \left\langle \xi_0^1 : \xi_0^1\right\rangle\right\rangle - 2\left\langle \xi_0^1 : \xi_0^2\right\rangle - \left\langle \xi_0^1 : \eta\right\rangle\Big) + O(\epsilon^4), \tag{A.1}$$

$$x(2\pi) = \epsilon 2\pi\xi_0^1 + \epsilon^2\pi\Big(2\xi_0^2 - \pi\left\langle \xi_0^1 : \xi_0^1\right\rangle + \eta\Big) + O(\epsilon^3). \tag{A.2}$$

*Proof.* Note that property (7.10) implies directly that $\overline{b^1}(2\pi) = \overline{\overline{b^1}}(2\pi) = \overline{\overline{\overline{b^1}}}(2\pi) = 0$, so that the terms in the Taylor expansion in Proposition 7.1 simplify to

$$\begin{aligned}
\xi^1(2\pi) &= \xi_0^1,\\
\xi^2(2\pi) &= \xi_0^2 - \pi\left\langle \xi_0^1 : \xi_0^1\right\rangle + \left(\overline{b^2 - \tfrac{1}{2}\left\langle \overline{b^1} : \overline{b^1}\right\rangle}\right)(2\pi),\\
\xi^3(2\pi) &= -2\pi\left\langle \xi_0^1 : \xi_0^2\right\rangle + \pi^2\left\langle \xi_0^1 : \left\langle \xi_0^1 : \xi_0^1\right\rangle\right\rangle - \left\langle \xi_0^1 : \left(\overline{\overline{b^2 - \tfrac{1}{2}\left\langle \overline{b^1} : \overline{b^1}\right\rangle}}\right)(2\pi)\right\rangle\\
&\quad + \overline{\left\langle \left\langle \xi_0^1 : \xi_0^1\right\rangle : \overline{b^1}\right\rangle \frac{t}{2}}(2\pi) + \overline{\left\langle \overline{b^1} : \left\langle \xi_0^1 : \overline{\overline{b^1}}\right\rangle\right\rangle}(2\pi)\\
&\quad - \overline{\left\langle \overline{b^1} : \overline{\left(b^2 - \tfrac{1}{2}\left\langle \overline{b^1} : \overline{b^1}\right\rangle\right)}\right\rangle}(2\pi),\\
x^1(2\pi) &= 2\pi\xi_0^1,\\
x^2(2\pi) &= 2\pi\xi_0^2 - \pi^2\left\langle \xi_0^1 : \xi_0^1\right\rangle + \left(\overline{\overline{b^2 - \tfrac{1}{2}\left\langle \overline{b^1} : \overline{b^1}\right\rangle}}\right)(2\pi) + \tfrac{1}{2}\overline{\left[\xi_0^1 + \overline{b^1}, \xi_0^1 t + \overline{\overline{b^1}}\right]}(2\pi).
\end{aligned}$$

Hence, $\xi^1(2\pi)$ and $x^1(2\pi)$ are as computed above. We employ Lemma 7.2 and prop-

erty (7.11) to simplify the remaining terms into

$$\xi^2(2\pi) = \xi_0^2 - \pi \left\langle \xi_0^1 : \xi_0^1 \right\rangle + \eta,$$

$$\xi^3(2\pi) = -2\pi \left\langle \xi_0^1 : \xi_0^2 \right\rangle + \pi^2 \left\langle \xi_0^1 : \left\langle \xi_0^1 : \xi_0^1 \right\rangle \right\rangle - \pi \left\langle \xi_0^1 : \eta \right\rangle + \overline{\left\langle \left\langle \xi_0^1 : \xi_0^1 \right\rangle : \overline{b^1} \right\rangle \frac{t}{2}}(2\pi)$$
$$+ \overline{\left\langle \overline{b^1} : \left\langle \xi_0^1 : \overline{\overline{b^1}} \right\rangle \right\rangle}(2\pi) - \overline{\left\langle \overline{b^1} : \overline{\left( b^2 - \tfrac{1}{2} \left\langle \overline{b^1} : \overline{b^1} \right\rangle \right)} \right\rangle}(2\pi),$$

$$x^2(2\pi) = 2\pi\xi_0^2 - \pi^2 \left\langle \xi_0^1 : \xi_0^1 \right\rangle + \pi\eta + \tfrac{1}{2} \overline{\left[ \xi_0^1 + \overline{b^1}, \xi_0^1 t + \overline{\overline{b^1}} \right]}(2\pi).$$

Regarding the term $\xi^3(t)$, the claim is proven if

$$\overline{\left\langle \left\langle \xi_0^1 : \xi_0^1 \right\rangle : \overline{b^1} \right\rangle \frac{t}{2}}(2\pi) = \overline{\left\langle \overline{b^1} : \left\langle \xi_0^1 : \overline{\overline{b^1}} \right\rangle \right\rangle}(2\pi) = \overline{\left\langle \overline{b^1} : \overline{\left( b^2 - \tfrac{1}{2} \left\langle \overline{b^1} : \overline{b^1} \right\rangle \right)} \right\rangle}(2\pi) = 0.$$

However, since $b^1(t)$ is linear combination of the functions $\psi_a(t)$, the latter relations correspond equality sign by equality sign to the properties in equation (7.12). Regarding the term $x^2(t)$, it holds that

$$\overline{\left[ \xi_0^1 + \overline{b^1}, \xi_0^1 t + \overline{\overline{b^1}} \right]}(2\pi) =$$
$$2\pi^2 \left[ \xi_0^1, \xi_0^1 \right] + \left[ \xi_0^1, \overline{\overline{b^1}}(2\pi) \right] + \overline{\left[ \overline{b^1}, \xi_0^1 t \right]}(2\pi) + \overline{\left[ \overline{b^1}, \overline{\overline{b^1}} \right]}(2\pi) = 0, \quad \text{(A.3)}$$

as all terms in the middle expression vanish. □

## A.3 Lemma 7.4

In what follows we abbreviate `Maintain-Velocity` to `Maintain`(and similarly for `Change`).

*Proof.* Given the descriptions of the primitives `Change` and `Maintain`, we compute the evolution of $\xi(t)$ as follows. Starting from $\xi(0) = O(\sigma^2)$, we have:

| | | | | |
|---|---|---|---|---|
| after first `Change`$(\sigma, \xi_{\text{nom}})$ | : | $\xi(2\pi)$ | = | $\sigma\xi_{\text{nom}} + O(\sigma^2)$, |
| after first `Maintain`$(\sigma, \xi_{\text{nom}})$ | : | $\xi(4\pi)$ | = | $\sigma\xi_{\text{nom}} + O(\sigma^3)$, |
| after $k$th step in the **for** loop | : | $\xi(2(k+1)\pi)$ | = | $\sigma\xi_{\text{nom}} + O(\sigma^3)$, |
| after the final `Change`$(\sigma, 0)$ | : | $\xi(2(N+1)\pi)$ | = | $O(\sigma^2)$. |

The final value of $\xi$ is therefore as in the claim. Similarly, we can compute the change in configuration during each interval:

| | | | | |
|---|---|---|---|---|
| after first `Change`$(\sigma, \xi_{\text{nom}})$ | : | $\log\big(h(0)\big)$ | = | $\pi\sigma\xi_{\text{nom}} + O(\sigma^{3/2})$, |
| after first `Maintain`$(\sigma, \xi_{\text{nom}})$ | : | $\log\big(h(2\pi)\big)$ | = | $2\pi\sigma\xi_{\text{nom}} + O(\sigma^2)$, |
| after $k$th step in the **for** loop | : | $\log\big(h(2k\pi)\big)$ | = | $2\pi\sigma\xi_{\text{nom}} + O(\sigma^3)$, |
| after final `Change`$(\sigma, 0)$ | : | $\log\big(h(2N\pi)\big)$ | = | $\pi\sigma\xi_{\text{nom}} + O(\sigma^{3/2})$. |

where we let $h(t) = g(t)^{-1} g(t + 2\pi)$.

We now need to sum the changes in configuration due to each interval by means of the approximation in Lemma 7.3. Combining the contributions during the first two intervals, and recalling that $[\xi_{\text{nom}}, \xi_{\text{nom}}]$ vanishes, we have

$$\log\big(g_0^{-1} g(4\pi)\big) = 3\pi\sigma\xi_{\text{nom}} + O(\sigma^{3/2}) =: 3\pi\sigma\xi_{\text{nom}} + \sigma^{3/2}\eta_1, \quad \text{(A.4)}$$

where $\eta_1 = O(1)$ is an appropriate vector in $\mathfrak{g}$. Next, we claim that for all $k = 1, \ldots, N-1$,

it holds

$$\log\left(g_0^{-1}g(2(k+1)\pi)\right) = a_k\xi_{\text{nom}} + \sigma^{3/2}\eta_k,$$

where the scalar $a_k$ and the vector $\eta_k$ are of order at most 1. We prove the claim by induction. At $k=1$, we recover equation (A.4), with $a_1 = 3\pi\sigma$. Next, we assume that the claim holds at $k$, and we prove it for $k+1$. As dictated by Lemma 7.3, we compute the bracket between the current value $a_k\xi_{\text{nom}} + \sigma^{3/2}\eta_k$ and the contribution $2\pi\sigma\xi_{\text{nom}} + O(\sigma^3) =: 2\pi\sigma\xi_{\text{nom}} + \sigma^3\zeta_k$, where $\zeta_k = O(1)$ is an appropriate vector in $\mathfrak{g}$. We have:

$$[a_k\xi_{\text{nom}} + \sigma^{3/2}\eta_k\ ,\ 2\pi\sigma\xi_{\text{nom}} + \sigma^3\zeta_k] = O(\sigma^{5/2}),$$

so that

$$\begin{aligned}\log\left(g_0^{-1}g(2(k+2)\pi)\right) &= \left(a_k\xi_{\text{nom}} + \sigma^{3/2}\eta_k\right) + \left(2\pi\sigma\xi_{\text{nom}} + \sigma^3\zeta_k\right) + O(\sigma^{5/2}) \\ &= \left(a_k + 2\pi\sigma\right)\xi_{\text{nom}} + \sigma^{3/2}\left(\eta_k + \sigma^{3/2}\zeta_k + \sigma\nu_k\right),\end{aligned}$$

where $\nu_k = O(1)$ is an appropriate vector in $\mathfrak{g}$. Hence, the claim holds at $k+1$, with $a_{k+1} = a_k + 2\pi\sigma$ and $\eta_{k+1} = \eta_k + \sigma^{3/2}\zeta_k + \sigma\nu_k$. At the end of the **for** loop, as $k = N-1$, we have

$$\log\left(g_0^{-1}g(2N\pi)\right) = a_{N-1}\xi_{\text{nom}} + \sigma^{3/2}\eta_{N-1},$$

where we can compute the coefficients as

$$a_{N-1} = a_1 + \sum_{k=2}^{N-1} 2\pi\sigma = (2N-1)\pi\sigma,$$

and

$$\eta_{N-1} = \eta_1 + \sum_{k=2}^{N-1}\left(\sigma^{3/2}\zeta_k + \sigma\nu_k\right) = O(1).$$

The contribution of the last interval is $\sigma\pi\xi_{\text{nom}}$ plus some higher-order terms, so that

$$\log\left(g_0^{-1}g(2(N+1)\pi)\right) = 2N\pi\sigma\xi_{\text{nom}} + O(\sigma^{3/2}).$$

Finally, we apply the approximation in Lemma 7.3 for a last time to obtain

$$\log(g(2(N+1)\pi)^{-1}g_1) = \log\left(\left(g_0^{-1}g(2(N+1)\pi)\right)^{-1}\left(g_0^{-1}g_1\right)\right) = O(\sigma^{3/2}),$$

where we recall that $\log(g_0^{-1}g_1) = 2N\pi\sigma\xi_{\text{nom}}$ and $\log(h^{-1}) = -\log(h)$. □

## A.4 Lemma 7.5

*Proof.* We start by investigating the two `Change` primitives described inside the **for** loop in Algorithm 7.2. Assuming that at time $t_k$ it holds

$$\left\|\left(\log(g(t_k)), \xi(t_k)\right)\right\| = \sigma_k \ll 1,$$

we claim that

$$\left\| \big( \log(g(t_{k+1})), \xi(t_{k+1}) \big) \right\| = O(\sigma_k^{3/2}). \tag{A.5}$$

This can be seen as follows. By assumption there exist two vectors $x_{\mathrm{err}}$ and $\xi_{\mathrm{err}}$ of order $O(1)$ such that

$$\begin{aligned} \log(g(t_k)) &= \sigma_k x_{\mathrm{err}}, \\ \xi(t_k) &= \sigma_k \xi_{\mathrm{err}}. \end{aligned}$$

With this notation, it holds $-\big( \log(g(t_k)) + \pi \xi(t_k) \big)/(2\pi\sigma_k) = -\big(x_{\mathrm{err}} + \pi \xi_{\mathrm{err}}\big)/(2\pi)$. After the primitive $\texttt{Change}(\sigma_k, -\big(x_{\mathrm{err}} + \pi\xi_{\mathrm{err}}\big)/(2\pi))$, we compute

$$\begin{aligned} \log(g(t_k + 2\pi)) &= \tfrac{1}{2}\sigma_k (x_{\mathrm{err}} + \pi \xi_{\mathrm{err}}) + O(\sigma_k^{3/2}) \\ \xi(t_k + 2\pi) &= -\sigma_k \big(x_{\mathrm{err}} + \pi \xi_{\mathrm{err}}\big)/(2\pi) + O(\sigma_k^2), \end{aligned}$$

and after the final $\texttt{Change}(\sigma_k, 0)$, we have

$$\begin{aligned} \log(g(t_k + 4\pi)) &= O(\sigma_k^{3/2}), \\ \xi(t_k + 4\pi) &= O(\sigma_k^2). \end{aligned}$$

As $t_{k+1} = t_k + 4\pi$, this proves equation (A.5). The latter equations are equivalent to

$$\left\| \big( \log(g(t_{k+1})), \xi(t_{k+1}) \big) \right\| \leq M_k \sigma_k^{3/2}, \tag{A.6}$$

where the positive scalar $M_k$ depends continuously on initial state and parameters of the system of ordinary differential equations (3.7) and (3.8). The parameters are $\sigma_k$ and the coefficients in the design of $(b^1(t), b^2(t))$, for $t_k < t < t_{k+1}$. By looking at the details of the inversion algorithm in Lemma 7.2, these parameters are seen to be continuous function of the initial conditions $\big( \log(g(t_k), \xi(t_k)) \big)$. Hence, we know that $M_k(g(t_k), \xi(t_k))$ is a continuous function of its arguments and it is therefore bounded in a neighborhood of the point $(g(t_k), \xi(t_k)) = (\mathrm{Id}, 0)$. In other words, there exist positive constants $B_1, B_2$ such that

$$\left\| \big( \log(g(t_k)), \xi(t_k) \big) \right\| < B_1 \quad \Longrightarrow \quad M_k(g(t_k), \xi(t_k)) < B_2.$$

Finally, for some $\alpha < 1$, we set $\sigma = \alpha \min\big(B_1, 1/B_2^2\big)$ and we prove by induction that $\sigma_k < \sigma$ and $M_k \sigma_k^{1/2} \leq \alpha$. At $k = 0$, we have by assumption

$$\sigma_0 = \|(\log(g(0)), \xi(0))\| \leq \sigma < B_1,$$

so that $M_0 < B_2$ and

$$M_0 \sigma_0^{1/2} < B_2 \sigma^{1/2} < \alpha < 1.$$

Therefore, the claim holds at $k = 0$. Next, we assume it at $k$, and prove it for $k + 1$. We rewrite equation (A.6) as

$$\sigma_{k+1} = \left\| \big( \log(g(t_{k+1}), \xi(t_{k+1}) \big) \right\| \leq \big( M_k \sigma_k^{1/2} \big) \sigma_k \leq \alpha\sigma < B_1.$$

Hence, $M_{k+1}$ is also bounded by $B_2$ and we have

$$\sigma_{k+1}^{1/2} M_{k+1} \leq \sigma^{1/2} B_2 < \alpha.$$

This proves that $M_k \sigma_k^{1/2} \leq \alpha$ for all $k$. In other words, we have that the sequence $\{\sigma_k, k \geq 0\}$ satisfies $\sigma_{k+1} \leq \alpha \sigma_k$ with $\alpha < 1$, or equivalently $\sigma_k \leq \alpha^k \sigma_0$. Therefore, for $\lambda = -\ln \alpha > 0$,

$$\left\| \left( \log(g(t_k)), \xi(t_k) \right) \right\| \leq \left\| \left( \log(g(0)), \xi(0) \right) \right\| e^{-\lambda k}.$$

Finally we prove the last statement in Lemma 7.5. From time $t_k$ to $t_{k+1}$, the system undergoes two `Change` primitives and evolves starting from a state of order $O(\sigma_k) = O(e^{-\lambda k})$ to a final state of higher order. During the two `Change` primitives, the input is of order $\sqrt{\sigma_k} = e^{-\lambda k/2}$ (with the notation in Section 7.2.1 and in Proposition 7.1, it holds $\epsilon = \sqrt{\sigma}$). Therefore, the expansions in Proposition 7.1 show that the state is of order $\sqrt{\sigma_k} = e^{-\lambda k/2}$ from time $t_k$ to $t_{k+1}$.

□

# Bibliography


[1] R. Abraham and J. E. Marsden. *Foundations of Mechanics*. Addison Wesley, Reading, MA, second edition, 1987.

[2] R. Abraham, J. E. Marsden, and T. Ratiu. *Manifolds, Tensor Analysis, and Applications*, volume 75 of *AMS*. Springer Verlag, New York, NY, second edition, 1988.

[3] A. A. Agračhev and R. V. Gamkrelidze. The exponential representation of flows and the chronological calculus. *Math. USSR Sbornik*, 35(6):727–785, 1978.

[4] S. Arimoto. *Control Theory of Non-linear Mechanical Systems: A Passivity-Based and Circuit-Theoretic Approach*, volume 49 of *OESS*. Oxford University Press, Oxford, UK, 1996.

[5] V. I. Arnold. Sur la geometrie differentielle des groupes de Lie de dimension infinie et ses applications a l'hydrodynamique des fluides parfaits. *Annale de l'Institut Fourier*, XVI(1):319–361, 1966.

[6] V. I. Arnold. *Mathematical Methods of Classical Mechanics*, volume 60 of *GTM*. Springer Verlag, New York, NY, second edition, 1989.

[7] J. Baillieul. Stable average motions of mechanical systems subject to periodic forcing. In M. J. Enos, editor, *Dynamics and Control of Mechanical Systems*, volume 1, pages 1–23. Field Institute Communications, 1993.

[8] N. S. Bedrossian and M. W. Spong. Feedback linearization of robot manipulators and Riemannian curvature. *Journal of Robotic Systems*, 12(8):541–552, 1995.

[9] A. M. Bloch and P. E. Crouch. Nonholonomic control systems on Riemannian manifolds. *SIAM Journal of Control and Optimization*, 33(1):126–148, 1995.

[10] A. M. Bloch, P. S. Krishnaprasad, J. E. Marsden, and G. S. de Alvarez. Stabilization of rigid body dynamics by internal and external torques. *Automatica*, 28(4):745–756, 1992.

[11] A. M. Bloch, N. E. Leonard, and J. E. Marsden. Stabilization of mechanical systems using controlled Lagrangians. In *IEEE Conf. on Decision and Control*, San Diego, CA, December 1997.

[12] B. Bonnard. Controllabilité de systémes mécaniques sur les groupes de Lie. *SIAM Journal of Control and Optimization*, 22(5):711–722, 1984.

[13] W. M. Boothby. *An Introduction to Differentiable Manifolds and Riemannian Geometry*. Academic Press, New York, NY, second edition, 1986.

[14] M. S. Branicky, V. S. Borkar, and S. K. Mitter. A unified framework for hybrid control: model and optimal-control theory. *IEEE Transactions on Automatic Control*, 43(1):31–45, 1998.

[15] R. W. Brockett. System theory on group manifolds and coset spaces. *SIAM Journal of Control*, 10(2):265–284, 1972.

[16] R. W. Brockett. Lie theory and control systems defined on spheres. *SIAM Journal of Applied Mathematics*, 25(2):213–225, 1973.

[17] R. W. Brockett. Control theory and analytical mechanics. In R. Hermann and C. Martin, editors, *Geometric Control Theory*, volume 7 of *Lie Groups: History Frontiers and Applications*, pages 1–46. Mathematical Scientific Press, Brookline, MA, 1977.

[18] R. W. Brockett. Feedback invariants for nonlinear systems. In *Proceedings of the International Congress of Mathematicians*, Helsinki, Finland, 1978.

[19] B. Brogliato. *Nonsmooth Impact Mechanics: Models, Dynamics, and Control*, volume 220 of *Lecture Notes in Control and Information Sciences*. Springer Verlag, New York, NY, 1996.

[20] F. Bullo. Exponential stabilization of relative equilibria for mechanical systems with symmetries. In *Mathematical Theory of Networks and Systems (MTNS)*, Padova, Italy, July 1998. Submitted. Available at `http://www.cds.caltech.edu/~bullo`.

[21] F. Bullo. A series describing the evolution of mechanical control systems. In *IFAC World Conference*, Beijing, China, August 1998. Submitted. Available at `http://www.cds.caltech.edu/~bullo`.

[22] F. Bullo and N. E. Leonard. Motion control for underactuated mechanical systems on Lie groups. In *European Control Conference*, Brussels, Belgium, July 1997.

[23] F. Bullo and N. E. Leonard. Motion primitives for stabilization and control of underactuated vehicles. In *Nonlinear Control Systems Design (NOLCOS)*, pages 133–138, Enschede, the Netherlands, July 1998.

[24] F. Bullo, N. E. Leonard, and A. D. Lewis. Controllability and motion algorithms for underactuated Lagrangian systems on Lie groups. Submitted to *IEEE Transactions on Automatic Control*. Also Technical Report CDS 97–013, California Institute of Technology, November 1997.

[25] F. Bullo and R. M. Murray. Proportional derivative (PD) control on the Euclidean group. In *European Control Conference*, pages 1091–1097, Rome, Italy, June 1995.

[26] F. Bullo and R. M. Murray. Tracking for fully actuated mechanical systems: A geometric framework. To appear, *Automatica*. Also Technical Report CDS 97–003, California Institute of Technology, January 1997.

[27] F. Bullo and R. M. Murray. Trajectory tracking for fully actuated mechanical systems. In *European Control Conference*, Brussels, Belgium, July 1997.

[28] F. Bullo, R. M. Murray, and A. Sarti. Control on the sphere and reduced attitude stabilization. In *Nonlinear Control Systems Design (NOLCOS)*, pages 495–501, Tahoe City, CA, June 1995.

[29] F. Bullo and M. Žefran. On modeling and locomotion of hybrid mechanical systems with impacts. In *IEEE Conf. on Decision and Control*, Tampa, FL, December 1998. To appear. Available at `http://www.cds.caltech.edu/~bullo`.

[30] C. I. Byrnes, A. Isidori, and J. C. Willems. Passivity, feedback equivalence, and the global stabilization of minimum phase nonlinear systems. *IEEE Transactions on Automatic Control*, AC-36(11):1228–1240, 1991.

[31] J. J. Craig. *Introduction to Robotics: Mechanics and Control*. Addison Wesley, Reading, MA, second edition, 1989.

[32] P. E. Crouch. Geometric structures in systems theory. *IEE Proceedings*, 128(5):242–252, 1981.

[33] P. E. Crouch. Spacecraft attitude control and stabilization: Application of geometric control theory to rigid body models. *IEEE Transactions on Automatic Control*, 29(4):321–331, 1984.

[34] P. E. Crouch and A. J. van der Schaft. *Variational and Hamiltonian Control Systems*, volume 101 of *Lecture Notes in Control and Information Sciences*. Springer Verlag, New York, NY, 1987.

[35] M. P. Do Carmo. *Riemannian Geometry*. Birkhäuser, Boston, MA, 1992.

[36] O. Egeland and J.-M. Godhavn. Passivity-based adaptive attitude control of a rigid spacecraft. *IEEE Transactions on Automatic Control*, 39(4):842–846, 1994.

[37] B. Etkin. *Dynamics of Flight: Stability and Control*. John Wiley and Sons, New York, NY, 1982.

[38] H. Flanders. *Differential Forms with Applications to Physical Sciences*. Dover Publications, New York, NY, 1989.

[39] A. T. Fomenko and R. V. Chakon. Recursion relations for homogeneous terms of a convergent series of the logarithm of a multiplicative integral on Lie groups. *Functional Analysis and its Applications*, 24(1):48–58, 1990. Translated from Russian.

[40] T. I. Fossen. *Guidance and Control of Ocean Vehicles*. John Wiley and Sons, New York, NY, 1994.

[41] H. Goldstein. *Classical Mechanics*. Addison Wesley, Reading, MA, second edition, 1980.

[42] B. Goodwine. *Control of Stratified Systems with Robotic Applications*. Ph.D. thesis, California Institute of Technology, June 1998.

[43] L. Gurvits. Averaging approach to nonholonomic motion planning. In *IEEE Conf. on Robotics and Automation*, pages 2541–2546, Nice, France, 1992.

[44] R. Hermann and A. J. Krener. Nonlinear controllability and observability. *IEEE Transactions on Automatic Control*, 22:728–740, 1977.

[45] A. Isidori. *Nonlinear Control Systems: an Introduction*. Springer Verlag, New York, NY, second edition, 1989.

[46] A. Isidori and A. J. Krener. On feedback equivalence of nonlinear systems. *Systems & Control Letters*, 2(2):118–121, 1982.

[47] S. M. Jalnapurkar and J. E. Marsden. Stabilization of relative equilibria. Technical Report CDS 98–007, California Institute of Technology, July 1998. Available at `http://www.cds.caltech.edu`.

[48] M. Kawski. Nonlinear control and combinatorics of words. In B. Jakubczyk and W. Respondek, editors, *Geometry of Feedback and Optimal Control*, pages 305–346. Dekker, New York, NY, 1998.

[49] S. D. Kelly and R. M. Murray. Geometric phases and robotic locomotion. *Journal of Robotic Systems*, 12(6):417–431, 1995.

[50] S. D. Kelly and R. M. Murray. Lagrangian mechanics and carangiform locomotion. In *Nonlinear Control Systems Design (NOLCOS)*, Enschede, The Netherlands, July 1998.

[51] H. Khalil. *Nonlinear Systems*. Macmillan Publishing Company, New York, NY, 1992.

[52] S. Kobayashi and K. Nomizu. *Foundations of Differential Geometry, Vol. I*, volume 15 of *Interscience Tracts in Pure and Applied Mathematics*. Interscience Publishers, New York, NY, 1963.

[53] D. E. Koditschek. The application of total energy as a Lyapunov function for mechanical control systems. In J. E. Marsden, P. S. Krishnaprasad, and J. C. Simo, editors, *Dynamics and Control of Multibody Systems*, volume 97, pages 131–157. AMS, 1989.

[54] P. S. Krishnaprasad. Lie Poisson structures, dual-spin spacecraft and asymptotic stability. *Nonlinear Analysis, Theory, Methods & Applications*, 9 (10):1011–1035, 1985.

[55] M. Krstic, I. Kanallakopoulos, and P. Kokotovic. *Nonlinear and Adaptive Control Design*. Addison Wesley, Reading, MA, 1995.

[56] G. Lafferriere and H. J. Sussmann. A differential geometric approach to motion planning. In Z. Li and J. F. Canny, editors, *Nonholonomic Motion Planning*, pages 235–270. Kluwer, 1993.

[57] H. Lamb. *Hydrodynamics*. Dover Publications, New York, NY, sixth edition, 1932.

[58] N. E. Leonard. Control synthesis and adaptation for an underactuated autonomous underwater vehicle. *IEEE Journal of Oceanic Engineering*, 20(9):211–220, 1995.

[59] N. E. Leonard. Stability of a bottom-heavy underwater vehicle. *Automatica*, 33(3):331–346, 1997.

[60] N. E. Leonard. Stabilization of underwater vehicle dynamics with symmetry-breaking potentials. *Systems & Control Letters*, 32:35–42, 1997.

[61] N. E. Leonard. Mechanics and nonlinear control: Making underwater vehicles ride and glide. In *Nonlinear Control Systems Design (NOLCOS)*, volume 1, pages 1–6, Enschede, The Netherlands, July 1998.

[62] N. E. Leonard and P. S. Krishnaprasad. Motion control of drift-free, left-invariant systems on Lie groups. *IEEE Transactions on Automatic Control*, 40(9):1539–1554, 1995.

[63] N. E. Leonard and J. E. Marsden. Stability and drift of underwater vehicle dynamics: Mechanical systems with rigid motion symmetry. *Physica D*, 105:130–162, 1997.

[64] A. D. Lewis. *Aspects of Geometric Mechanics and Control of Mechanical Systems.* Ph.D. thesis, California Institute of Technology, Pasadena, CA, April 1995. Available at `http://www.cds.caltech.edu/reports`.

[65] A. D. Lewis. Local configuration controllability for a class of mechanical systems with a single input. In *European Control Conference*, Brussels, Belgium, July 1997.

[66] A. D. Lewis. Simple mechanical control systems with constraints. Submitted to the *IEEE Transactions on Automatic Control.* Special issue on Mechanics and Nonlinear Control Systems, 1997.

[67] A. D. Lewis and R. M. Murray. Controllability of simple mechanical control systems. *SIAM Journal of Control and Optimization*, 35(3):766–790, 1997.

[68] A. D. Lewis and R. M. Murray. Decompositions of control systems on manifolds with an affine connection. *Systems & Control Letters*, 31(4):199–205, 1997.

[69] J. Luh, Walker, and R. Paul. Resolved acceleration control. *IEEE Transactions on Automatic Control*, 25(3):468–474, 1980.

[70] V. Manikonda and P. S. Krishnaprasad. Controllability of Lie-Poisson reduced dynamics. In *American Control Conference*, Albuquerque, NM, June 1997.

[71] J. E. Marsden. *Lectures on Mechanics.* Cambridge University Press, New York, NY, 1992.

[72] J. E. Marsden and T. S. Ratiu. *Introduction to Mechanics and Symmetry.* Springer Verlag, New York, NY, 1994.

[73] G. Meyer. Design and global analysis of spacecraft attitude control systems. Technical Report R-361, NASA, March 1971.

[74] P. Morin and C. Samson. Time-varying exponential stabilization of a rigid spacecraft with two control torques. *IEEE Transactions on Automatic Control*, 42(4):528–534, 1997.

[75] R. M. Murray. Nonlinear control of mechanical systems: a Lagrangian perspective. In *Nonlinear Control Systems Design (NOLCOS)*, pages 378–389, Lake Tahoe, CA, June 1995. *Annual Reviews in Control*, v21, pp 31-45, 1997.

[76] R. M. Murray, Z. X. Li, and S. S. Sastry. *A Mathematical Introduction to Robotic Manipulation.* CRC Press, Boca Raton, FL, 1994.

[77] R. M. Murray and S. S. Sastry. Nonholonomic motion planning: Steering using sinusoids. *IEEE Transactions on Automatic Control*, 5(38):700–726, 1993.

[78] H. Nijmeijer and A. van der Schaft. *Nonlinear Dynamical Control Systems.* Springer Verlag, New York, NY, 1990.

[79] L. Noakes, G. Heinzinger, and B. Paden. Cubic splines on curved spaces. *IMA Journal of Mathematical Control & Information*, 6:465–473, 1989.

[80] J. P. Ostrowski and J. W. Burdick. Controllability tests for mechanical systems with symmetries and constraints. *Journal Applied Mathematics and Computer Science*, 7(2):101–127, 1997.

[81] F. C. Park. Distance metrics on the rigid–body motions with applications to mechanism design. *ASME Journal of Mechanical Design*, 117(1):48–54, 1995.

[82] K. Y. Pettersen and O. Egeland. Robust attitude stabilization of an underactuated AUV. In *European Control Conference*, Brussels, Belgium, July 1997.

[83] M. Rathinam and R. M. Murray. Configuration flatness of Lagrangian systems underactuated by one control. *SIAM Journal of Control and Optimization*, 36(1):164–179, 1998.

[84] C. Rui, I. V. Kolmanovsky, P. J. McNally, and N. H. McClamroch. Attitude control of underactuated multibody spacecraft. In *IFAC World Conference*, San Francisco, CA, July 1996.

[85] D. H. Sattinger and O. L. Weaver. *Lie Groups and Algebras, with Applications to Physics, Geometry and Mechanics*, volume 61 of *AMS*. Springer Verlag, New York, NY, 1986.

[86] J. C. Simo, D. R. Lewis, and J. E. Marsden. Stability of relative equilibria I: The reduced energy momentum method. *Archive for Rational Mechanics and Analysis*, 115:15–59, 1991.

[87] J.-J. E. Slotine and M. D. Di Benedetto. Hamiltonian adaptive control of spacecraft. *IEEE Transactions on Automatic Control*, 35:848–852, 1990.

[88] J.-J. E. Slotine and W. Li. Composite adaptive control of robot manipulators. *Automatica*, 25:509–519, 1989.

[89] S. Smale. Topology and mechanics. *Inventionae Mathematicae*, 10:305–331, 1970.

[90] E. D. Sontag. *Mathematical Control Theory*, volume 6 of *TAM*. Springer Verlag, New York, NY, 1990.

[91] E. D. Sontag. On the input-to-state stability property. *European Journal of Control*, 1:24–36, 1995.

[92] O. J. Sordalen and O. Egeland. Exponential stabilization of nonholonomic chained systems. *IEEE Transactions on Automatic Control*, 40(1):35–49, 1995.

[93] H. J. Sussmann. A general theorem on local controllability. *SIAM Journal of Control and Optimization*, 25(1):158–194, 1987.

[94] H. J. Sussmann and W. Liu. Limits of highly oscillatory controls and the approximation of general paths by admissible trajectories. In *IEEE Conf. on Decision and Control*, pages 437–442, Brighton, UK, December 1991.

[95] M. Takegaki and S. Arimoto. A new feedback method for dynamic control of manipulators. *Journal of Dynamic Systems, Measurement, and Control*, 102:119–125, 1981.

[96] P. Tsiotras and Y. M. Longuski. Spin-axis stabilization of symmetrical spacecraft with 2 control torque. *Systems & Control Letters*, 23(6):395–402, 1994.

[97] A. J. van der Schaft. Linearization of Hamiltonian and gradient systems. *IMA Journal of Mathematical Control & Information*, 1:185–198, 1984.

[98] A. J. van der Schaft. Stabilization of Hamiltonian systems. *Nonlinear Analysis, Theory, Methods & Applications*, 10(10):1021–1035, 1986.

[99] M. J. van Nieuwstadt and R. M. Murray. Rapid hover to forward flight transitions for a thrust vectored aircraft. *Journal of Guidance, Control, and Dynamics*, 21(1):93–100, 1998.

[100] M. J. van Nieuwstadt and R. M. Murray. Real time trajectory generation for differentially flat systems. *International Journal of Robust and Nonlinear Control*, 1998. To appear.

[101] F. W. Warner. *Foundations of Differentiable Manifolds and Lie Groups*, volume 94 of *GTM*. Springer Verlag, New York, NY, second edition, 1989.

[102] J. T.-Y. Wen and D. S. Bayard. A new class of control laws for robotic manipulators. Part I: Non–adaptive case. *International Journal of Control*, 47(5):1361–1385, 1988.

[103] J. T.-Y. Wen and K. Kreutz-Delgado. The attitude control problem. *IEEE Transactions on Automatic Control*, 36:1148–1162, 1991.

[104] L. L. Whitcomb, A. A. Rizzi, and D. E. Koditschek. Comparative experiments with a new adaptive controller for robot arms. *IEEE Transactions on Automatic Control*, 9(1):59–70, 1993.

[105] E. T. Whittaker. *A Treatise on the Analytical Dynamics of Particles and Rigid Bodies*. Cambridge University Press, New York, NY, 1927.

[106] M. Žefran. *Continuous methods for motion planning*. Ph.D. thesis, University of Pennsylvania, Philadelphia, PA, December 1996.

# Index